



UNIVERSIDAD DE CÓRDOBA

FACULTAD DE MEDICINA

**DEPARTAMENTO DE BIOLOGÍA CELULAR, FISIOLOGÍA E
INMUNOLOGÍA**

PROGRAMA DE DOCTORADO EN BIOMEDICINA

TESIS DOCTORAL

***MODULATION BY POST-TRANSLATIONAL
MODIFICATIONS OF KINASES IMPLIED IN GENOTOXIC
STRESS***

**Memoria presentada para optar al grado de Doctor en Biología por
Moisés Pérez Aguilera**

Directores

Marco Antonio Calzado Canale

Eduardo Muñoz Blanco

Córdoba, Marzo de 2012

TÍTULO: Modulation by Post-Translational Modifications of Kinases implied in Genotoxic Stress

AUTOR: Moisés Pérez Aguilera

© Edita: Servicio de Publicaciones de la Universidad de Córdoba. 2012
Campus de Rabanales Ctra. Nacional IV, Km. 396 A
14071 Córdoba

www.uco.es/publicaciones
publicaciones@uco.es

D. Marco Antonio Calzado Canale, Investigador Ramón y Cajal de la Universidad de Córdoba,

CERTIFICA

Que **D. Moisés Pérez Aguilera** ha realizado en el Departamento de Biología Celular, Fisiología e Inmunología bajo su dirección el trabajo titulado *“Modulation by Post-Translational Modifications of Kinases implied in Genotoxic Stress”*, que a mi juicio reúne los requisitos necesarios para optar al grado de doctor.



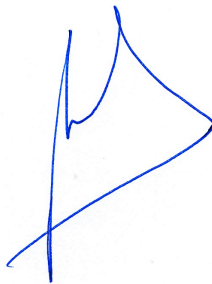
Y para que conste, firmo el presente, en Córdoba a 22 Marzo 2012.



D. Eduardo Muñoz Blanco, Catedrático del Departamento de Biología Celular,
Fisiología e Inmunología de la Universidad de Córdoba,

CERTIFICA

Que **D. Moisés Pérez Aguilera** ha realizado en el Departamento de Biología Celular,
Fisiología e Inmunología bajo su dirección el trabajo titulado *“Modulation by Post-
Translational Modifications of Kinases implied in Genotoxic Stress”*, que a mi juicio
reúne los requisitos necesarios para optar al grado de doctor.



Y para que conste, firmo el presente, en Córdoba a 22 Marzo 2012.



Acknowledgements

After an enormously amusing, difficult, enjoyable, thrilling, and also sometimes exhausting and frustrating almost 5 years, there are a lot of people whom I want to thank for being with me and supporting me in many different ways during that time.

I am truly indebted and thankful to my supervisors Eduardo Muñoz and Marco A. Calzado. Needless to say about their exceptional international scientific performance, I have the need to let everyone know about them personally. They have selflessly helped me reach my goals, given me the chances of traveling to Germany and shortly to England, supported me in all the publications and always having a nice mood towards me. Marco deserves special considerations for having put up with my weekly meetings, supports me for further career in science and his endlessly struggle to make the best out of me.

I owe sincere and earnest thankfulness to all members of the lab. You all have been good friends and compatriots. Hope you never forget the “delicious” meal we had after the IMIBIC award we won in 2011; Lol! I would like to show my especial gratitude to Carmen G. L. She has helped me more than anyone can think to accomplish this dissertation and my main article to be published. I’ve enjoyed her stories, our endless debates over the issues outside of science, and just interacting with her.

Those, who were not directly involved in my scientific research but share a major portion of satisfaction and happiness for my achievements, are my beloved parents, grandparents, brother, sister and my amazing and delightful girlfriend Maribel. I hereby offer my proud salutations to all of them for their love and encouragement. Their belief in me, gave me the energy to move on. Dad, I have learnt how to be a man from you. Mum, I will never forget your eagerness to make us all happy and be always in a nice mood. Isra and María, I eventually have the chance to tell you publicly how proud I am of yourselves, thank you for helping me. Hope you are having a nice time in Greece María. My grandparents deserve to be mentioned; to them I owe an extra strenght. Maribel, thank you for waiting so patiently so many hours outside the lab, deprive yourself many weekends for this dissertation, listen to my worries and encourage me to achieve my ambitions, that as you know science is not the only one...

Abbreviations

2-AG	2-Arachidonoylglycerol
AEA	Anandamide
AKT	Protein kinase B
ATM	Ataxia telangiectasia mutated
ATR	Ataxia telangiectasia and Rad3 related
ATX	ATM- related X protein
BBB	Blood–brain barrier
CB	Cannabinoid receptors
CHK	Csk-homologous kinase
CHX	Cycloheximide
COX-2	Ciclooxigenase-2
DAPI	4',6-diamidino-2-phenylindole
DNA-PK	DNA-dependent protein kinase
DSB	Double-strand break
DXR	Doxorubicin
DYRK	Dual-specificity tyrosine-regulated kinases
ECs	Endocannabinoid system
EPO	Erythropoietin
HIF	Hypoxia-inducible factor
HIPK	Homeodomain-interacting protein kinase
IKK	I κ B kinase
IL-1β	Interleukin-1 alpha
IP	Immunoprecipitation
LPS	Lipopolysaccharide
MAPK	Mitogen-Activated Protein Kinase
MDM2	Murine doble minute 2
NADA	<i>N</i> -arachidonoyl-dopamine
Ni-NTA	Nickel-nitrilotriacetic acid
NLS	Nuclear localization signal
OLDA	<i>N</i> -oleoyl-dopamine
PALDA	<i>N</i> -palmitoyl-dopamine
PG	Prostaglandin

PHD	Prolyl hydroxylase
PI3K	Phosphoinositide 3-kinase
PKCδ	Protein kinase C
qPCR	Quantitative real time polymerase chain reaction
RING	Really Interesting New Gene
SIAH	Seven in absentia homolog
STEARDA	<i>N</i> -stearoyl-dopamine
TNFα	Tumor necrosis factor alpha
TRPV	Transient Receptor Potential Vanilloid
UV	Ultraviolet light

Table of Contents

1. Introduction	1
1.1. The endocannabinoid system	2
1.2. <i>N</i> -arachidonoyl-dopamine, NADA	2
1.3. The Cyclooxygenase catalysis	3
1.4. Genomic instability in cancer	3
1.5. Protein kinase signaling networks in cancer	6
1.6. DYRK	7
1.7. SIAH 7 (seven in absentia homolog)	10
1.8. SIAH2 and Hypoxia	13
2. Aims	16
3. Materials and Methods	18
3.1. Cell lines, transfections and reagents	19
3.2. Antibodies	19
3.3. Plasmids	20
3.4. Western blotting	21
3.5. Phosphatase treatment	21
3.6. Immunoprecipitation	22
3.7. Luciferase reporter assays	22
3.8. Enrichment of His-Tagged Proteins	22
3.9. Immunofluorescence	22
3.10. GST pulldown assay	23
3.11. <i>In vitro</i> phosphorylation analysis	23
3.12. Mass spectrometry	23
3.13. Peptide array binding assay	25
3.14. mRNA extraction and qPCR	25
3.15. Angiogenesis assay	26
3.16. Determination of COX-2 protein degradation half-life	26
4. Results	27
4.1. <i>N</i> -Arachidonoyl-dopamine induces the expression of COX-2 on brain endothelial cells	28
4.2. <i>N</i> -Arachidonoyl-dopamine stabilizes COX-2 mRNA in brain endothelial cells	29
4.3. <i>N</i> -Arachidonoyl-dopamine stabilizes COX-2 mRNA through a p38 MAPK pathway	30
4.4. <i>N</i> -Arachidonoyl-dopamine up-regulates HIF-1 α	31

4.5.	DYRK2 phosphorylates SIAH2 <i>in vivo</i> and <i>in vitro</i>	32
4.6.	DYRK2 phosphorylates SIAH2 in at least five residues	34
4.7.	SIAH2 colocalizes and interacts with DYRK2	38
4.8.	SIAH2 mediates DYRK2 ubiquitination	39
4.9.	SIAH2 controls DYRK2 expression in response to hypoxia	42
4.10.	Phosphorylation of SIAH2 by DYRK2 affects its localization and ability to degrade PHD3	47
5.	Discussion	52
6.	Conclusions	58
7.	References	60
8.	Oral presentation and publications	74

Introduction

1. The endocannabinoid system

The past decade has seen a sudden spurt of interest in the endocannabinoid system (ECs). This system regulates a plethora of biological effects and is composed of cannabinoid and vanilloid receptors, endogenous signaling molecules (called endocannabinoids) and metabolism-related enzymes (De Petrocellis et al, 2000; Di et al, 2000). Endocannabinoids are a class of lipid mediators found in several tissues and based on a polyunsaturated fatty acid amide or ester motifs (Di Marzo et al, 2002). Anandamide (AEA) and 2-arachidonoylglycerol (2-AG) are the most characterized endocannabinoids acting in the brain and in peripheral tissues mainly through the activation CB₁ and CB₂ cannabinoid receptors, respectively. AEA can also interact with the vanilloid receptor type 1 TRPV1 (Smart et al, 2000; Zygmunt et al, 1999). This non-selective cation channel is activated by vanilloids, such as capsaicin, and also by endogenous ligands *N*-acyl-dopamines (neurolipins), such as *N*-arachidonoyl-dopamine (NADA) and *N*-oleoyl-dopamine (OLDA) (Caterina et al, 1997; Chu et al, 2003; Huang et al, 2002).

2. *N*-arachidonoyl-dopamine, NADA

While NADA binds TRPV1 (Huang et al, 2002; Toth et al, 2003), and CB₁ receptor and induces several biological activities such as hyperalgesia (Chu et al, 2003), smooth muscle contraction in the guinea pig bronchi and bladder (Harrison et al, 2003), vasorelaxation in blood vessels (O'Sullivan et al, 2004), and also has immunomodulatory, neuroprotective and antiinflammatory properties (Bobrov et al, 2008; Navarrete et al, 2009; Sancho et al, 2004). Their saturated analogs *N*-palmitoyl-dopamine (PALDA) and *N*-stearoyl-dopamine (STEARDA) were also identified as endogenous substances not activating TRPV1, although they significantly enhanced the TRPV1-mediated effects of NADA (Chu et al, 2003).

Endocannabinoids may play a major role in the central nervous system (CNS), immune control and neuroprotection by regulating the cellular network of communication between the nervous and immune system during neuroinflammation and neuronal damage (Achiron et al, 2000; Malfitano et al, 2006; Pryce et al, 2003). In addition, *N*-acyl-dopamines influence the lipoxygenase pathway of arachidonic acid cascade as substrates or inhibitors and may also be involved in the regulation of inflammation (Bezuglov et al, 1997; Tseng et al, 1992).

3. The Cyclooxygenase catalysis

Cyclooxygenases catalyse the first step in the synthesis of prostanoids, a large family of arachidonic acid metabolites, including prostaglandins (PGs), prostacyclins and thromboxanes. The inducible isoform COX-2 is involved in the mediation of inflammation, immunomodulation, blood flow, apoptosis and fever (Cao et al, 2001; Dubois et al, 1998). COX-2 is rapidly expressed on several cell types in response to growth factors, proinflammatory molecules and cytokines (Caughey et al, 2001; Moolwaney & Igwe, 2005). Proinflammatory cytokines such as IL-1 β and TNF- α increase the expression of COX-2 in brain microvessel endothelial cells and this has been related to increases in permeability of the cerebral microvasculature (Cao et al, 2001; Mark et al, 2001). The production of several PGs, secondary to induction of COX-2, by the cells lining the blood–brain barrier (BBB), which may diffuse to the brain parenchyma, may have important consequences in brain inflammatory processes by modulating blood flow and also the intracerebral immune responses.

We were interested in studying the effect of NADA on key MAP kinases on genome stability (i.e. p38 MAPK) as well as on other regulators of inflammatory processes and tumorigenesis (i.e. COX-2, SIAH2). In this dissertation we have also studied very in detail how SIAH2 phosphorylation by DYRK2 (another important kinase in genome stability) influences tumorigenesis and the outcomes of DYRK2 degradation by SIAH2 on cell apoptosis pathways.

4. Genomic instability in cancer

To maintain genome integrity and fidelity, cells present complex signaling networks that are activated when genomic material is damaged as a consequence of exposition to oncogenic stress. The failure or loss of functionality of some of these control systems largely threatens the viability of the organism, thereby causing cytotoxicity, blocks in the correct DNA transcription and replication and, eventually, mutagenesis.

Genetic instability can be defined as a number of events capable of causing a wide number of unscheduled alterations that can be easily classified as single nucleotide mutations and chromosomal instabilities (Charames & Bapat, 2003). Along the same line, genomic instability is also due to chromosomal double-strand DNA

breaks (DSBs) that occur after exposure to ionizing radiation, after the collapse of replication forks when replication blocks at DNA intra-strand cross-links brought about by UV light or after chemotherapeutic agents (Hoeijmakers, 2001).

The DNA damage response network involves a number of pathways such as the PI3-kinase/AKT, I κ K/NF κ B and various MAP Kinases (MAPKs)(Huang et al, 2003; Kyriakis & Avruch, 2001; Saleem et al, 1995). These pathways start as response to number of events occurs at the DSB region in the DNA. First of all, a mediator complex consisting of Mre11, Rad50 and Nbs1 (MRN) is recruited and phosphorylation of a variant H2A histone (H2AX) takes place (Fernandez-Capetillo et al, 2004). This serves to intensify the signal and recruit new molecules to the DSB lesion, where finally the ATM (ataxia-telangiectasia) and ATR (ATM- and Rad3- Related) signaling pathways come into play (Falck et al, 2005).

ATM and ATR signaling pathways orchestrate downstream effectors by targeting them with phosphate residues (Figure 1). Once active ATM phosphorylates p53 on serine 15 and CHK2 on threonine 68 that likewise phosphorylates p53, but on serine 20 instead (Khosravi et al, 1999). Once p53 is phosphorylated on those two residues it escapes from Mdm2-dependent proteasomal degradation and act as an active transcription factor. ATM directly interferes with p53-Mdm2 interaction by phosphorylating Mdm2 on serine 395 (Maya et al, 2001).

Besides ruling p53-CHK2-Mdm2 axis, ATM regulates many other important substrates. It phosphorylates the tumor-suppressor protein BRCA1 on serines 1387 and 1423 following DNA damage (Cortez et al, 1999; Gatei et al, 2001). It also inhibits CtIP which is an inhibitor of BRCA1. In this regard, CHK2, previously activated by ATM, likewise phosphorylates and activates BRCA1. Other important ATM targets in the DSB response are NBS1, SIAH-1 and DYRK2 (Lim et al, 2000; Taira et al; Winter et al, 2008). Furthermore, CHK1 is activated by ATR on serines 315 and 345 by means of the mediator protein claspin (Kumagai et al, 2004; Zhao & Piwnica-Worms, 2001). Both CHKs proteins converge to inactivate members of the Cdc25 family of dual-specificity phosphatases, responsible for ruling cell cycle divisions (Donzelli & Draetta, 2003). However, while the ATM/Chk2 pathway is primarily involved in DNA double-strand breaks, the ATR-Chk1 pathway is mainly required for replication-associated DNA lesions (Bartek & Lukas, 2003; Pommier et al, 2006).

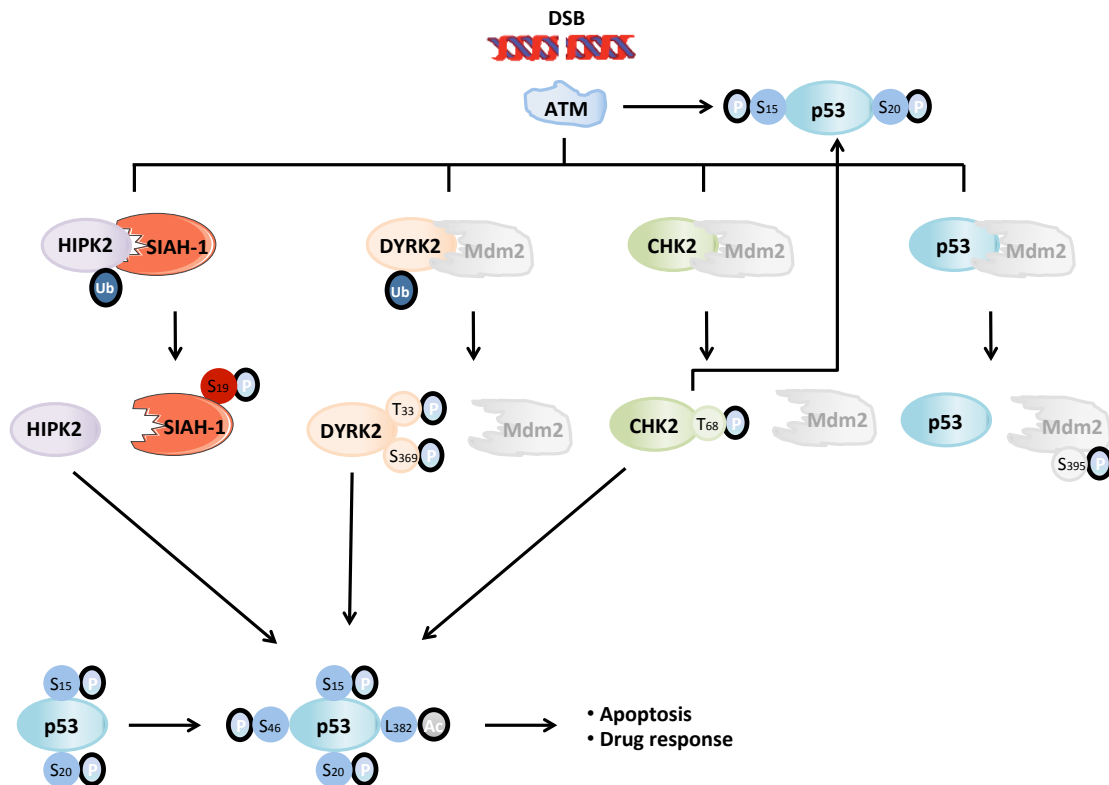


Figure 1. Important signaling pathways involved in cell cycle regulation

As well as the regulations mentioned straightforwardly above that end up activating cell-cycle checkpoints, further modifications of p53 enhance such responses driving the cell to apoptosis (Oda et al, 2000). In this respect, it has been reported since 2002 that ATM, DNA-PK, PKC δ , DYRK2 and HIPK2 phosphorylate p53 on serine 46 (D'Orazi et al, 2002; Komiyama et al, 2004; Saito et al, 2002; Taira et al, 2007; Yoshida et al, 2006). HIPK2-dependent p53 regulation has been extensively and thoroughly reported ever since, and not so much about the DYRK2-p53 axis which first came to light in 2007. As regards HIPK2 regulation over p53 it is worth pointing out a number of findings. Once HIPK2 phosphorylates p53 at Ser 46, it stimulates CBP-mediated p53 acetylation at Lys 382 (D'Orazi et al, 2002; Hofmann et al, 2002; Puca et al, 2009).

Among HIPK2 upstream control proteins we should have a close look at the role of both SIAH-1 and SIAH-2. Under DSB lesions, ATM phosphorylates SIAH-1 on serine 19 which disrupts its binding with HIPK2, whereupon it locates to the nucleus and targets p53 for phosphorylation on serine 46 (Figure 1). In addition, ATM hinders MDM2 levels making HIPK2 unavailable for degradation. Under hypoxia events WSB-

1, SIAH-1L, SIAH1 and SIAH2 downregulate HIPK2 levels, and thus inactivate the p53 apoptotic response. Under these circumstances, HIF-1 α levels increase high enough to restrain HIPK2 accumulation. Likewise HIPK2 rescue from MDM2-dependent degradation by ATM, DYRK2 interaction with MDM2 is inhibited once the kinase is phosphorylated by ATM. Once this happens, DYRK2 phosphorylates p53 on serine 46 and the apoptotic response finally takes place (Figure 2).

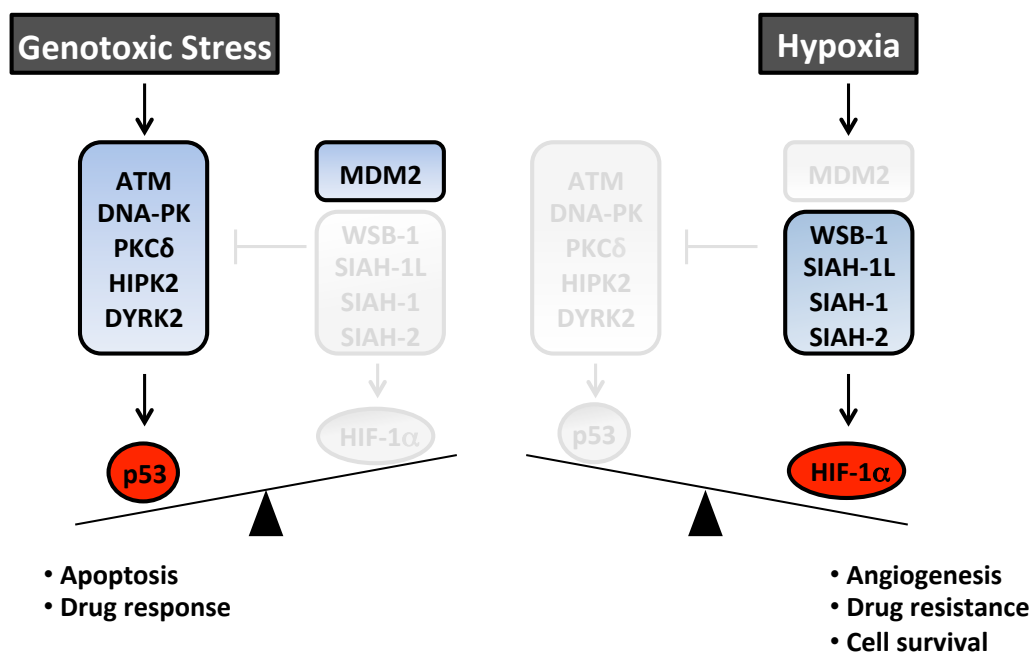


Figure 2. Balance outcome when either DNA damage or hypoxia takes place.

5. Protein kinase signaling networks in cancer

Protein kinases are enzymes able that phosphorylate precise tyrosine, serine or threonine residues on other kinases or other substrates so as to spread signals from extra- and intracellular stimuli. They rule many signaling pathways to control important physiological processes such as cell survival, proliferation and cell growth. Both the vast number of kinases, 539, encoded by the genome and the abundance of phosphorylation sites reported so far explain how mutations or abnormal protein expression may lead to many diseases such as rheumatoid arthritis, cardiovascular and neurological disorders, asthma, psoriasis and cancer. While some mutations enhance the protein catalytic activity of the proteins (such as PI3KCA), other mutations reduce their activity (c-FES and MAP2K4). More than 400 diseases have been related

so far to an impairment of kinases roles (Brognard & Hunter; Melnikova & Golden, 2004). So much so, that a number of signaling pathways controlled by kinases have been reported to be tied up with transformations processes: the cytoplasmic (Ras-Raf-MEK-ERK)-, the Wnt/ β -catenin-, Hedgehog-, the JAK/STAT-, PI3K/PKB- and the Notch pathway (Rennefahrt et al, 2005).

As the literature reports, kinase activity can be controlled by different mechanisms: blocking ATP binding so as to inhibit the catalytic activity, hampering protein interactions, knocking down by antisense or RNA interference approaches genes encoding kinases (Melnikova & Golden, 2004), etc. Thus, further knowledge of kinases control mechanisms urges to be brought to light. In this respect we have come upon a compelling and far-reaching regulation of a kinase reported to drive the cell to apoptosis under genotoxic stress.

6. DYRK

Dual-specificity tyrosine-regulated kinases (DYRKs) belong to the CMGC group, which also includes cyclin-dependent kinases (CDKs), mitogen-activated protein kinases (MAPKs), glycogen synthase kinase-3 (GSK3), CDK-like kinases, serine/arginine-rich protein kinases, cdc2-like kinases, and RCK kinases. The DYRK family is divided in turn into three subfamilies: DYRK kinases, homeodomain-interacting protein kinases (HIPKs), and pre-mRNA processing protein 4 kinases (PRP4s). Two members of the family have been reported in *Caenorhabditis elegans* (MBK-1 and MBK-2), whereas 3 members exist in *Drosophila melanogaster* (minibrain, dDyrk2, and dDyrk3). As respect to mammals, DYRKs comprise DYRK1A, DYRK1B (or MIRK), DYRK2, DYRK3 (or REDK), and DYRK4 (Figure 3)(Aranda et al; Becker et al, 1998).

DYRKs autophosphorylate on tyrosine residues so as to become active and phosphorylate on serine/threonine residues on exogenous substrates (Becker & Joost, 1999; Campbell & Proud, 2002; Himpel et al, 2001; Li et al, 2002a; Lochhead et al, 2003). Likewise the TXY motif that MAPKs (mitogen-activated protein kinases) have to phosphorylate their substrates, DYRKs have an YXY sequence in the activation loop of their catalytic domain (Kentrup et al, 1996). This fact suggests that DYRKs proteins could be involved in very similar pathways as the MAPKs are (Miyata & Nishida, 1999). The five members in mammals share a kinase domain as well as a sequence just upstream of the kinase domain named the DYRK homology (DH)-box which is

characteristic of the subfamily in question. Besides, the paralogous pair DYRK1A-DYRK1B shares a NLS (nuclear localization Signal) and a PEST (motif rich in proline, glutamic acid, serine, and threonine residues) domain. The other three members have a NAPA (N-terminal autophosphorylation accessory region) domain that provides a chaperone-like function for the intermediate form with tyrosine autophosphorylation activity.

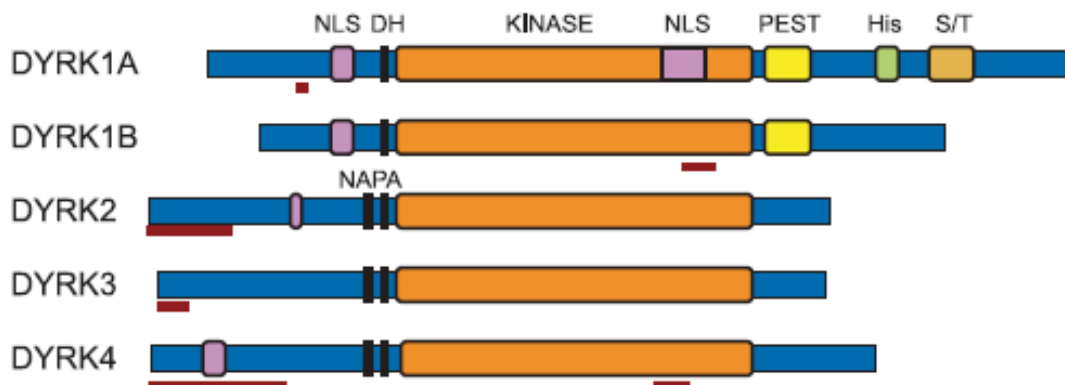


Figure 3. The 5 mammalian DYRKs structure. Yellow squares represent polyhistidine stretch. Brown squares represent regions enriched in Ser and Thr residues.

DYRK1A is the founding member of this family, is the best well known among the rest isotypes and maps to the DSCR (Down Syndrome Critical Region) of chromosome 21 (Guimera et al, 1996; Shindoh et al, 1996; Song et al, 1996). Besides being involved in neurological disorders such as Down syndrome, it is also implicated in calcium signaling by phosphorylating NFAT (Gwack et al, 2006) and cell polarity maintenance in *Schizosaccharomyces pombe* (Tatebe et al, 2005). Furthermore it is embroiled in various biochemical pathways as it is able to phosphorylate many other substrates such as: STAT3 (Matsuo et al, 2001), eIF2B and Tau (Woods et al, 2001) (Aranda et al). As concerns DYRK1B, it mediates cell survival and differentiation and is highly expressed in muscle tissues (Lee et al, 2000; Mercer et al, 2005; Mercer & Friedman, 2006). It has been reported to phosphorylate among other substrates: p21^{Cip1} (Zhou et al, 2001) and class II HDACs (Deng et al, 2005) (Aranda et al).

As it is reported further on in this dissertation, DYRK2 is the isoform we report as a new protein of interest in the response to hypoxia and genotoxic stress. DYRK2 is involved in regulating key developmental and cellular processes such as neurogenesis,

cell proliferation, cytokinesis, and cellular differentiation. A wide number of substrates have been reported to be phosphorylated by DYRK2. Some of these are: Katanin p60 (Maddika & Chen, 2009), NFAT (Gwack et al, 2006), p53 (Taira et al, 2007), Stat3 (Matsuo et al, 2001), Tau (Woods et al, 2001), and very recently c-Jun and c-Myc (Taira et al) (Aranda et al). A number of publications relate DYRK2 to an adequate prognosis (Yamashita et al, 2009) (Taira et al) and also as responsible for the regulation of tumour progression via c-Jun and c-Myc.

As it was mentioned above, in 2007 a finding of great importance shed light a major role of DYRK2 as concern the regulation of cell physiology upon DNA damage (Taira et al, 2007). Since then many publications have brought into light the importance of getting to know the regulation of DYRK2 in a comprehensive, accurate and exhaustive way. In this dissertation we would like to put forward a new molecular mechanism whereby DYRK2 is ruled under hypoxia events by the ubiquitin ligase SIAH2. Under these circumstances we have seen how p53 regulation is altered both at a protein and at a transcriptional level. Nevertheless, we describe SIAH2 as a new and direct substrate of DYRK2 whose activity is enhanced over some substrates (i.e. PHD3) by a DYRK2-phosphorylation dependent manner.

DYRK3 is highly produced in hematopoietic cells and testis. It reduces apoptosis in response to cytokine starvation in hematopoietic cells (Geiger et al, 2001) and has been reported to phosphorylate SIRT1 (Guo et al), myelin basic protein and histones H2b and H3 (Lord et al, 2000). DYRK4 is the least known isoform of all the DYRK family members. It is exclusively expressed in the testis and helps the process of spermiogenesis (Sacher et al, 2007). As regards DYRK subcellular localization, DYRK1A and DYRK1B contain a NLS domain that confers them nuclear localization. Concerning DYRK2, it has been reported a cytoplasmic localization under normal conditions (Becker et al, 1998; Leder et al, 1999) that following genotoxic stress moves into the nucleus (Taira et al, 2007). This nuclear accumulation depends on an NLS in the N terminus of the protein and on an Mdm2-dependent increase in protein stability (Taira et al). Despite the absence of NLS domain on DYRK3, it shows nuclear localization (Lord et al, 2000). Finally, as regards DYRK4 localization it has not been clarified so far.

7. SIAH (seven in absentia homolog)

The SIAH (seven in absentia homolog) protein family belongs to the RING finger E3 ubiquitin ligases family, which are involved in ubiquitination and proteasome-mediated degradation of specific substrates (Lorick et al, 1999; Schnell & Hicke, 2003; Tang et al, 1997). The first member of this highly homologue family was initially identified in *Drosophila melanogaster* as seven in absentia (*sina*), a protein needed for photoreceptor R7 formation (Carthew et al, 1994; Li et al, 1997). Other three genes were later identified in mice (*Siah1a*, *Siah1b* and *Siah2*)(Della et al, 1993; Holloway et al, 1997). The human SIAH family consists of two proteins (*SIAH1* and *SIAH2*) from different genes, which perform different but in some cases, redundant functions (Hu et al, 1997a).

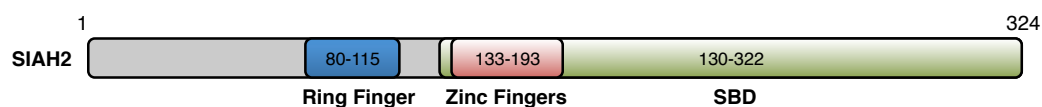


Figure 4. SIAH2 full sequence showing the three basic domains: RING, Zinc Fingers and SBD.

Human SIAH2 is a 324 amino acid dimeric protein presenting a RING (Real Interesting New Gen) catalytic domain in its N-terminal that recruits E2 ubiquitin-conjugating enzymes, two zinc-finger motifs and a substrate-binding domain (SDB) in its C-terminal (House et al, 2006; Polekhina et al, 2002)(Figure 4). SIAH2 may exert its activity as ubiquitin ligase E3 either through its binding to adapting proteins such as phyllopod (PHYL) and Siah-interacting protein (SIP)(Li et al, 2002b; Matsuzawa & Reed, 2001) or through direct interaction to the substrate protein (Calzado et al, 2009b; Roysarkar et al). A wide number of SIAH2 substrates implied in the regulation of important signalling pathways have been described (Nakayama et al, 2009). These are: PML (Promyelocytic leukemia protein)(Fanelli et al, 2004), PHD (prolyl hydroxylases)(Nakayama et al, 2004), Sprouty (Nadeau et al, 2007), TRAF2 (receptor-associated factor 2)(Habelhah et al, 2002), DCC (Hu et al, 1997b), β -catenin (Topol et al, 2003), N-CoR (Zhang et al, 1998), HIPK2 (Calzado et al, 2009b), PPAR γ (Kilroy et al), OGDHC-E2 (2-oxoglutarate dehydrogenase complex)(Habelhah et al, 2004), TIN2 (Bhanot & Smith), HDAC3 (Zhao et al), AKAP121 (Carlucci et al, 2008) and α -synuclein (Liani et al, 2004). *Siah2* knock-out mice show faint phenotypes, such as fewer

amounts of hematopoietic progenitor cells. In contrast, Siah1a and Siah2 double knock-out mice are embryonic lethal, denoting an key purpose in embryogenesis and putting forward that the two Siah homologs have both overlapping and distinct rolls *in vivo* (Frew et al, 2003).

As it was said above, SIAH2 degrades specific substrates by means of its ubiquitin ligase activity. Ubiquitination consists of attaching minor proteins to the target protein of interest driving it to either attenuating its function or putting them on a spurt. That appurtenance is called ubiquitin. This protein, lacking in archaeal or eubacterial, attaches covalently to those proteins that are going to get rid of by proteolysis. Also, non degrading reasons have been ascribed to ubiquitins (Hochstrasser, 2000). The process of ubiquitination consists of three consecutive steps that involves three different enzymes (Figure 5). The first step comprise the activation of ubiquitin using ATP by the use of E1 activating enzyme, the second steps involves a second protein, called E2 conjugating enzyme that, by means of a thioester bond, transfers the activated ubiquitin from E1 to E3, which is the last enzyme used in this process. The E3 ligase enzyme ties the activated ubiquitin to the ϵ -amino group of a lysine residue in a specific substrate (Hershko & Ciechanover, 1998).

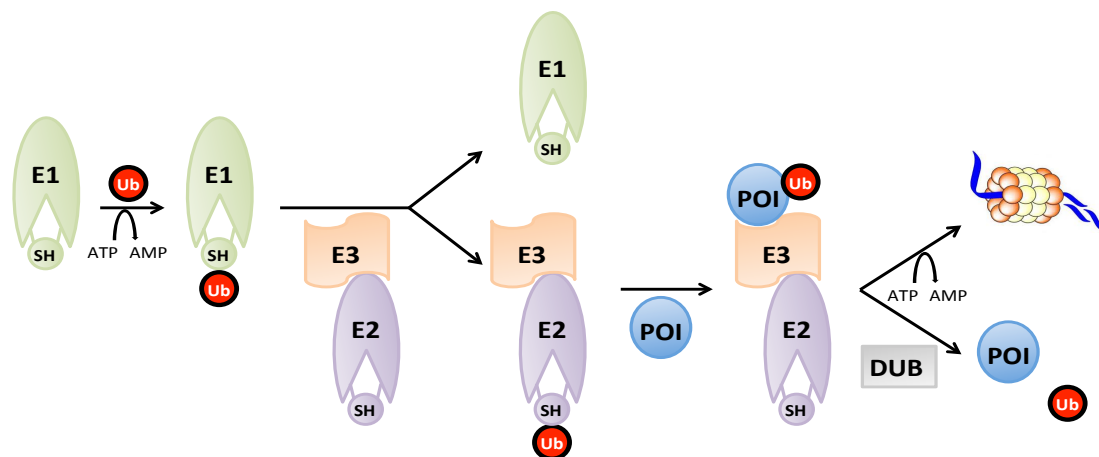


Figure 5. Ubiquitin conjugation scheme that depicts a straightforward representation of how ubiquitin enzymes work.

Whereas not many E1 activating enzymes have been described, more than 20 different E2 conjugating enzymes have been reported in humans. In contrast, among 500 to 1000 different E3 ligase enzymes are present in humans (Hicke et al, 2005). E3 enzymes are classified in two leading groups: RING (really interesting new gene) and

HECT (homologous to the E6-AP carboxy terminus) domain-containing E3s. The main difference among them is that while RING ligases directly transfer ubiquitin from E2 to the target protein, HECT ligases bind ubiquitin to one of their Cys aminoacid right before transferring it to the target protein (de Bie & Ciechanover). Once the ubiquitin is bound to the protein of interest, the latter can either be driven to degradation through the 26S proteasome (the ubiquitin proteins will be recycled), or de-ubiquitinated by DUBs (de-ubiquitylating enzymes) enzymes, which only a few types are known at present.

Some studies seem to suggest that labeling proteins by means of ubiquitination is not only a direction for degradation but also a target to enroll the cell in many other processes such as cell cycle, DNA repair, endocytosis, antigen processing and apoptosis (Di Fiore et al, 2003; Haglund & Dikic, 2005). In addition to that, it has been shown that besides ubiquitin there are other kinds of similar modifications known as ubiquitin-like proteins (Ubl) (figure 6) which include: sumoylation (small ubiquitin-related modifier; SUMO) (S), fatylation (FAT10) (F), neddylation (NEDD8) (N) and ISGylation (interferon-stimulated gene 15; ISG15) (figure 6, i), in a functionally distinct manner (Hoeller et al, 2006).

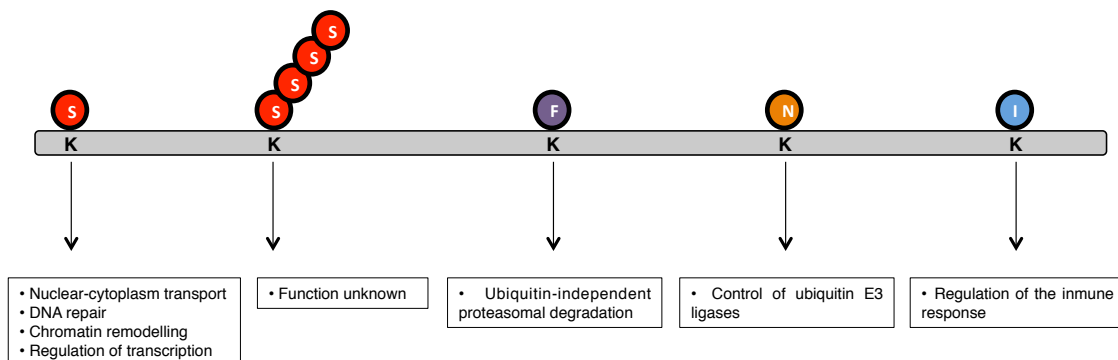


Figure 6. Summary of the most important ubiquitin-like proteins (Ubl). The arrows point to the outcomes each Ubl has in the cell.

It is not surprising to think that this important cell signalling regulation must be ruled very tightly. SIAH2 expression is controlled either at the mRNA level or at the protein level by restriction via self-ubiquitination, while its activity can be regulated through the association with different binding proteins (Depaux et al, 2006; Matsuzawa & Reed, 2001; Nakayama et al, 2004). Nevertheless, it is surprising how little is known

as regards how post-translational modifications are able to alter SIAH2 activity. Murine Siah2 is phosphorylated by p38 MAPK, which in turn increases its ability to degrade PHD3 (Khurana et al, 2006), while previous work from us showed that phosphorylation of human SIAH2 by the serine/threonine kinase HIPK2 (homeodomain-interacting protein kinase) occurs at three residues, affecting its activity through the modification of substrate interaction (Calzado et al, 2009a). This work also revealed the strong phosphorylation of SIAH2 at many residues, raising the possibility that several kinases mediate SIAH2 phosphorylation. The phosphorylation of SIAH2 weakens its interaction with HIPK2, a kinase that belongs to the CMGC (containing CDK, MAPK, GSK, CLK families) group of protein kinases. The CMGC group, also comprises the dual-specificity tyrosine phosphorylation regulated (DYRK) kinases which includes DYRK1a, DYRK1b and DYRK2 (Becker et al, 1998).

8. SIAH2 and Hypoxia

Oxygen tension in the body is crucial for the maintenance of body balance upon different physiological conditions. For instance, O₂ regulation is critical on stroke, cancer, hypertension, sleep apnoea, heart failure and sudden infant death syndrome. The reason why hypoxia occurs is mainly due to three different motives: lack of O₂ transport, low partial pressure and inability of tissues to accept O₂. According to the oxygen level in the tissue in question hypoxia can be divided into four major types: a) Hypoxic hypoxia, due to pulmonary diseases or low oxygen abundance in the atmosphere, typically present at high altitudes; b) Anaemic hypoxia, due to a lack of haemoglobin which is normally caused by a loss of blood, reduced red cell production, genetic defect of haemoglobin or carbon monoxide poisoning; c) Ischemic or Stagnant hypoxia, which results as low flow of blood due to vasospasms, atherosclerosis or heart failure and d) Histotoxic hypoxia, which prevents the tissue to accept coming oxygen due to poisoning of oxidative enzymes. In order to face these abnormal situations, the organism undergoes a wide number of changes. At a cellular level for instance, the oxygen-sensitive ion channels (K⁺ and Ca²⁺ channels) are inhibited (Peers, 1997) and, on the other hand, HIF-1 action comes into play.

As it is reported in the literature, SIAH2 has been described as a key protein in cancer, hypoxia and inflammation processes (House et al, 2006; House et al, 2009; Kim et al; Nakayama et al, 2004; Qi et al). As regards the role of SIAH2 in hypoxia, it is

worth pointing out its ability to alter the expression of hypoxia-inducible transcription factor 1 alpha (HIF-1 α) (Nakayama et al, 2009) (Appelhoff et al, 2004) (Nakayama et al, 2004) by down-regulating PHDs 1 and 3 enzymes. Furthermore, it has been reported very recently that under hypoxia events the intracellular domain of p75 Neurotrophin Receptor increases SIAH2 stabilization by decreasing its auto-ubiquitination, and therefore a rise in HIF-1 α levels occurs (Le Moan et al). In contrast, under normal conditions of O₂, SIAH2 basal levels are not enough to degrade PHDs which in turn hydroxylate HIF-1 α sparking off its proteasomal degradation (Ivan et al, 2001; Jaakkola et al, 2001).

HIF-1, whose levels vary the opposite way as O₂ concentration does (Ferguson et al, 2007), is a transcription factor that rule a wide number of genes involved in important cellular processes (Kaelin, 2005; Schofield & Ratcliffe, 2004; Semenza, 2003). It is a heterodimer made up of two Basic Helix-Loop-Helix (bHLH) proteins that belong to the PAS family of proteins. While HIF-1 β or aryl hydrocarbon nuclear translocator (91-94 kDa) subunit is constitutively expressed, the other component, HIF-1 α (120 kDa), is induced upon a lack of oxygen and very fast degraded by the proteasome. Besides HIF-1 α , HIF-2 α and HIF-3 α proteins have been described (Hirota & Semenza, 2005). As it is seen in figure 7, PHD hydroxylates HIF-1 α at Pro-402 and Pro-564 in normoxia and mild hypoxia conditions. Once this occurs pVHL (the von Hippel-Landau tumour suppressor gene product) recognizes hydroxylated HIF-1 α and forms a complex with elongin B, elongin C, RBX1 and Cullin 2 for further HIF-1 α ubiquitination and subsequent degradation by means of the proteasome. Acetylation of HIF-1 α at lysine-532 by the ARD1 acetyltransferase enhances the interaction of VHL with HIF-1 α . Under hypoxa events, SIAH2 limits PHD1 and PHD3 availability, thereby increasing HIF-1 α expression (Hon et al, 2002; Iwai et al, 1999; Jeong et al, 2002; Kibel et al, 1995; Nakayama et al, 2004; Pause et al, 1997).

HIF-1 regulation in the cell is not only achieved at a protein level, but also at a transcriptional level by means of FIH (factor inhibiting HIF-1 α) (Mahon et al, 2001), which is another hydroxylase factor that belongs to the Fe²⁺- and 2-oxoglutarate-dependent dioxygenase superfamily (Hirota & Semenza, 2005; Mahon et al, 2001). It hydroxylates HIF-1 α at Asparagine-803 residue, thereby preventing its phosphorylation prior to dimerize with HIF-1 β . This modification makes it unavailable to associate with p300/CREB for transcriptional activation of some genes (i.e. HIF-1 α for self regulation). The levels of FIH in mammalian cells are not O₂-dependent (Stolze et al, 2004) and its

regulation still remains to be elucidated. However, it has been reported in the literature that SIAH1 mediates FIH degradation under normoxic conditions (Fukuba et al, 2008). Also, it has been shown that ISWI is required for full expression of FIH mRNA and protein levels by changing RNA polymerase II loading to the FIH promoter (Melvin et al). In short, under hypoxic conditions prolyl- and asparaginyl-hydroxylases are inhibited, thereby preventing hydroxylation of HIF-1 α which will dimerize with HIF-1 β to activate HRE (hypoxia-response elements) in HIF target genes.

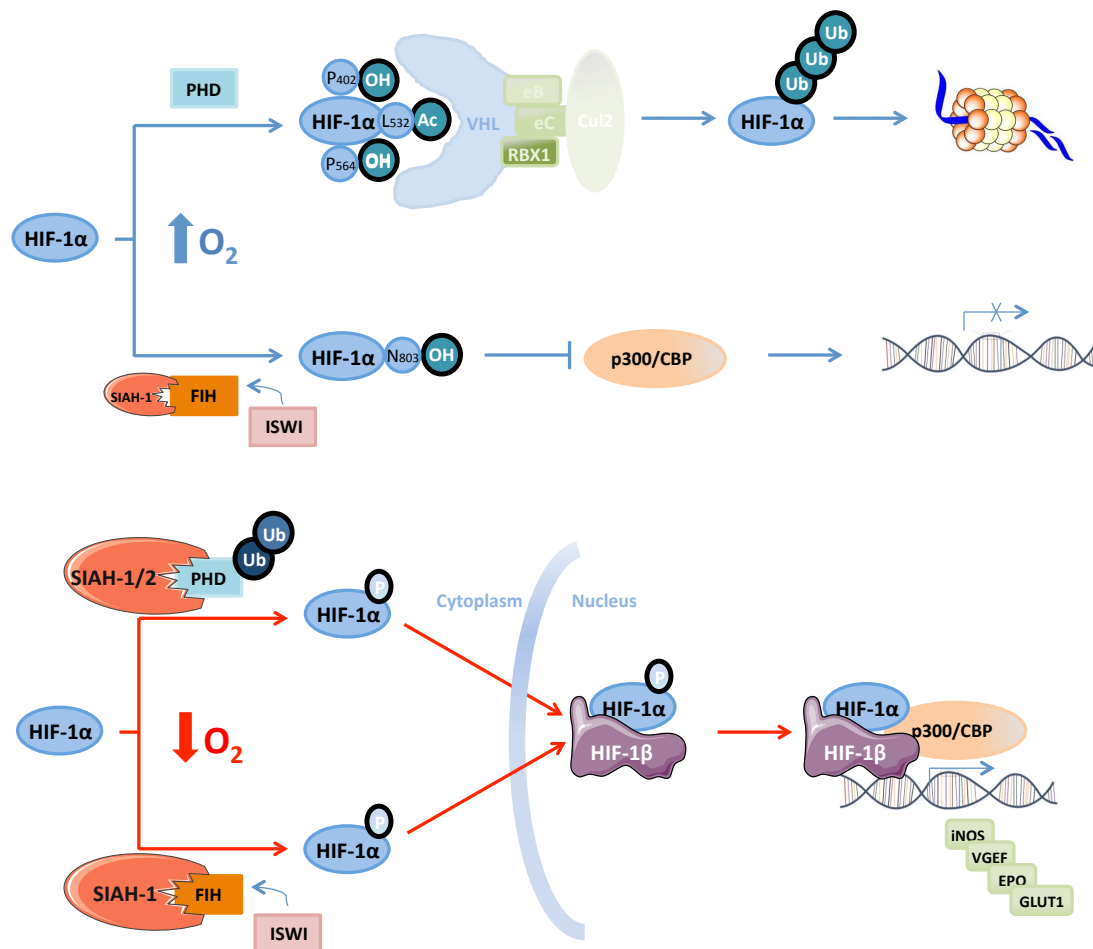


Figure 7. A straightforward model on how HIF regulation occurs.

Aims

Endocannabinoids may play a major role in the central nervous system (CNS), immune control and neuroprotection by regulating the cellular network of communication between the nervous and immune system during neuroinflammation and neuronal damage. In this sense, we define how NADA is able to regulate the activity of p38 and SIAH2 proteins, being the latter an important regulator of the hypoxic and cancer responses. This thesis drove us to the discovery of new kinases able to phosphorylate and regulate SIAH2 activity and to understand a new molecular mechanism by which hypoxic cancer cells could escape chemotherapeutic drug treatment.

The aims of this search project have been the followings:

- 1. Studying the effects of NADA on target proteins that mediate inflammation and tumorigenesis.**
- 2. Identifying new kinases able to phosphorylate SIAH2.**
- 3. Resolving one possible molecular mechanism whereby SIAH2 regulation alters angiogenesis.**

Material and Methods

1. Cell lines, transfections and reagents

U2OS (human osteosarcoma cell line), b.end5 (murine brain endothelial cell line), HeLa (cervical cancer cells), H1299 (human non-small cell lung carcinoma cell) and HEK 293T (human embryonic kidney cells) cells were maintained in DMEM supplemented with 10% FCS, 2 mM L-glutamine and 1% (v/v) penicillin/streptomycin at 37 °C in a humidified atmosphere containing 5% CO₂. HUVEC (Human Umbilical Vein Endothelial Cells) cells were maintained in Medium 199 supplemented with 20% FBS, 2 mM penicillin/streptomycin (10000 U y 10 mg/ml, respectively), 2 mM amphotericin B, 2 mM L-glutamine, 10 mM HEPES, 30 µg/ml ECGS and 100 µg/ml heparine. Transient transfections were performed with Rotifect (Roth) according to manufacturer instructions and harvested 48h after transfection. HUVEC cells were transfected using the nucleofector technology (Lonza). DNA amounts in each transfection were kept constant upon addition of empty expression vector.

Hypoxia was induced by cultivation of cells in a New Brunswick Innova-48 incubator at defined O₂ concentrations. MG-132 was purchased from Enzo biolabs. Doxorubicin, *N*-arachidonoyl-dopamine (NADA), cycloheximide (CHX), SB203580, Harmine and the rest of reagents were from Sigma Aldrich. Scramble control oligonucleotides siRNA (#D-001810-10-20) and the siGENOME SMARTpool (#M-006561-02) against SIAH-2 were purchased from Dharmacon (#M-006561-02). Oligonucleotides Stealth siRNA against DYRK2 (5'-AUACCUGUAAGCCACGUGAUCGUGG-3') were from Invitrogen. The effect of siRNA on protein expression was assessed 2 days after transfection.

2. Antibodies

Antibodies against FLAG epitope (clone M2), β-actin (AC-74) and α-tubulin were purchased from Sigma Aldrich. Anti-phospho-JNK 1+2 (9255S), anti-phospho p38 (Thr180/Tyr182, 9211), anti-p53 (sc-126), anti-p53 phospho Ser46 (2521) and anti-ubiquitin (P4D1) from Cell Signaling Technology. Antibodies against COX-2 (M-19), COX-1 (M-20), phospho-ERK 1+2 (sc-7383) and SIAH2 (sc-5507) were from Santa Cruz. Anti-DYRK2 (AP7534a) from Abgent, anti-HA (clone 3F10) and anti-myc (clone 9E10) from Roche Molecular Biochemicals, anti-phosphoserine (AB1603) from Millipore. Rabbit polyclonal antibodies recognizing phosphorylated threonine 26 and serines 28 and 68 of SIAH2 were raised by NeoMPS. Rabbit polyclonal antibodies

recognizing phosphorylated threonine 119 of SIAH2 were raised by Abyntek. Secondary horseradish peroxidase-coupled antibodies were purchased from Jackson ImmunoResearch Laboratories. The Alexa Fluor 647 goat anti-mouse IgG1 and Alexa Fluor 488 goat anti-rabbit IgG antibodies were purchased from Invitrogen.

3. Plasmids

Flag-SIAH-2 wild type sequence, Flag-SIAH-2-RM (Ring Mutant, H98A/C101A), HA-Ubiquitin and His-Ubiquitin were described previously (Calzado et al, 2009). Flag-DYRK1A and Flag-DYRK1B were reported formerly (Ritterhoff et al). Flag-DYRK2 and Flag-DYRK2-KD (Kinase Death, K251R) plasmids were detailed earlier (Gwack et al, 2006). HA-SIAH2 and HA-SIAH2-RM were generated by PCR following standard protocols. Myc-DYRK2 was cloned into pCMV-Tag3B-Myc by amplification by PCR using the following primers: Forward: 5' GGGGGAATTCATGAATGATCACCTGCATGT 3' y Reverse: 5' GGGGAAGCTTTCAGCTAACAAGTTTTGGCA 3'. The PCR program consisted of a first denaturing cycle (2 min at 94°C), followed by 35 cycles of three steps: denaturing (30 sec at 94°C), annealing (30 sec at 65°C) and elongation (1 min and 15 sec at 68°C), finally the DNA was further elongated in the last cycle (10 min at 72°C). As a result we obtained two new restriction enzyme cuts (EcoRI y HindIII) that were checked on an agarose gel. Finally, the sequence was confirmed by sequencing. The p53-Luc (containing multimers of p53-binding sites) and Bax-Luc reporter plasmids were previously described (Fogal et al, 2000; Hofmann et al, 2002). The plasmid COX-2-Luc was a gift from Dr. M. Iñiguez (UAM, Spain); this plasmid contains the COX-2 promoter followed by the luciferase gene. The COX-2 translational reporter COX-2-3'-UTR-luciferase contains the 3'-UTR of COX-2 sequence (763 bp) fused to the 3' end of the luciferase gene under control of the SV40 promoter and enhancer elements (Yeo et al, 2003). pcDNA3-Flag-PHD3 was a gift from Dr. Frank S. Lee (Pennsylvania School of Medicine), pGEX-2TK-DYRK2 was a gift from Dr W Becker (Aachen, Germany) and Epo-Luc was a gift from Dr. ML. Schmitz (Giessen, Germany). Human SIAH-2-WT, SIAH-2-ΔC (aminoacids 117-324) and SIAH-2-ΔN (aminoacids 1-116) were cloned in pGEX-2TK allowing prokaryotic expression of SIAH-2 as a GST fusion protein. The primers used were:

			SIAH-2-WT-Fwd:	5'
GCAGGAATTCATGAGCCGCCCGTCCTCCACCGGC	3',		SIAH-2-WT-Rev:	5'
CCCCCTCGAGTCATGGACAACATGTAGAAATAGTAAC	3',		SIAH-2-ΔC-Fwd:	5'
GCAGGAATTCATGAGCCGCCCGTCCTCCACCGGC	3',		SIAH-2-ΔC-Rev:	5'

GGGCCTCGAGTCAGCCCCTGCACGTCGGGCAG 3', SIAH-2-ΔN-Fwd: 5'
GATTGAATTCGCCCTGACGCCCAGCATCAG 3', SIAH-2-ΔN-Rev: 5'
CCCCCTCGAGTCATGGACAACATGTAGAAATAGTAAC 3'. The PCR program consisted of a first denaturing cycle (2 min at 95°C), followed by 40 cycles of three steps: denaturing (1 min at 95°C), annealing (1 min at 95°C) and elongation (1 min at 72°C), finally the DNA was further elongated in the last cycle (5 min at 72°C). The following SIAH-2 point mutants were previously described: T26A, S28A, S68A, TS2628AA, SS2868AA y TSS262868AAA, T113A, T119A, S121A y S279A (Ritterhoff et al). The following SIAH-2 point mutants: S16A, S16D, TS2628DD, S68D and T119D used to create the final SIAH-2-STSST16262868119AAAAA (SIAH-2-5A) y SIAH-2-STSST16262868119DDDDD (SIAH-2-5D) mutants, were prepared using the QuickChange site-directed Mutagenesis Kit (Stratagene, # 210518). The authenticity of the constructs was verified by DNA sequencing. The PCR program consisted of a first denaturing cycle (2 min at 95°C), followed by 18 cycles of three steps: denaturing (1 min at 95°C), annealing (1 min at 60°C) and elongation (8 min at 68°C), finally the DNA was further elongated in the last cycle (10 min at 68°C).

4. Western blotting

Soluble fractions were obtained after lysis of cells in NP-40 buffer (20 mM Tris-HCl pH 7.5, 150 mM NaCl, 1 mM phenylmethylsulfonylfluoride, 10 mM NaF, 0.5 mM sodium orthovanadate, leupeptine (10 µg/ml), aprotinin (10 µg/ml), 1% (v/v) NP-40, and 10% (v/v) glycerol). After centrifugation the supernatants were mixed with SDS sample buffer (50mM Tris-HCl pH6.8, 100mM DTT, 2% SDS, 0.1% bromophenol blue and 10% glycerol). Proteins were resolved on SDS-PAGE gels and blotted to polyvinylidene difluoride membranes using a semi-dry transfer. After blocking with non fat milk or BSA in TBST buffer, primary antibodies were added. Appropriate secondary antibodies coupled to horseradish peroxidase were detected by enhanced chemiluminescence system (USB).

5. Phosphatase treatment

Cells were lysed in NP-40 buffer without phosphatase inhibitors. Then samples were treated with γ -phosphatase following manufacturer's instructions (New England Biolabs). Reactions were stopped with SDS buffer and samples immunoblotted.

6. Immunoprecipitation

Cells were washed in PBS and collected by centrifugation. The cell pellet was lysed in IP buffer [50 mM Hepes pH 7.5, 50 mM NaCl, 1% (v/v) Triton X-100, 2 mM EDTA, 10 mM sodium fluoride, 0.5 mM sodium orthovanadate, 10 µg/ml leupeptine, 10 µg/ml aprotinin, 10 µg/ml aprotinin, 10 µg/ml leupeptin and 1 mM PMSF]. Cell lysates were incubated with 1 µg of the indicated antibodies for 6 h at 4 °C. Antibodies were then isolated with 25 µl of protein A/G Sepharose (Santa Cruz). Immunoprecipitated proteins were then washed five times in IP buffer and eluted in 1.5X SDS sample buffer. Samples were immunoblotted as described before.

7. Luciferase reporter assays

Cells were collected in PBS and lysed in NP-40 buffer or Triton buffer (25 mM Tris-phosphate pH 7.8, 8 mM MgCl₂, 1 mM DTT, 1% Triton X-100, and 7% glycerol). Luciferase assay was performed using Luciferase Assay Reagent (Promega) according to the manufacturer's instructions and measured in a luminometer Autolumat LB9510 (Berthold). Luciferase activity in different samples was normalized with protein concentration.

8. Enrichment of His-Tagged Proteins

Cells were collected in PBS and pellets were dissolved in lysis buffer (50 mM Tris-HCl buffer pH 8.0 containing 8M urea, 50 mM Na₂HPO₄, 300mM NaCl, 0.5 % (v/v) NP-40, 10 mM imidazole and 1 mM β-mercaptoethanol). Samples were sonified and cell debris were removed by centrifugation. His-ubiquitin tagged proteins were isolated with 40 µl of equilibrated Ni-NTA resin (Qiagen) for 4h at room temperature. After centrifugation precipitates were washed once with lysis buffer, once with wash buffer 1 (10 mM Tris HCl, pH 8.0 containing 8M Urea, Na₂HPO₄ 100 mM, 10 mM imidazole and 1 mM β-Mercaptoethanol) and twice with Wash buffer 2 (the same composition of wash buffer 1 but at pH 6.3). Proteins were eluted in SDS sample buffer containing 200 mM imidazole and analyzed by immunoblotting.

9. Immunofluorescence

Cells were grown on coverslips and 48h after transfection fixed with 3,7% of pre-warmed paraformaldehyde/PBS for 10 minutes. Cells were then permeabilized with 0,1% Triton X-100/PBS for 15 min, blocked with 3% BSA/PBS and incubated overnight with primary antibodies. After being washed with PBS and incubated for 45

min with the secondary antibody they were mounted on glass slides with mounting medium with DAPI (Vectashield). Fluorescence images were captured using confocal laser scanning microscope LSM 5 EXCITER (Carl Zeiss MicroImaging GmbH) using a 40X/1.30 oil objective (EC Plan-Neofluar) and ZEN 2008 software (Carl Zeiss MicroImaging GmbH). Images were analysed using the ImageJ v 1.45 software (<http://rsbweb.nih.gov/ij/>). The Costes' approach was employed for co-localization analysis between green (Alexa 488) and red (Alexa 647) images to determinate the Pearson's correlation coefficient (R). SIAH2 wild type and phospho mutant versions were visualized on a BD Pathway 855 Bioimager in a non-confocal mode.

10. GST pulldown assay

Recombinant GST-SIAH2 proteins (Wt, ΔC and ΔN) were produced in *Escherichia coli* BL21 cells and purified with Glutathione-Sepharose 4B (GE Healthcare) according to standard protocols. HEK 293T cells expressing Flag-DYRK2 were lysed in IP buffer. Then 400 μg of protein from each lysate were incubated at 4 °C overnight with soluble fusion proteins (10 μg) and 30 μl of glutathione-sepharose beads. Sepharose beads were then washed with IP buffer and resuspended in SDS sample buffer for further immunoblot analysis

11. *In vitro* phosphorylation analysis

GST-SIAH2 fusion protein (8 μg) was incubated with 0.5 μg of commercial recombinant DYRK2 protein (Abnova) in kinase buffer assay (20 mM Hepes, pH 7.5, 10 mM MgCl_2 , 1 mM DTT and 0.1 mM ATP). After 60 min of incubation at 30 °C reactions were stopped adding SDS sample buffer. Samples were then immunoblotted with anti-phosphoserine antibody.

12. Mass spectrometry

SIAH2 protein was immunoprecipitated with anti-Flag M2 affinity gel (Sigma Aldrich) from HEK-293T cells transfected with SIAH2-Flag plasmid alone or combined with DYRK2-Myc. Cells were treated with 10 μM 12 h before lysis. After collection pellets were lysed in IP buffer. The precipitated proteins were eluted by boiling in 1.5X SDS sample buffer for 5 min and resolved in SDS-PAGE gels. SIAH2 bands were excised from gels and destained in acetonitrile:water (ACN:H₂O, 1:1). Gel bands were digested with trypsin (Promega, Madison, WI) as previously described (Shevchenko et

al, 1996). Disulfide bonds from cysteinyl residues were reduced with 10 mM dithiothreitol (DTT) for 1 h at 57 °C, and then thiol groups were alkylated with 55 mM iodoacetamide for 1 h at room temperature in darkness, and washed once in ACN:H₂O (1:1) in order to remove excess iodoacetamide. The gel pieces were shrunk by removing all liquid using sufficient ACN. Acetonitrile was pipetted out prior to desiccation via speedvac. The dried gel pieces were re-swollen in 50 mM ammonium bicarbonate with trypsin (12.5 ng/μl). The tubes were kept in ice for 2 h. The digestion buffer was removed and gels were covered again with 50 mM ammonium bicarbonate and incubated at 37°C for 12 h. Digestion was stopped by the addition of 1% TFA, trifluoroacetic acid. Whole supernatants were dried down and then desalted until the mass spectrometric analysis. After digestion, TFA was added to a final concentration of 0.1% and samples were desalted on ZipTip C18 tips (Millipore) using as elution solution 50% ACN in 0.1% TFA.

The desalted protein digest was dried, resuspended in 7 μl of 0.1% formic acid and analyzed by RP-LC-MS/MS in an Agilent 1100 system coupled to a linear ion trap LTQ-Velos mass spectrometer (Thermo Fisher Scientific, Waltham, MA, USA). The peptides were separated by reverse phase chromatography using a 0.18 mm × 150 mm Bio-Basic C18 RP column (Thermo Fisher Scientific), operating at 1.8 μl/min. Peptides were eluted using a 35-min gradient from 5 to 40% solvent (Solvent A: 0,1% formic acid in water, solvent B 0,1% formic acid, 80% acetonitrile in water). ESI ionization was done using a microspray “metal needle kit” (Thermo Fisher Scientific) interface. Peptides were detected in survey scans from 400 to 1600 amu (1 μscan), followed by five data dependent MS/MS scans (Top 5), using an isolation width of 2 u (in mass-to-charge ratio units), normalized collision energy of 35%, and dynamic exclusion applied during 30 seconds periods. Peptide identification from raw data was carried out using the SEQUEST algorithm (Proteome Discoverer 1.2, Thermo Fisher Scientific). Database search was performed against a small home database containing Siah-2 sequence. The following constraints were used for the searches: tryptic cleavage after Arg and Lys, up to two missed cleavage sites, and tolerances of 1 Da for precursor ions and 0.8 Da for MS/MS fragment ions and the searches were performed allowing optional Met oxidation and Cys carbamidomethylation. To identify phosphorylated peptides, phosphorylation on Ser or Thr was added as a variable modification.

In order to confirm the phosphorylations identified by the above method and to identify new sites, the mass spectrometer was operated in the selected MS/MS ion

monitoring mode. In this mode, the LTQ-Velos detector was programmed to perform, along the entire gradient, a continuous sequential operation in the MS/MS mode on the doubly charged and triple charged ions corresponding to the peptide/s selected previously. The MS/MS spectra from the peptide were analyzed by assigning the fragments to the candidate sequence, after calculation the series of theoretical fragmentations, according to the nomenclature of the series as previously described (Roepstorff & Fohlman, 1984). The proportion of each phosphorylated peptide was estimated using the fragments of MS / MS spectra which are common to the modified and unmodified peptides. In order to normalize we used a non-phosphorylated control peptide present in all samples.

13. Peptide array binding assay

Overlapping dodecapeptides of SIAH2 protein were automated spotted on cellulose membranes by using Fmoc-protection chemistry. Membrane was blocked overnight in non fat milk in TBS buffer and incubated during 6 hours with 60 nmol of recombinant GST-DYRK2 protein or GST protein for control. Then primary anti-DYRK antibody was added and rabbit secondary antibodies coupled to horseradish peroxidase were revealed by enhanced chemiluminescence system (USB) on autoradiographic films.

14. mRNA extraction and qPCR

Cells were harvested and washed twice with PBS. The cell pellet was lysed using the RNeasy Mini Kit (Qiagen) so as to isolate the RNA. After being quantified in a spectrophotometer (Genensis 10 uv Scanning, Thermo Scientific), RNA integrity was checked on an agarose gel (Bio-Rad Universal Hood II). mRNA retrotranscription was performed with the iScript cDNA Synthesis kit (Bio-Rad). Real time PCR was employed with go taq qPCR Master Mix (Promega) in an iCYCLER detection system (Bio-Rad). The qPCR program for COX-2 amplification consisted of a first denaturing cycle (3 min at 95 °C), followed by 40 cycles of four steps: denaturing (30 sec at 95 °C), annealing (30 sec at 50 °C), elongation (30 sec at 72 °C) and a further step (10 sec at 83 °C) . The DNA was finally elongated in the last cycle (1 min at 72 °C). The qPCR program for DYRK2 amplification consisted of a first denaturing cycle (2 min at 95 °C), followed by 35 cycles of three steps: denaturing (15 sec at 95 °C), annealing (59 sec at 59 °C) and elongation (30 sec at 72 °C), finally the DNA was further elongated in the last cycle (10 min at 72 °C). The following primers were used: COX-2-Forward: 5´

TGAGCAACTATTCCAAACCAGC 3'; COX-2-Reverse: 5'
 GCACGTAGTCTTCGATCACTATC 3' GAPDH-Forward: 5'
 TGGCAAAGTGGAGATTGTTGCC 3' and GAPDH-Reverse, 5' AAGATGGTGA
 TGGGCTTCCCG 3', DYRK2-Forward: 5' GTGGTCAAGGCCTACGATCACA 3',
 DYRK2-Reverse: 5' CCGCAGGTGTTCCAGGATTC 3', β -Actin-Forward: 5'
 GCTCCTCCTGAGCGCAAG 3' and β -Actin-Reverse: 5'
 CATCTGCTGGAAGGTGGACA 3'. Amplification efficiencies of COX-2 and DYRK2
 were validated and normalized against GAPDH and β -Actin, respectively. The fold
 change in gene expression was calculated using delta CT method.

15. Angiogenesis assay

5×10^5 HUVEC cells were transfected by electroporation using the nucleofector technology (Lonza). Twenty-four hours after transfection, cells were harvested and 2×10^4 cells were reseeded over a uniform layer of matrigel (BD Biosciences) in 96 well plate. After twelve hours cells were washed with PBS and stained with $5 \mu\text{M}$ Calcein (Invitrogen). Tubes formations were analyzed using a 4X objective and the BD Pathway 855 Bioimager. For quantification of tubes total length and tubes branch points Attovision v 1.7 BD software was used. The remainder of cells was reseeded on 6 well plates and twelve hours later were collected for expression analysis of SIAH2 levels by immunoblotting.

16. Determination of COX-2 protein degradation half-life

b.end5 cells were preincubated with vehicle or NADA ($2.5 \mu\text{M}$) during 12 hours and then cycloheximide (CHX, $10 \mu\text{M}$) was added to inhibit further protein synthesis. Following incubation for 1, 2, 4 and 6 h, cells were harvested and lysed, and cell lysates were collected as described above. Western blotting was performed in the same way as described above. Normalized density ratio of COX-2 over α -tubulin was performed using the Quantity One program (Bio-Rad). Protein degradation rate is expressed as half-life ($t_{1/2}$), the time for degradation of 50% of the protein.

Results

1. N-Arachidonoyl-dopamine induces the expression of COX-2 on brain endothelial cells

To study the effects of NADA on COX-1 and COX-2 protein expression we treated b.end5 cells with increasing concentration of NADA during 20 h and the steady state levels of COX-1, COX-2 and α -tubulin were investigated by western blots. COX-2/COX-1 optical density values were normalized to α -tubulin and represented in arbitrary units. In Figure 8, it is shown that NADA, at the concentration of 1 mM and higher, clearly increased the expression of COX-2, but not COX-1, in b.end5 cells.

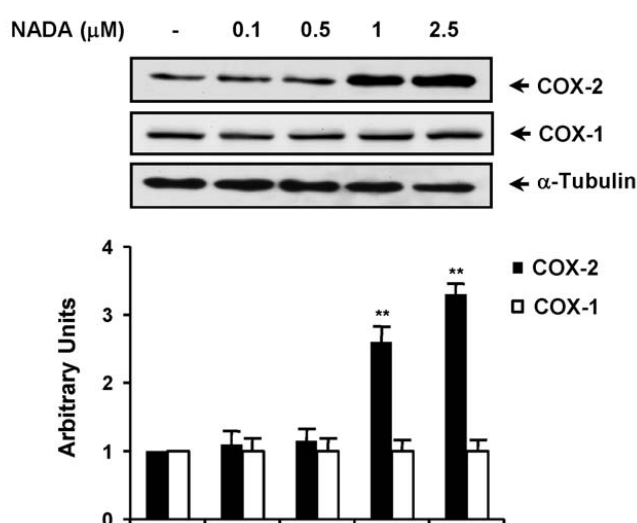


Figure 8. NADA induces COX-2 protein expression in b.end5 cell line in a dose-dependent manner. b.end5 cells were incubated with NADA at the indicated doses during 20 hours. The expression of COX-1 and COX-2 protein was determined by immunoblot analysis of protein levels. We reported the representative blots and mean \pm S.D. values of optical density of three independent experiments (one-way ANOVA with Student's t-test ** P < 0.001 and for NADA versus control).

2. N-Arachidonoyl-dopamine stabilizes COX-2 mRNA in brain endothelial cells

It has been reported that COX-2 undergoes proteasomal degradation via the endoplasmic reticulum-associated degradation pathway (Mbonye et al, 2006). To investigate the mechanisms by which NADA induces the expression of COX-2 in b.end5 cells firstly we studied the half-life of the COX-2 protein. The cells were treated with vehicle or with NADA (2.5 mM) during 12 h, then CHX (10 mM) was added and the cells were collected at the indicated times. Finally, the expression of COX-2 and α -tubulin protein was analyzed by immunoblots. As expected, NADA induced a clear increase in COX-2 expression (Figure 9A). The specific bands were quantified and the ratio COX-2/ α -tubulin calculated for every point and plotted to calculate the decay rates

for COX-2 protein expression (Figure 9B). We found that the half-life ($t_{1/2}$) for COX-2 protein in b.end5 cells was approximately 6 h and this half-life was not modified by the treatment with NADA. These results, together with the inability of NADA to induce COX-2 phosphorylation (data not shown), suggest that protein post-translational modifications are not involved in COX-2 stabilization in NADA-treated cells.

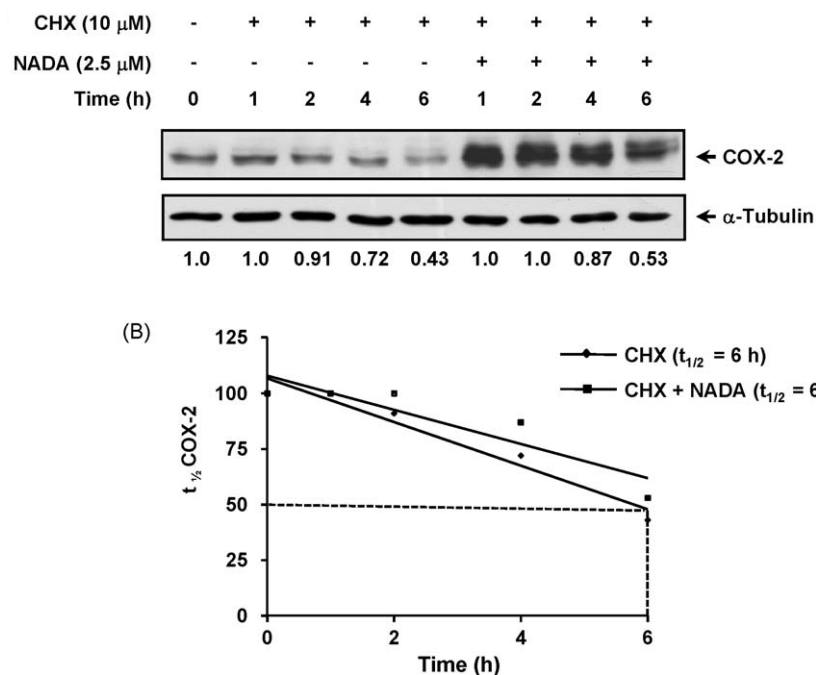


Figure 9. NADA does not affect the half-life of COX-2 protein. **A.** b.end5 cells were pre-incubated with vehicle or NADA (2.5 μ M) during 12 hours and then cycloheximide (CHX 10 μ M) was added to inhibit further protein synthesis. Following incubation from 0 to 6 hours, the cells were harvested and the expression of COX-2 protein was determined by immunoblot analysis. Normalized density ratio of COX-2 over α -tubulin is indicated for each band. A representative blot out of three independent experiments is shown. **B.** The graph represents the COX-2 protein levels normalized to α -tubulin. Results from the densitometry analysis were expressed as arbitrary values and plotted relative to the zero time point.

Next, we studied whether or not NADA had some effect on the COX-2 gene at the transcriptional level. The cells were transiently transfected with the COX-2-Luc plasmid and 24 h later stimulated with either LPS or NADA during 12 h and the cell lysates tested for luciferase activity. We show in Figure 10A that LPS clearly induced luciferase expression driven by the COX-2 promoter (4.2-fold induction). In contrast, NADA did not affect the basal levels of luciferase when compared to untreated cells. However, qRT-PCR experiments demonstrated that NADA induced a clear induction of the COX-2 mRNA levels in b.end5 cells (Figure 10B). These results suggest that the effects of NADA on COX-2 expression could be mediated by a mechanism that involves COX-2 mRNA stabilization.

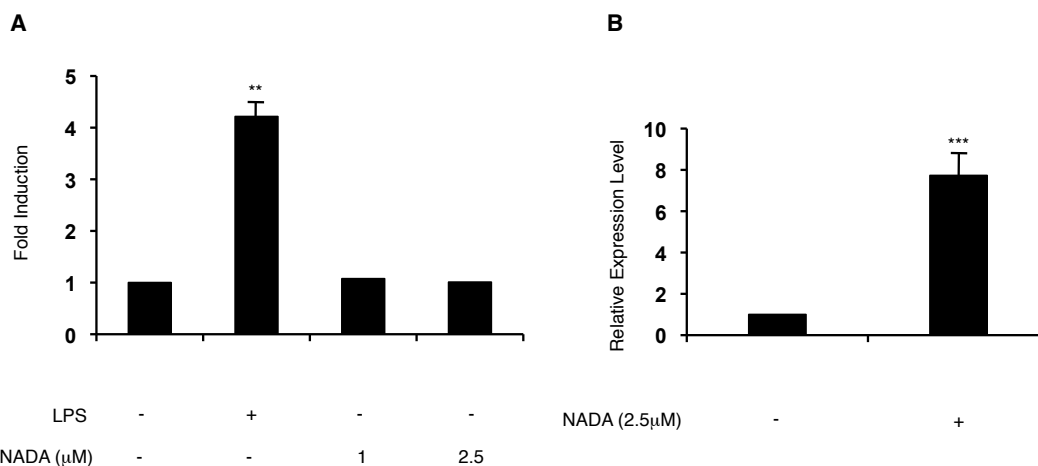


Figure 10. NADA stabilizes COX-2 mRNA. **A.** b.end5 cells were transiently transfected with the luciferase reporter plasmid COX-2-Luc as described in Materials and Methods and 24 h after transfection the cells were incubated for 12 h with LPS or NADA, and the luciferase activity measured in the cell lysates. Results are the means \pm S.D. of three determinations expressed as fold induction (observed experimental RLU/basal RLU in absence of any stimuli) (one-way ANOVA with Student's t-test **P < 0.001 LPS versus control). **B.** For the qRT-PCR analysis of COX-2 expression, b.end5 cells were stimulated with NADA 2.5 μ M for 12 h, total RNA extracted and qRT-PCR assay was performed. The graph shows the means \pm S.D. of three experiments (***P < 0.0001 NADA versus control).

3. N-Arachidonoyl-dopamine stabilizes COX-2 mRNA through a p38 MAPK pathway

The COX-2 mRNA is stabilized by p38 MAPK activation in different cell types (Lasa et al, 2000; Mifflin et al, 2002; Ridley et al, 1998). To study the role of p38 MAPK on NADA-induced COX-2 mRNA stabilization we transiently transfected b.end5 cells with the COX-2-30-UTR-luciferase plasmid for 24 h and then the cells were stimulated with either LPS or NADA, in the presence or absence of SB203580, a chemical p38 MAPK inhibitor. After 12 h of treatment the cells were collected and the luciferase activity measured in the cell lysates. As depicted in Figure 11A, both LPS and NADA clearly induced COX-2 mRNA stabilization that was prevented in the presence of SB203580.

To further confirm the specific role of p38 on NADA-induced COX-2 protein expression we stimulated b.end5 cells with NADA for 12 h in the absence or the presence of SB203085. In Figure 11B, it is shown that NADA-induced upregulation of COX-2 protein was completely prevented by the p38 MAPK inhibitor SB203085. To study directly the effect of NADA on p38 MAPK activation, we incubated b.end5 cells with NADA (2.5 mM) for the indicated times, and the phosphorylation/activation status of p38, JNK, and ERK was investigated by western blots using specific mAbs that recognize the phosphorylated forms of these MAPKs. As depicted in Figure 11C,

NADA induced a sustained activation of the p38 MAPK and did not affect significantly the phosphorylation of the MAPKs JNK and ERK.

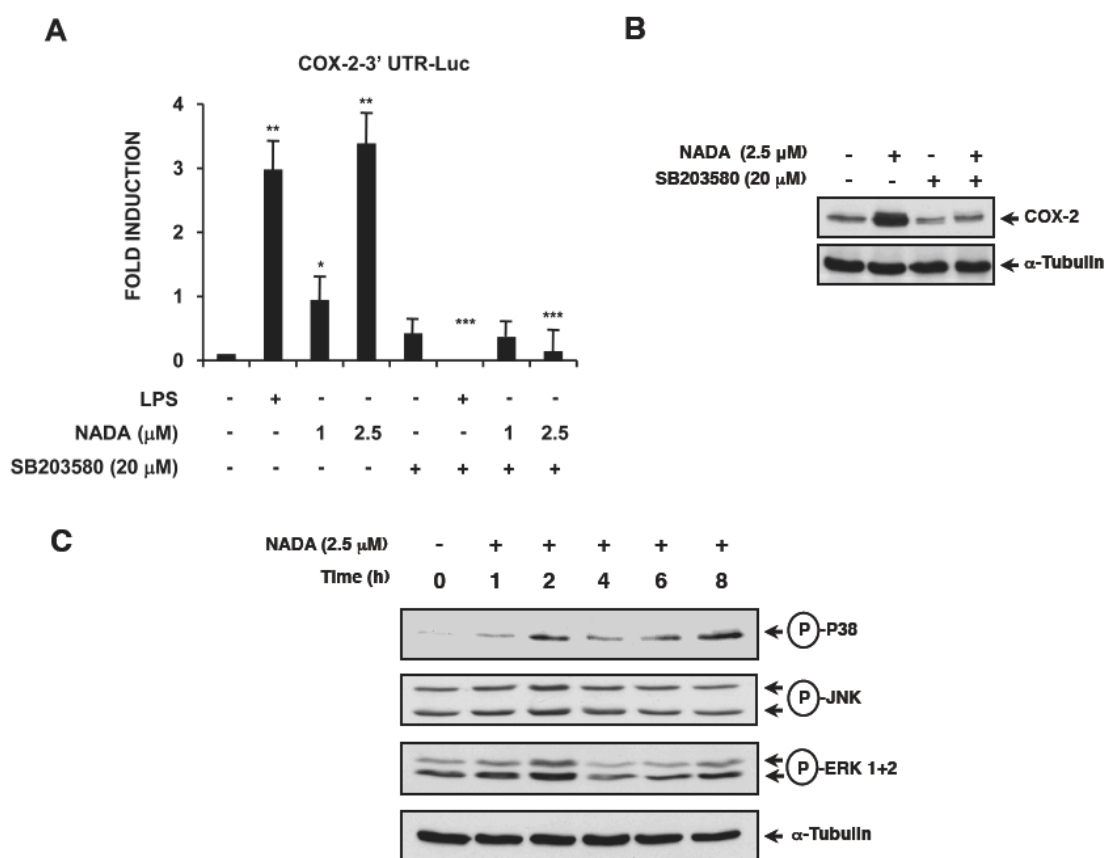


Figure 11. NADA induces COX-2 expression by stabilizing mRNA through a p38 dependent pathway. **A.** b.end5 cells were transiently transfected with the plasmid COX-2-3'UTR-Luc and 24 h later the cells were pre-incubated for 30 min with SB203580 (20 μM) and stimulated with LPS or NADA as indicated for 12 h. Luciferase activity was measured and the results are the means ± S.D. of three determinations expressed as fold induction (observed experimental RLU/basal RLU in absence of any stimuli) (one-way ANOVA with post-hoc Bonferroni's test * $P < 0.05$ for NADA versus control and ** $P < 0.001$ for LPS / NADA versus control; *** $P < 0.0001$ for LPS+SB203580 versus LPS and for NADA+SB203580 versus NADA). **B.** b.end5 cells were pretreated with SB203580 (20 μM), PD98059 (20 μM) or SP600125 (10 μM) for 30 min, and then incubated with NADA 2.5 μM for 20 h. The expression of COX-2 protein was determined by immunoblot analysis of protein levels. We reported the representative blots of three independent experiments. **C.** The cells were incubated with NADA 2.5 μM at the indicated times and MAPKs activation detected by immunoblots using specific phospho-antibodies.

4. N-Arachidonoyl-dopamine up-regulates HIF-1α

Since both endocannabinoids and HIF-1α share common properties in neuroprotection (Giusti & Fiszer de Plazas; Harten et al; Pryce et al, 2003) we hypothesized whether NADA could influence HIF-1α at a protein level. The human neuroblastoma cell line SK-N-SH was stimulated with deferoxamine (DFX) and

increasing amounts of NADA, and HIF-1 α expression was analyzed. As observed, larger amounts of HIF-1 α were detected. As SIAH2 is one of the upper stream proteins in the hypoxia response we wondered whether HIF-1 α degradation was a collateral effect of NADA-dependent SIAH2 degradation. To assess this, 293T cells were treated with MG-132 to avoid SIAH2 auto-degradation and SIAH2 protein was analyzed. We observed (Figure 12) a decrease in SIAH2 protein in the presence of NADA, which explains the mechanism whereby HIF-1 α up-regulation is accomplished.

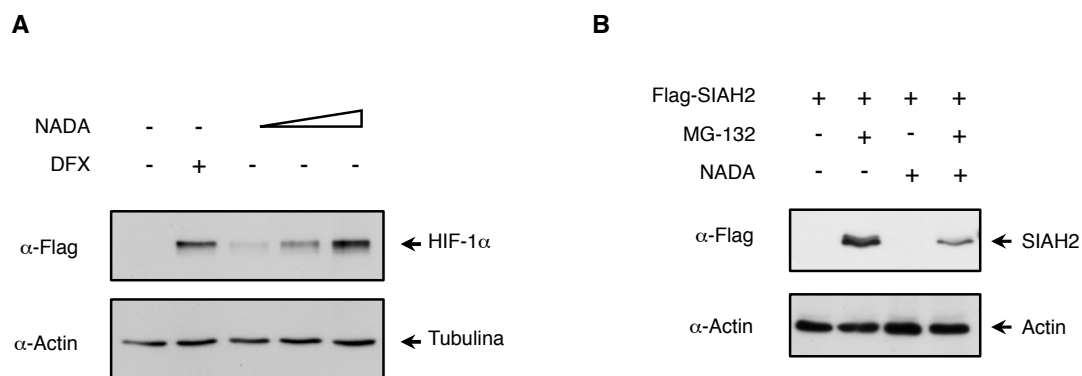


Figure 12. NADA up-regulates HIF-1 α protein. **A.** SK-N-SH cell were treated with 100 μ M of DFX and 12 hours later cells were stimulated with 1, 5 and 10 μ M NADA for 6 hours before lysis. Protein expression was analyzed by immunoblotting. **B.** 293T cells were transfected with the indicated plasmids and 36 h later cells were treated with 10 μ M NADA and 30 min later with 10 μ M MG-132 for 12 h before lysis. Protein expression was evaluated by immunoblot with the indicated antibodies.

As the literature reports SIAH2 as a new protein of interest in hypoxia and tumorigenesis whose activity depends on the degree of its phosphorylation state, we were interested in getting to know the molecular mechanism by which SIAH2 activity is ruled. To achieve this, we performed a kinase screening to find out new kinases able to phosphorylate SIAH2. Among others, we spotted DYRK2 as a new kinase of interest.

5. DYRK2 phosphorylates SIAH2 *in vivo* and *in vitro*

As our previous work showed that SIAH2 is heavily phosphorylated (Calzado et al, 2009) we aimed to identify further kinases with the ability to modify this important E3 ligase. A set of different kinases was tested to for their ability to phosphorylate SIAH2 *in vitro*. As DYRK kinases showed robust SIAH2 phosphorylation we initially decided to focus on this protein family in more detail. To study the ability of these kinases to phosphorylate SIAH2 *in vivo*, 293T cells were transfected to express SIAH2 and the most relevant members of human DYRK kinases (DYRK1A, DYRK1B and DYRK2) in

the presence of the proteasome inhibitor MG-132 to avoid SIAH2 auto-degradation. As shown in figure 13A, DYRK1B and DYRK2 overexpression resulted in the appearance of several slower migrating SIAH2 bands, an effect not observed with DYRK1A. Similar results were obtained when SIAH2 phosphorylation was scored with an antibody specifically recognizing SIAH2 phosphorylation at Ser28 (Calzado et al, 2009), as DYRK2 caused the strongest signal. To test whether the upshifted SIAH2 band represents the phosphorylated form of the E3 ligase, cell extracts were incubated with λ phosphatase and analyzed for their electrophoretic mobility by Western blotting. Treatment with λ phosphatase converted the slower electrophoretic mobility of SIAH2 back to that of the faster migrating bands as they occur upon expression of SIAH2 alone (Figure 13B), indicating that DYRK2-mediated SIAH2 phosphorylation can be revealed by the differential electrophoretic mobility of SIAH2 bands.

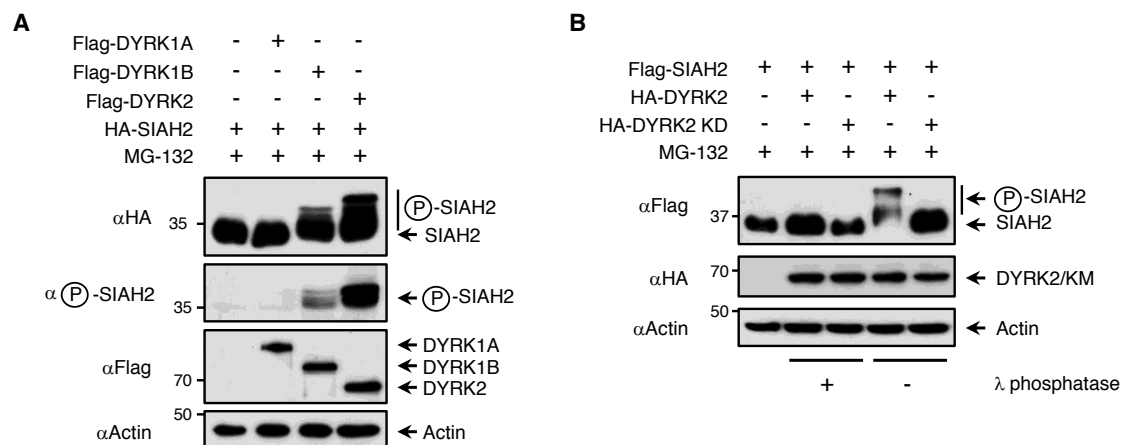


Figure 13. DYRK2 phosphorylates SIAH2. **A.** 293T cells were transfected with the indicated plasmids and 36 h later cells were treated with 10 μ M MG-132 for 12 h before lysis. Protein expression was evaluated by immunoblot with the indicated antibodies and SIAH2 phosphorylation studied with a specific antibody against SIAH2 phospho-Ser28. **B.** Cells were transfected with the indicated combinations of plasmids and treated with MG-132 for 12 h. The sample was lysed in phosphatase inhibitor-free buffer containing λ phosphatase as shown and the electrophoretic mobility of SIAH2 determined by immunoblotting.

The upshifted SIAH2 form only occurred upon expression of the wildtype kinase, while a DYRK2 kinase dead mutant did not cause any alterations in the electrophoretic mobility of SIAH2 (Figure 14A). The relevance of the DYRK2 kinase activity for SIAH2 was underscored by experiments where increasing amounts of Harmine, a natural compound able to inhibit DYRK2 activity (Bain et al, 2007), caused a clear decrease in the bands with a slower mobility as well as SIAH2 phosphorylation at Ser28 (Figure 14B).

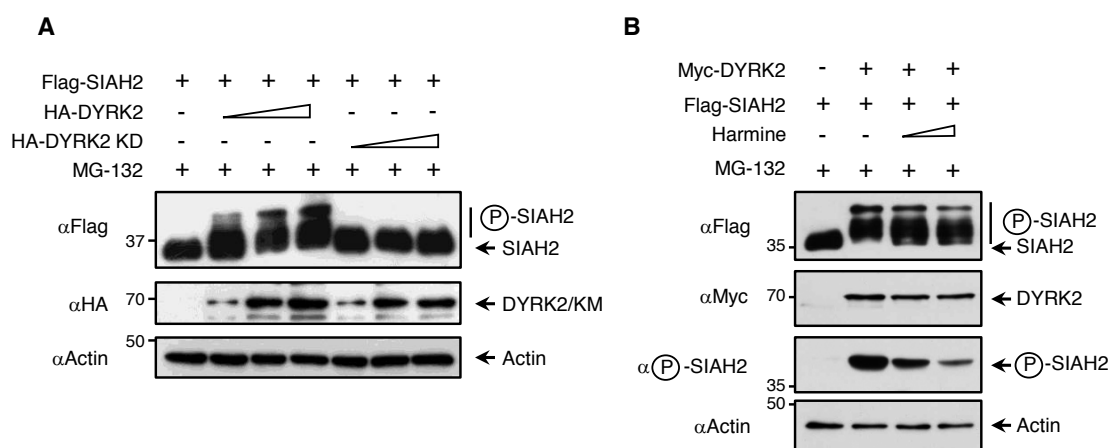


Figure 14. DYRK2 phosphorylates SIAH2. **A.** 293T cells expressing Flag-tagged SIAH2 and wild-type or kinase-inactive HA-DYRK2 KD were grown in the presence of MG-132. Cell lysates were analyzed by immunoblotting. **B.** Flag-SIAH2 was expressed either alone or along with DYRK2 in the presence of MG-132 and incubated with 2,5 and 5 μ M of Harmine during 12 h before lysis. SIAH2 was analyzed for its electrophoretic mobility by immunoblotting and the phosphorylation level studied with a specific antibody against SIAH2 phospho-Ser28.

To study whether DYRK2 is directly mediating SIAH2 phosphorylation, we performed an *in vitro* kinase assay with purified recombinant proteins GST fusion proteins. GST-DYRK2 caused the phosphorylation of GST-SIAH2, as revealed by immunoblotting with a specific phosphoserine antibody (Figure 15A). To study the function of DYRK2 for phosphorylation of the endogenous SIAH2 protein, 293T cells were transfected with a specific DYRK2 siRNA, followed by the analysis of SIAH2 Ser28 phosphorylation with specific antibodies. The inhibition of DYRK2 expression resulted in decreased constitutive SIAH2 Ser28 phosphorylation (Figure 15B), thus revealing the physiological importance of DYRK2 for SIAH2 phosphorylation. Collectively, these experiments identify DYRK2 as a kinase with the ability to directly phosphorylate SIAH2.

6. DYRK2 phosphorylates SIAH2 in at least five residues

To identify the putative SIAH2 sites phosphorylated by DYRK2, we mutated proline-flanked serines and threonines to alanine. Coexpression of the mutants with DYRK2 and subsequent analysis of their electrophoretic behaviour showed that mutation of Thr26, Ser28 and Ser68 resulted in increased electrophoretic mobility (Figure 16A). A SIAH2 mutant with mutations in all three residues (SIAH2-3A) was still upshifted by DYRK2 (Figure 16B), indicating the existence of further phosphorylation sites.

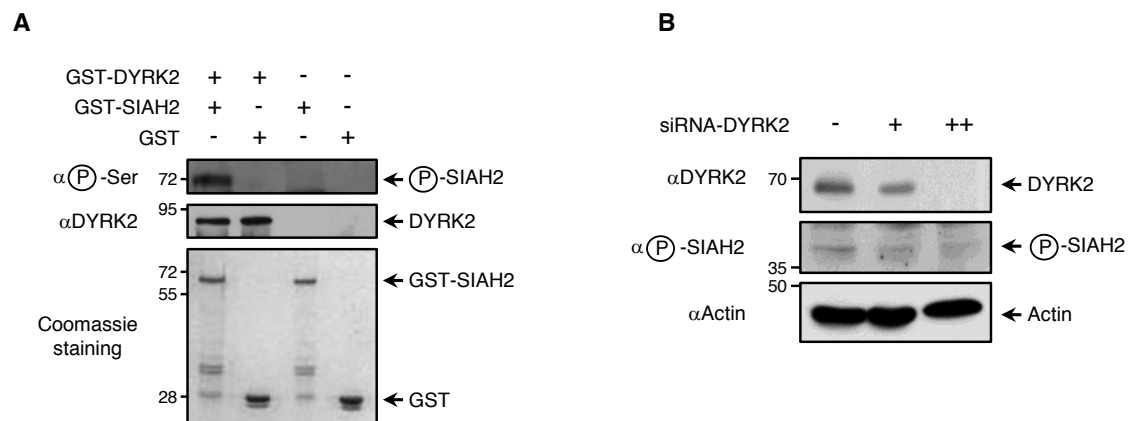


Figure 15. DYRK2 phosphorylates SIAH2. A. *In vitro* Kinase assay was employed with bacterially purified GST-SIAH2 and commercial recombinant DYRK2 protein. SIAH2 phosphorylation was evaluated by immunoblot with anti-phosphoserine antibody. Protein levels were visualized by coomassie staining. **B.** Endogenous levels of phospho SIAH2 were analyzed by western blot using a specific antibody against SIAH2 phospho Ser28. DYRK2 protein was immunoprecipitated using a specific antibody and its expression evaluated by immunoblot.

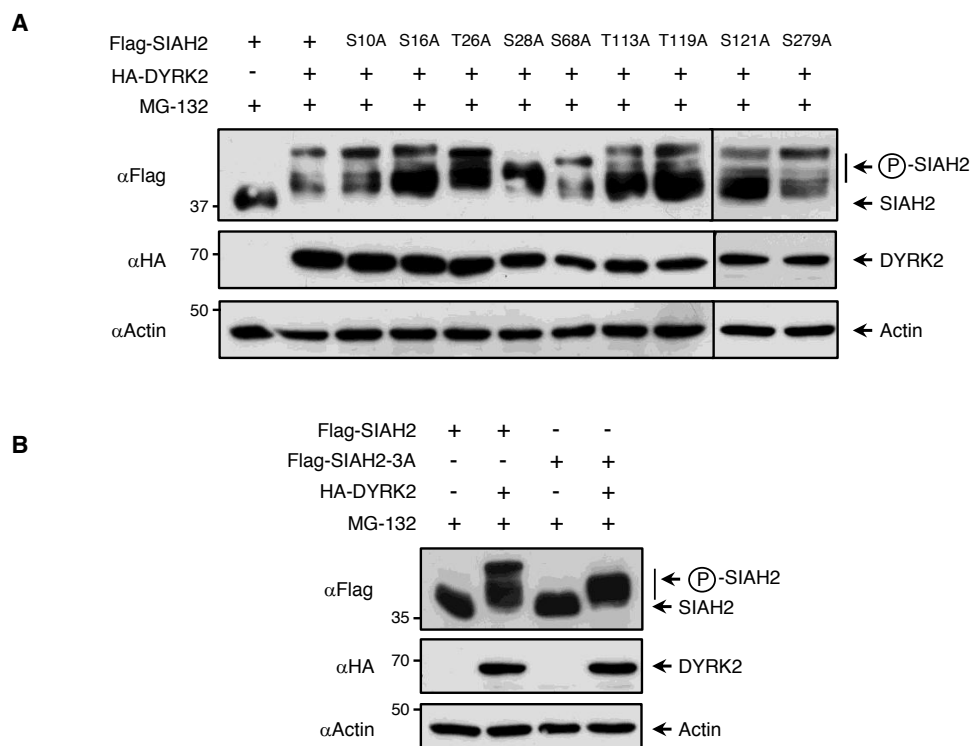


Figure 16. DYRK2 phosphorylates SIAH2. A. 293T cells were transfected with the indicated plasmids and treated 12 h before lysis with 10 μ M of MG-132. Electrophoretic mobility shift of different SIAH2 phospho mutants was analyzed by immunoblotting. **B.** 293T cells transiently transfected with Flag-SIAH2 or 3A mutant (T26A, S28A and S68A) were grown in the presence of 10 μ M MG-132. SIAH2 and -3A electrophoretic mobilities were analyzed by immunoblotting.

To identify the phosphorylation sites by an unbiased approach, SIAH2 was coexpressed either alone or together with DYRK2, followed by isolation of the E3 ligase via immunoprecipitation and analysis by mass spectrometry. We were able to achieve protein coverage up to 64% (Figure 17A). Phosphorylation site analysis confirmed the three phosphorylated residues described above and also allowed the identification of Ser16 and Thr119 as new phosphorylation sites (Figure 17B). Mutation of the five residues (SIAH2-5A) significantly decreased SIAH2 migration (compare first and last lanes), although the slight remaining upshift may harbor further phosphorylation sites contained in sequences not covered by the mass spectrometry analysis (Figure 17C).

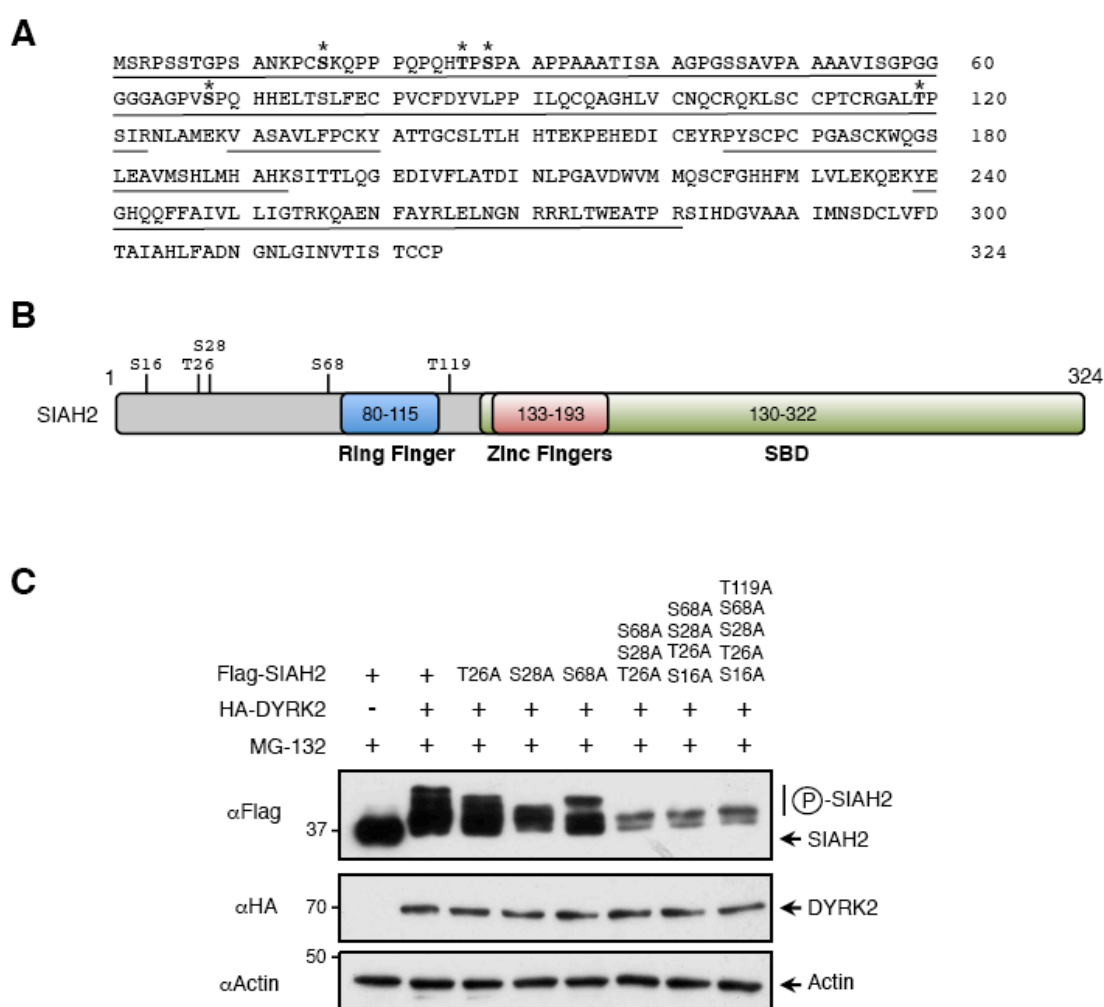


Figure 17. DYRK2 phosphorylates SIAH2 in at least five residues. **A.** SIAH2 full length protein sequence. Underlying text show the SIAH2 sequence covered by tandem mass spectrometry analysis. In bold are show the amino acids phosphorylated identified in this study. **B.** Schematic representation of SIAH2 structure showing the phosphorylated residues revealed by Mass Spectrometry analyses. **(C)** 293T cells expressing the indicated SIAH2 point mutants together with DYRK2 were treated during 12 h with MG-132. Cell lysates were analysed by immunoblotting.

To study DYRK2-mediated phosphorylation the individual SIAH2 sites we generated phosphospecific antibodies against each phosphorylated SIAH2 residue. While we successfully raised highly specific antibodies for most of the phosphorylation sites we failed to produce Ser16-specific antibodies. DYRK2 can function as a priming kinase for substrates such as c-Jun and c-Myc (Taira et al), raising the possibility that phosphorylation at specific residues is the prerequisite for phosphorylation at other sites. To test this, SIAH2 and phosphorylation site mutants were expressed alone or together with DYRK2, followed by detection of single site phosphorylation with the phospho-specific antibodies (Figure 18). DYRK expression caused phosphorylation at all sites, while Ser28 mutation precluded also phosphorylation at the neighboring Thr26.

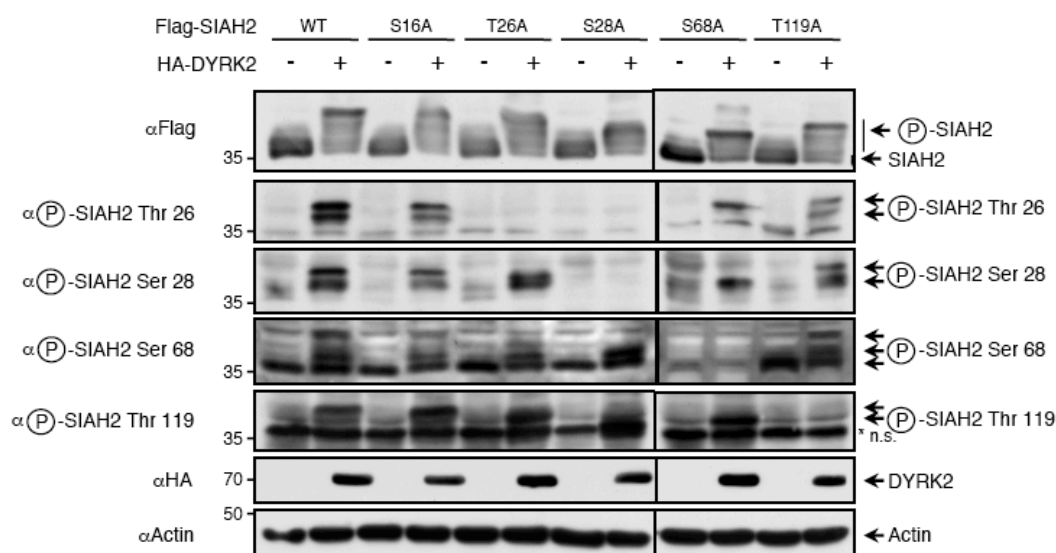


Figure 18. Influence of phosphorylation in phospho-SIAH2 mutants. Flag-SIAH2 or the different SIAH2 point mutants were expressed either alone or along with DYRK2 in 293T cells in the presence of MG-132. SIAH2 was analyzed for its electrophoretic mobility by immunoblotting and the phosphorylation level studied with the indicated specific antibodies.

As these sites are closely adjacent and also Ser28 will be part of the epitope recognized by the phospho-Thr26 antibody, we do not consider Ser28 as a priming phosphorylation site. Ser68 showed highly phosphorylated in basal conditions as compared to the others residues. We did not observe any significant changes in the phosphorylation of the different residues in response to points mutations, which probably indicate that at least in the case of DYRK2 no clear phosphorylation hierarchy exists. Taken together, all these results clearly indicate that DYRK2 can specifically phosphorylate SIAH2 at minimal five residues.

7. SIAH2 colocalizes and interacts with DYRK2

To study the subcellular localization of both proteins by indirect immunofluorescence, U2OS cells were stained for endogenous DYRK2 and for ectopically expressed SIAH2, as the detection of the endogenous E3 ligase is precluded by low protein levels and the limited quality of available antibodies. Confocal microscopy showed that the Flag-tagged SIAH2 protein (mutated in the RING domain to avoid its self-degradation) and endogenous DYRK2 mainly colocalize in the cytoplasm and partially in the nucleus (Figure 19). Correlation analysis revealed a value of 0.79 ± 0.06 for Pearson's coefficient indicating a high degree of colocalization between SIAH2 and DYRK2.

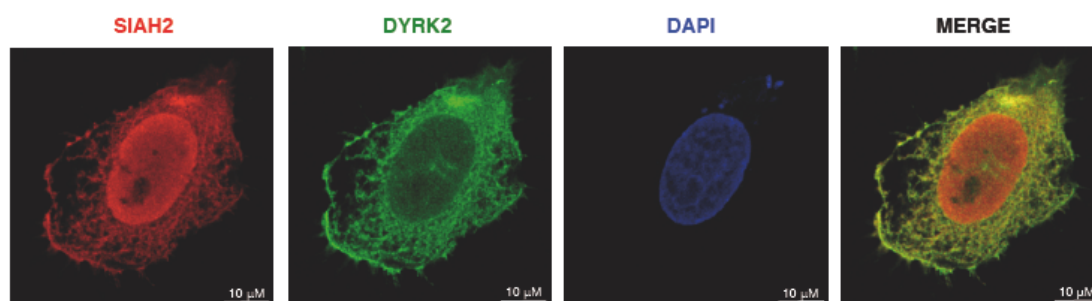


Figure 19. SIAH2 colocalizes with DYRK2. U2OS cells were transfected with Flag-SIAH2 RM and analyzed for SIAH2 and endogenous DYRK2 localization by indirect immunofluorescence. Overlapping localization in merged pictures is shown in yellow. Nuclear DNA was stained with DAPI. Scale bar = 10 μ M.

To assess whether SIAH2 interacts with endogenous DYRK2, we expressed Flag-SIAH2 in 293T cells and performed co-immunoprecipitation assays. Endogenous DYRK2 co-immunoprecipitated efficiently with SIAH2. Similarly, endogenous SIAH2 also co-immunoprecipitated with DYRK2, thus confirming the existence of DYRK2-SIAH2 complex under physiological conditions (Figure 20A). To test whether the interaction between SIAH2 and DYRK2 is direct and to characterize the responsible domain, we performed GST-pulldown assays (Figure 20B). Flag-tagged DYRK2 was efficiently captured by full-length SIAH2, but also by mutants lacking parts of the N- and C-terminus, suggesting the existence of more than one SIAH2 domain responsible for binding to DYRK2.

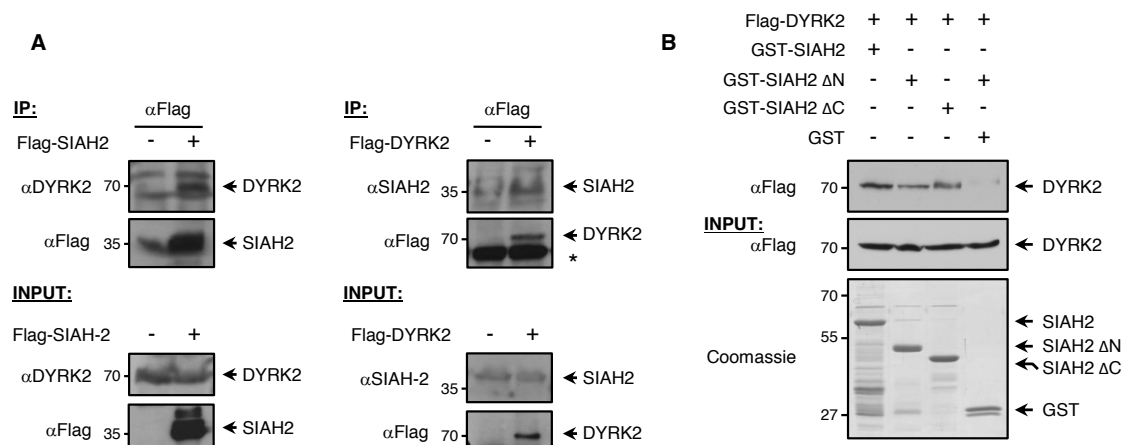


Figure 20. SIAH2 interacts *in vivo* and *in vitro* with DYRK2. **A.** 293T cells were transfected with Flag-SIAH2 or Flag-DYRK2 and treated with 10 μ M of MG-132 during 12 h before lysis. A fraction was subjected to immunoprecipitation (IP) using anti-Flag antibody. After elution, DYRK2 or SIAH2 proteins were detected by western blotting with antibodies specific for DYRK2 and SIAH2. The remaining extract fraction was tested for the occurrence of the indicated proteins by immunoblotting (INPUT). **B.** GST pull down assay was carried out incubating soluble GST-SIAH2 or deleted versions Δ N (117-324) and Δ C (1-116) with 293T cell extracts expressing Flag-DYRK2. DYRK2 bound proteins were detected by immunoblotting with anti-Flag antibody. A fraction of the cell extracts used and the Coomassie-stained display the input material.

To characterize SIAH2 interaction sites with DYRK2 in detail we performed a peptide array experiment. This technique has been widely used to define sites of direct interaction on many proteins including SIAH2 (Le Moan et al). A peptide library consisting of overlapping fragments representing the entire SIAH2 protein was incubated with GST-DYRK2 or the GST. Detection of the bound material by antibodies showed that DYRK2 binds two distinct domains of SIAH2: the N-terminal domain (aa 1-28, peptides 1-9) and an area comprising the first zinc finger domain (aa 119-150, peptides 60-70) present in the substrate-binding domain (SBD) (Figure 21). Overall, these results prove the direct interaction between DYRK2 and SIAH2 as well as the possible relevant role of the first zinc finger domain present in the substrate-binding domain of SIAH2.

8. SIAH2 mediates DYRK2 ubiquitination

As SIAH2 leads to ubiquitination and degradation of many of its interaction partners we tested the impact of SIAH2 expression at different optimum levels on the endogenous DYRK2. Expression of increasing amounts of SIAH2 resulted in a dose-dependent decrease of DYRK2 protein levels. While the protein levels decreased, the

mRNA levels of DYRK2 were not significantly changed, as revealed by qPCR (Figure 22A). A comparative analysis of SIAH1 and SIAH2 showed that SIAH2 was much more efficient in its ability to trigger DYRK2 degradation (Figure 22B).

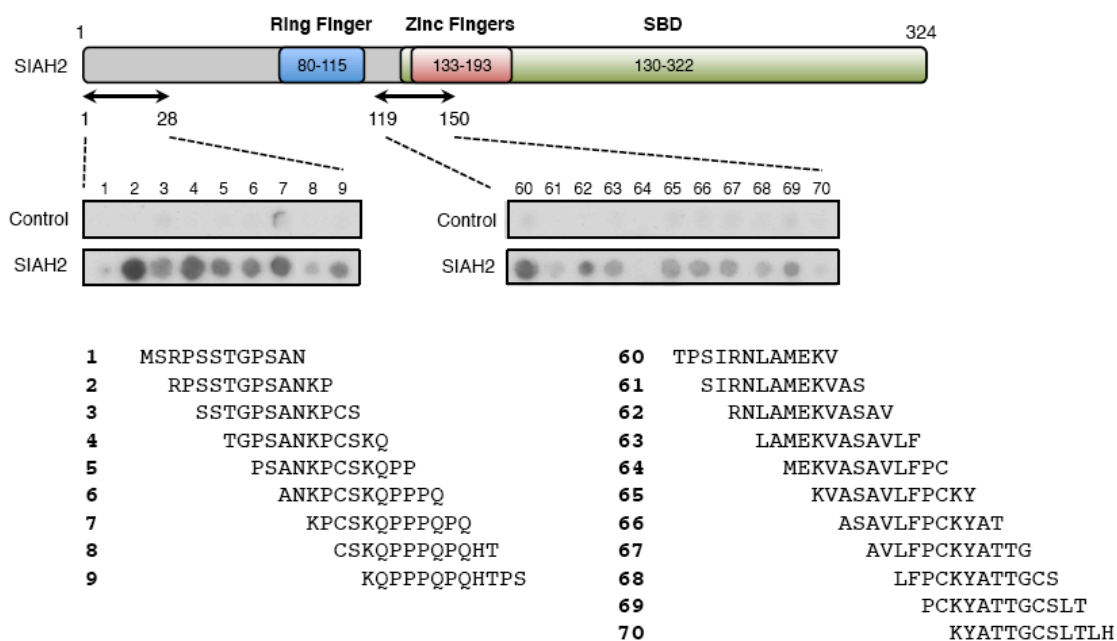


Figure 21. Peptide array assay. (Upper panel) Schematic diagram of peptide array binding assay. Peptide array library covering the complete sequence of SIAH2 was screened with recombinant GST-DYRK2 protein or GST protein for control. Recombinant GST-DYRK2 revealed two distinct domains of interaction with SIAH2 (shown in box): N-terminal domain (aa 1-28, peptides 1-9) and an area comprising the first zinc finger domain (aa 119-150, peptides 60-70). (Lower panel) Sequences of SIAH2 peptides interacting with DYRK2.

To assess whether SIAH2 can degrade DYRK2 through an ubiquitin/proteasome-dependent process, increasing amounts of SIAH2 were coexpressed with DYRK2 in the presence or absence of MG-132. The addition of this proteasome inhibitor prevented DYRK2 degradation and also stabilized the SIAH2 protein (Figure 23A). Along this line, the expression of ligase-deficient SIAH2 point mutant (SIAH2 RM) failed to cause DYRK2 degradation (Figure 23B). This degradation is specific for DYRK2, as expression of either SIAH1 or SIAH2 could not change the protein levels of the DYRK family members DYRK1A or DYRK1B (Figure 23C). All these data show that SIAH2-mediated DYRK2 degradation is performed by the proteasome, depends on SIAH2 ligase activity and is DYRK2-specific.

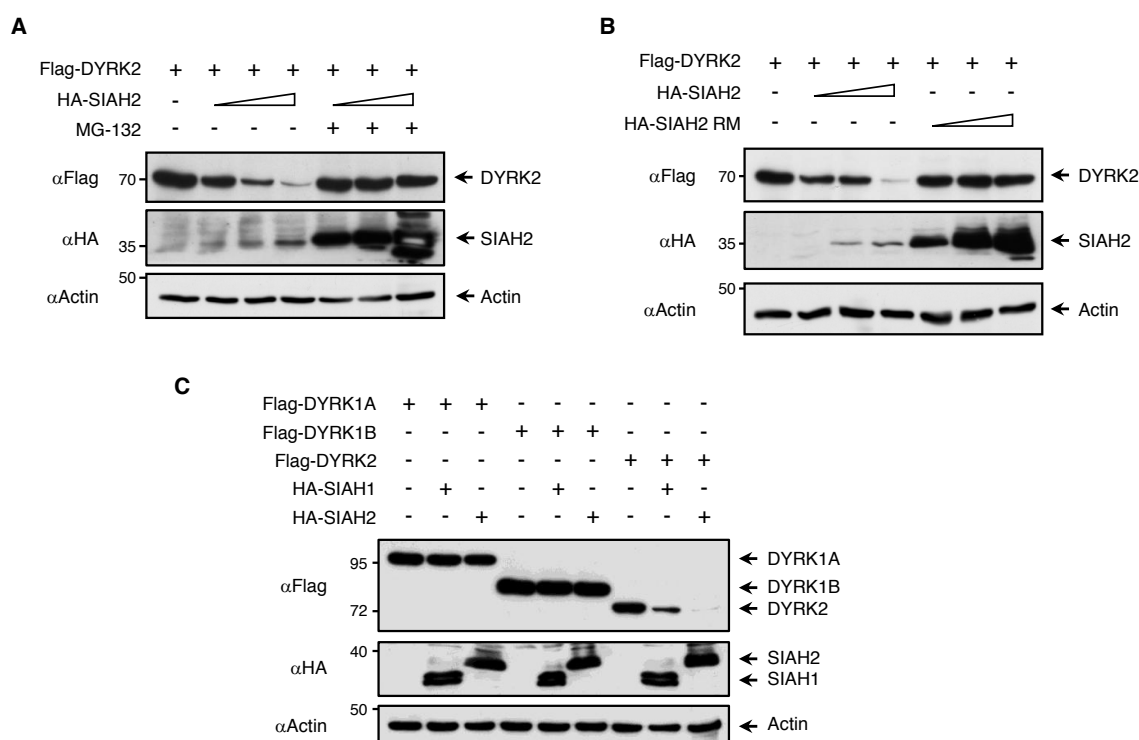


Figure 23. SIAH2 catalyzes DYRK2 degradation through the proteasome. A. Cells transfected to express Flag-DYRK2 and increasing amounts of SIAH2 were grown in the presence or absence of MG-132. Cell lysates were analyzed by immunoblot with the indicated antibodies. **B.** 293T cells were transfected with the indicated plasmids and DYRK2 protein levels were evaluated by immunoblot in response to increasing concentration of SIAH2 wild type or SIAH2 ring mutant (RM). **(C)** Cells were transfected to express Flag-DYRK1A, Flag-DYRK1B and Flag-DYRK2 in the presence of HA-SIAH1 or HA-SIAH2. Cells were further grown, lysed and the protein expression analyzed by immunoblot with the indicated antibodies.

9. SIAH2 controls DYRK2 expression in response to hypoxia

As SIAH2 is an important regulator of the hypoxic response, it was interesting to test whether SIAH2 has the ability to regulate DYRK2 expression levels in response to low oxygen levels. Cells expressing low levels of DYRK2 were subjected to hypoxia (1% O₂) for different periods and subsequently analyzed by immunoblotting for the occurrence of the kinase. Hypoxia caused DYRK2 degradation in a time-dependent manner (Figure 25A). Treatment with MG-132 prevented hypoxia-mediated DYRK2 degradation and also stabilized the kinase under normoxic conditions (Figure 25B).

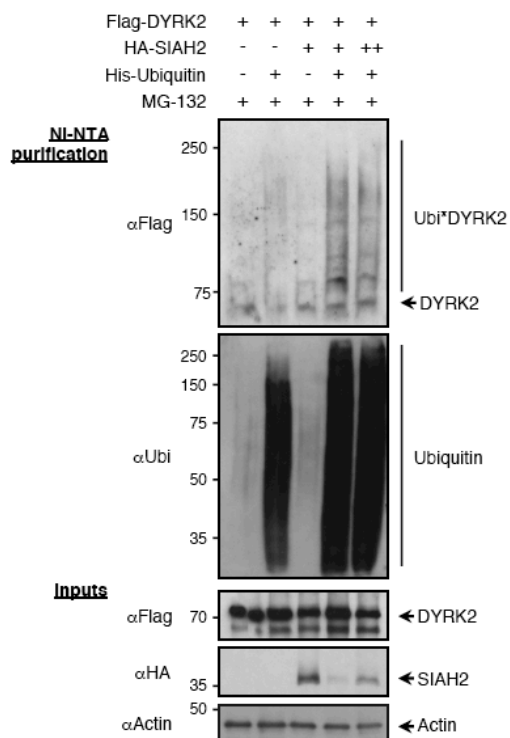


Figure 24. SIAH2 mediates DYRK2 ubiquitination. Cells were transfected with Flag-DYRK2, His-tagged ubiquitin and increasing amounts of SIAH2. A fraction was tested for the occurrence of the indicated proteins by immunoblotting (INPUT). Another aliquot was lysed under denaturing conditions, followed by purification of His-tagged ubiquitin on Ni-NTA agarose columns and detection of ubiquitylated DYRK2 by immunoblotting.

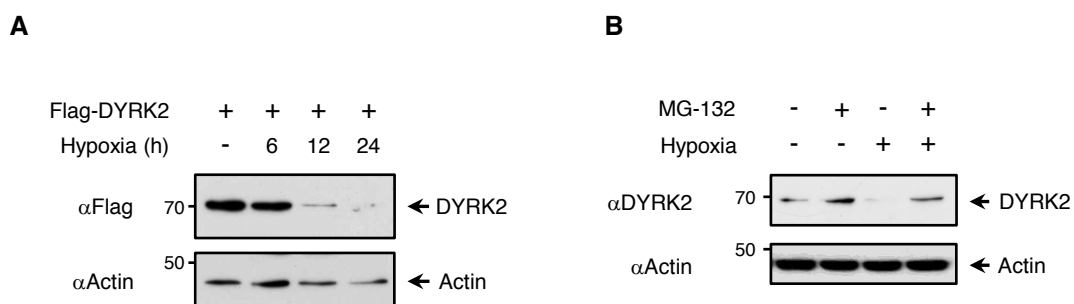


Figure 25. Hypoxia regulates DYRK2 levels. **A.** 293T cells expressing Flag-DYRK2 were grown in normoxia or hypoxia (1% O₂) for the indicated times and DYRK2 expression was analyzed by immunoblotting. **B.** 293T cells were incubated under normoxic or hypoxic (12 h) conditions in the presence of 10 μM of MG-132 as shown, and analyzed by immunoblotting with an anti-DYRK2 antibody.

To demonstrate the contribution of SIAH2 to this process, hypoxia-mediated DYRK2 decay was compared between control cells and cells where endogenous SIAH2 was knocked down by siRNA treatment. These experiments showed that hypoxia-mediated DYRK2 degradation only occurred in the presence of SIAH2 (Figure 26). SIAH2 depletion also increased DYRK2 levels under normoxic conditions, indicating that both basal and SIAH2-mediated ubiquitin/proteasome-dependent DYRK2 degradation also occurs in well-oxygenated cells.

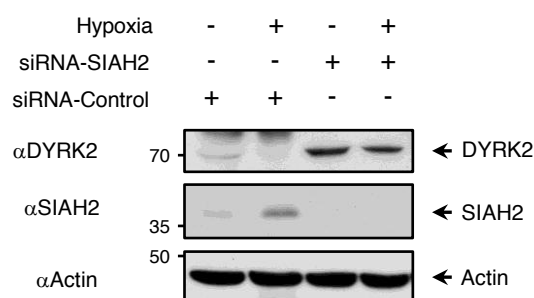


Figure 26. DYRK2 expression is regulated by SIAH2 on hypoxia. 293T cells were transfected with 100 nM of scrambled (control) or SIAH2 siRNA. After 4 days, cells were cultivated under normoxic or hypoxic conditions and analyzed for DYRK2 and SIAH2 as shown.

Next we were interested in determining the phosphorylation state of the endogenous SIAH2 protein under normoxic and hypoxic conditions as compared to DYRK2 endogenous protein levels. 293T cells were treated with or without MG-132, and SIAH2 phosphorylation endogenous levels analysed in hypoxia and normoxia (Figure 27A). Hypoxia-mediated DYRK2 decrease was accompanied by a clear reduction in endogenous SIAH2 basal phosphorylation. Treatment with MG-132 caused the accumulation of DYRK2 endogenous levels, which were accompanied by a very significant increase in SIAH2 phosphorylation. Hypoxic conditions also resulted in diminished SIAH2 phosphorylation when the phosphorylation was triggered by DYRK2 expression (Figure 27B).

The effect of hypoxia on ubiquitination of DYRK2 in vivo was tested in cells that were cotransfected to express low amounts of His-Ubiquitin and Flag-DYRK2. These cells were incubated in the presence of MG-132 for various periods under hypoxic conditions. After purification of ubiquitinated proteins under denaturing conditions by Ni-NTA pull-down the ubiquitination status of DYRK2 was analyzed by Western blotting. These experiments showed a clear increase in DYRK2 polyubiquitination in response to low O₂ concentrations (Figure 28).

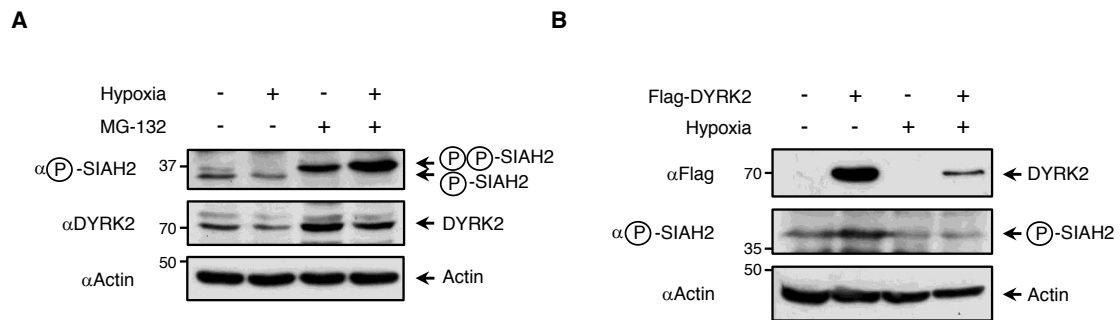


Figure 27. DYRK2 expression is regulated by SIAH2 on hypoxia. A. Cells were grown under normoxic or hypoxic conditions as shown, in the presence or absence of MG-132. Immunoblot analysis of endogenous DYRK2 and phospho SIAH2 was employed using anti-DYRK2 and a specific antibody against SIAH2 phosphorylated Ser28. **B.** 293T cells expressing Flag-DYRK2 were grown in normoxia or hypoxia (1% O₂) 12 h before lysis. Endogenous levels of phospho-SIAH2 were analyzed by immunoblotting with a specific antibody against SIAH2 Ser28 phosphorylated.

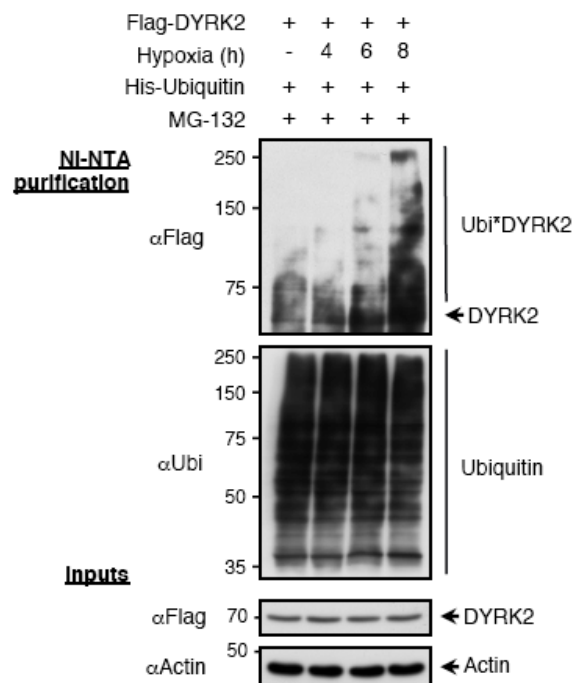


Figure 28. Hypoxia regulates DYRK2 ubiquitination. Cells were transfected with Flag-DYRK2, His-tagged ubiquitin and were grown in normoxia or hypoxia (1% O₂) for the indicated times in the presence of MG-132. A fraction was tested for the occurrence of DYRK2 by immunoblotting (INPUT). Another aliquot was lysed under denaturing conditions, followed by purification of His-tagged ubiquitin on Ni-NTA agarose columns and detection of ubiquitylated DYRK2 by immunoblotting.

To test the functional consequences of DYRK2 degradation by SIAH2, we studied whether SIAH2 expression affected DYRK2 ability to phosphorylate p53. U2OS cells were exposed to genotoxic damage by Doxorubicin and subjected to hypoxia conditions (Figure 29). DYRK2 inhibition in response to hypoxia caused a clear delay and decrease in p53 phosphorylation in Ser46 (Upper panel). The residual phosphorylation is probably due other kinases such as ATM, PKC δ , AMPK α or p38 which target the same site (Smeenk et al, 2011). As p53 phosphorylation at Ser46 triggers its ability to induce the transcription of proapoptotic genes, it was interesting to investigate the effect of DYRK2 and SIAH2 on the transcriptional activity of p53. H1299 cells deficient for p53 were transfected with a p53-inducible luciferase reporter construct (p53-Luc) together with p53 and various combinations of the p53 kinase DYRK2 and SIAH2. Luciferase assays showed that p53-induced transcription was further boosted by DYRK2, while coexpression of SIAH2 antagonized this stimulatory effect. Very similar results were obtained with another reporter gene consisting of the p53-dependent Bax promoter fused to the luciferase gene (Figure 23 lower panel).

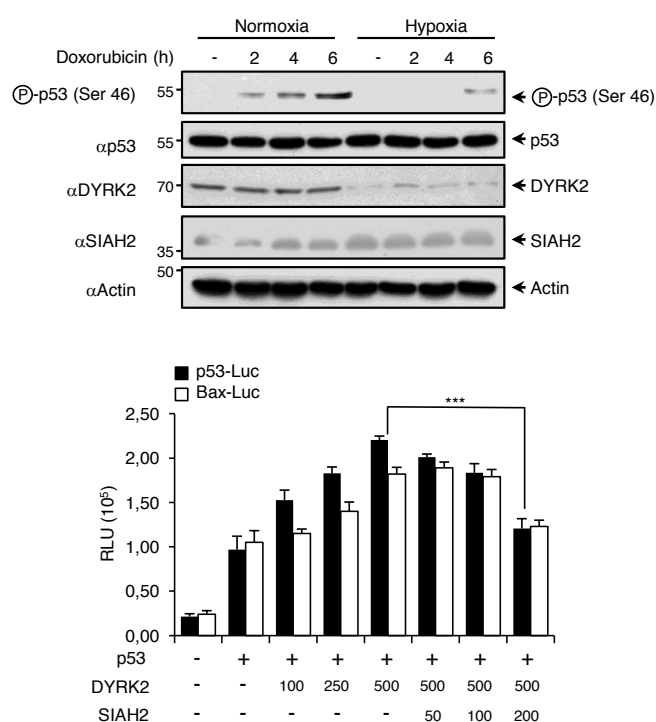


Figure 29. SIAH2-dependent p53 regulation on hypoxia. (Upper panel) H1299 cells were treated with 2 μ g/ml doxorubicin for the indicated times. After the addition of doxorubicin cells were further incubated for the indicated periods under normoxic or hypoxic conditions. Cell lysates were evaluated by immunoblot with the indicated antibodies. (Lower panel) H1299 cells were transfected with p53-Luc or Bax-Luc reporter plasmids together with expression plasmid for DYRK2, SIAH2 and p53 and luciferase activity analyzed. Data are means \pm S.D of n=3 experiments.

10. Phosphorylation of SIAH2 by DYRK2 affects its localization and ability to degrade PHD3

Is DYRK2-mediated phosphorylation of SIAH2 affecting its activity? To study the effect of SIAH2 phosphorylation on its ability to degrade DYRK2 we transfected 293T cells with an expression vector for HA-SIAH2 together with increasing amounts of Flag-DYRK2 or the kinase inactive mutant Flag-DYRK2 KD. Immunoblotting revealed that DYRK2 was equally degraded by SIAH2 irrespective of the presence of its kinase activity (Figure 30A). A similar result was observed in DYRK2 degradation by hypoxia treatment (Figure 30B). To determine in detail the effect of SIAH2 phosphorylation on DYRK2, we compared the ability of the SIAH2-5A phosphorylation mutant and the SIAH2-5D phospho-mimic mutant (Ser16, Thr26, Ser28, Ser68 and Thr119 to Asp) to degrade DYRK2. 293T cells were transfected with DYRK2 together with Flag-SIAH2-wt, Flag-SIAH2-5A and Flag-SIAH2-5D and DYRK2 expression was studied by immunoblotting (Figure 30C). Consistent with the previous experiments, DYRK2 was equally degraded by SIAH2 wild type compared with the SIAH2 mutants. Taken together, these results show that SIAH2 phosphorylation has no effects on its capacity to degrade DYRK2.

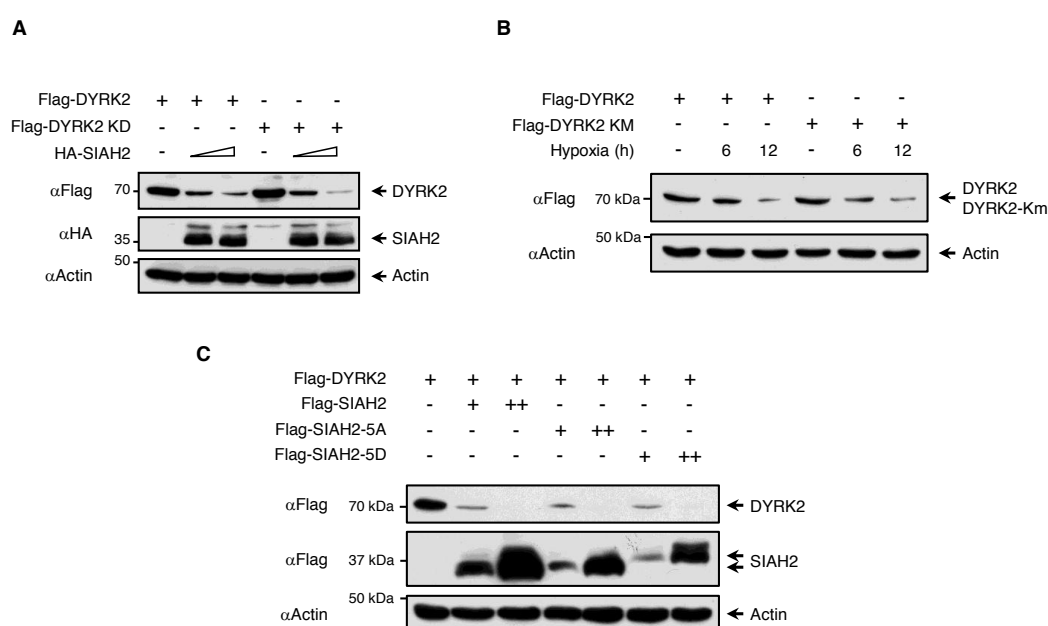


Figure 30. SIAH2 phosphorylation has no effect upon DYRK2 stability. **A.** 293T cells were transfected with expression vectors encoding Flag-DYRK2 and Flag-DYRK2 kinase dead mutant with increasing concentration of HA-SIAH2. The next day cells were lysed and the stability of DYRK2 was revealed by immunoblotting. **B.** 293T cells were transfected with Flag-DYRK2 or Flag-DYRK2-KD (kinase death) and grown under normoxia or hypoxia (1% O₂) for the indicated times before lysis. DYRK2 protein levels were analyzed by immunoblotting. **C.** 293T cells were co-transfected with Flag-DYRK2 and an increasing concentration of Flag-SIAH2 or mutants -5A, 5D. Cell lysates were evaluated by immunoblot with the indicated antibodies.

Next we were interested in studying how SIAH2 phosphorylation affects its stability. To confirm this possibility 293T cells were transfected with Flag-SIAH2 or Flag-SIAH2-5A with or without HA-DYRK2 in the presence or absence of MG-132 (Figure 31A). Both SIAH2 and SIAH2-5A mutants were able to degrade DYRK2 equally, which reinforces the hypothesis that the phosphorylation state does not alter SIAH2 ability to degrade DYRK2. However, Flag-SIAH2-5A mutant showed much more stability than Flag-SIAH2-wt in the absence of MG-132. This indicates that SIAH2 phosphorylation in these 5 sites can affect SIAH2 stability. To assess whether the stability change of SIAH2 could be due to an alteration in its activity, we compared SIAH2-wt self-ubiquitination activity to that of SIAH2-5A mutant. As shown in Figure 31B, both of them showed a similar ubiquitination pattern, pointing that the phosphorylation state does not seem to affect SIAH2 ligase ubiquitin activity.

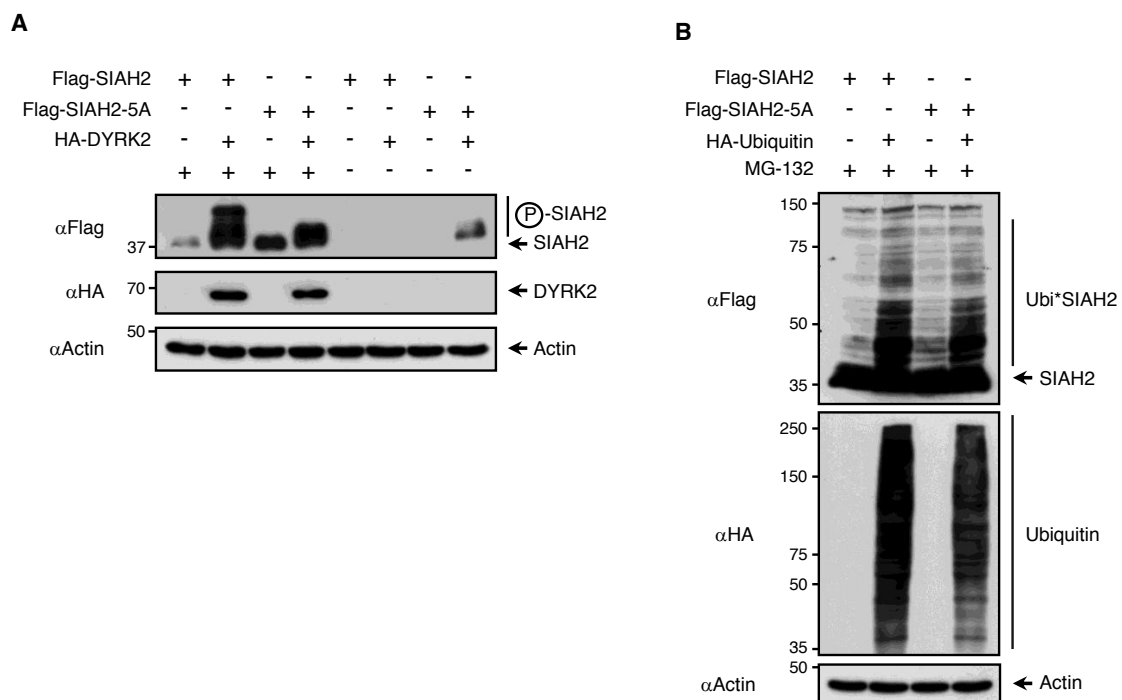


Figure 31. Phosphorylated SIAH2 is less stable. **A.** Cells were transfected with expression vectors encoding HA-DYRK2 and limiting amounts of Flag tagged versions of SIAH2 or SIAH2-5A with or without MG-132. Cell lysates were analysed by immunoblotting. **B.** 293T cells were transfected with expression vectors encoding HA-Ubiquitin, Flag-SIAH2 or Flag-SIAH2-5A, and treated with MG-132 during 12 h before lysis. Cell lysates were analysed by immunoblotting.

To investigate the consequences of SIAH2 phosphorylation for its intracellular localization, HeLa cells were transfected with Flag-SIAH2, Flag-SIAH2-5A and Flag-SIAH2-5D and analyzed by immunofluorescence microscopy. SIAH2 wild type and SIAH2-5A showed a similar localization pattern and were found mainly in the nucleus

and partially in cytoplasm (Figure 32). In contrast, the phosphomimic mutant showed a decrease in its nuclear localization which was paralleled by an increased localization in the perinuclear region. These results suggest that SIAH2 phosphorylation state can affect its stability, without affecting its self-ubiquitination activity probably because of a change in its subcellular localization.

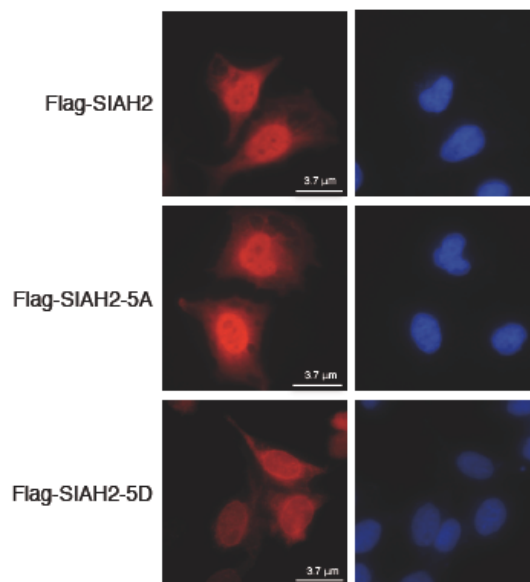


Figure 32. Phosphorylated SIAH2 locates differently. U2OS cells expressing the indicate plasmids were treated with MG-132, fixed and SIAH2 wild type, SIAH2-5A, and SIAH2-5D were detected by indirect immunofluorescence microscopy. Nuclear DNA (blue) was stained with DAPI.

While the phosphorylation state of SIAH2 had no impact on DYRK2 it was interesting to investigate possible effects for other SIAH2 substrates. Thus we examined the effect of the SIAH2 phosphorylation state on its ability to degrade PHD3, one of the most relevant SIAH2 substrates and a key protein in the hypoxia response pathway. Cells were transfected with PHD3 together with different SIAH2 variants and a luciferase construct controlled by the HIF-1-dependent erythropoietin promoter (Epo-Luc) as indicated (Figure 33). SIAH2 expression produced a clear decrease in PHD3 expression, which was reflected in a significant increase of HIF-dependent Epo-Luc promoter activity. The SIAH2-5A phosphorylation mutant showed a reduced ability to degrade PHD3 (compare lanes 3 and 2), which was reflected in a lower response to Epo-Luc promoter. In contrast, the phospho-mimetic SIAH2-5D mutant showed a strongly increased ability to degrade PHD3 (compare lanes 4 and 1), which was also reflected by a further increase of the Epo-Luc promoter response. Similar results were observed when SIAH2 phosphorylation was triggered upon co-expression of DYRK2.

These data suggest that SIAH2 phosphorylation state can modulate its ability to degrade PHD3.

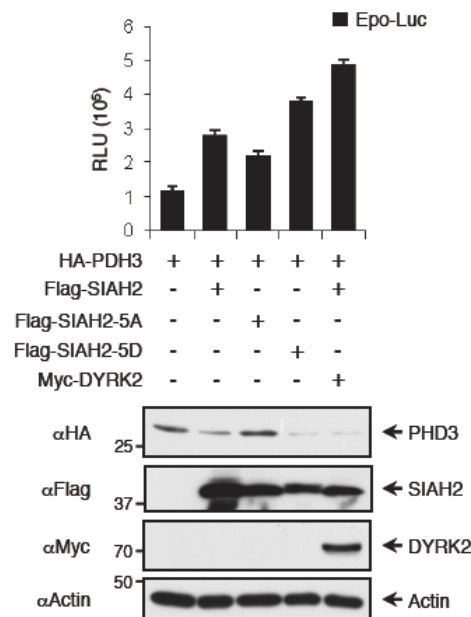


Figure 33. Phosphorylation of SIAH2 by DYRK2 affects its ability to degrade PHD3. Cells were transfected with the indicated expression vectors together with an HIF-responsive, erythropoietin promoter-derived luciferase construct (Epo-Luc). An empty expression vector was included for normalization of the transfections. Two days later, cells were cultured and analysed for luciferase expression (upper panel) or by immunoblotting (lower panel). Data are means \pm S.D of n=3 experiments.

To test the functional consequences of SIAH2 phosphorylation on the hypoxia response pathway in a physiological model, we measured endothelial cell tube formation as a model of angiogenesis. HUVEC cells were transfected with the different SIAH2 variants and tubule formation was quantified using a BD PathwayTM Bioimager (Figure 34). SIAH2 expression resulted in an increased tube total length and tube branch points. The tubular structures in HUVEC transfected with the SIAH-5A mutant were significantly (tubes total length $P < 0.05$, tubes branch points $P < 0.01$) shorter than those transfected with SIAH2 wild type. On the other hand, SIAH2-5D expression resulted in an increased number of tubular structures, strongly corroborating the finding that phosphorylated SIAH2 has an augmented ability to trigger the hypoxic response. These results identify the phosphorylation state of SIAH2 as a critical step in the control of the hypoxia response pathway, which has a clear consequence on angiogenesis.

On the whole these results emphasize the use of NADA, SIAH2 and DYRK2 as potential targets of therapeutic intervention for advanced cancers,

which may be achieved by restoring and inhibiting DYRK2 and SIAH2 expression and function, respectively.

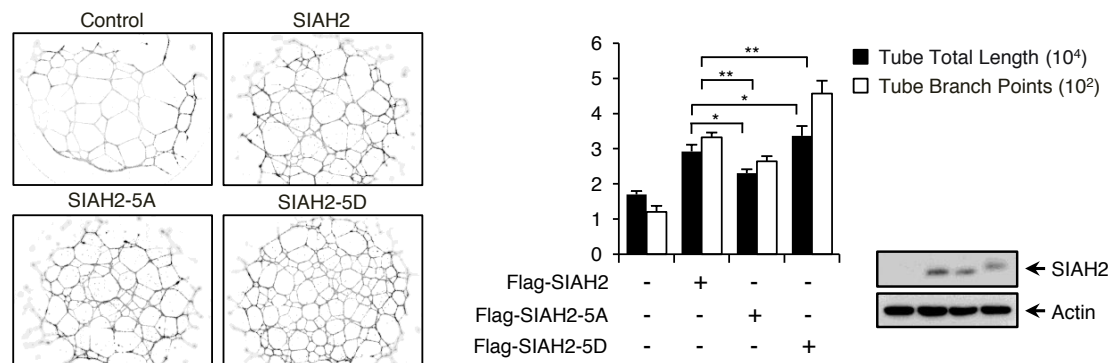


Figure 34. Enhanced down-regulation of PHD3 in the presence of phosphorylated SIAH2. HUVEC cells were transfected with expression vectors encoding Flag-SIAH2 and the variant mutants Flag-SIAH2-5A and Flag-SIAH2-5D two days prior to plating on Matrigel-coated culture dishes. Quantitative analysis of tube formation was performed in a BD Pathway 855 Bioimager using Attovision v 1.7 BD software. Protein levels were analysed by immunoblot. Three independent experiments were performed. Data are means \pm S.D of n=3 experiments.

Discussion

Discussion

The metabolism of the arachidonic acid by cyclooxygenases plays an important role both in physiological and pathological events in the CNS (Hewett et al, 2006). At the CNS level it has been demonstrated that the hippocampus and the striatum are the regions of the brain containing higher concentrations of NADA (Huang et al, 2002). Thus, the cells in these regions may also have a biosynthetic pathway of N-acyl-dopamines similar to the cells of the carotid body and under pro-inflammatory conditions CNS cells could release NADA in the brain and induce not only activities inherent to the activation of TRPV1 and CB1 receptors but also neuroprotective activities.

Like many genes coding for mRNA short half-life (i.e. cytokines), the COX-2 gene also contains ARE sequences (composed by six elements AUUUA), which regulate the stability of mRNA within the 30-UTR region. Previous studies have shown that ARE sequences present in the 30-UTR of COX-2 gene are responsible for the mRNA stabilization (Cok & Morrison, 2001; Dixon et al, 2000; Lasa et al, 2000). Our results indicate that NADA, and probably other N-acyl-dopamines, increase the half-life of the COX-2 mRNA in microvascular endothelial cells and this mechanism is dependent on the activation of p38. In other cell models it has been demonstrated that the activation of p38 allows the activation of MAPKAPK-2, which in turn activates a heat shock protein 27 (HSP27). This HSP27 has been implicated in the stabilization of COX-2 mRNA and, therefore, it is very likely that the final mechanism by which NADA induces the stabilization of COX-2 is due to activation of HSP27. All these results clearly show a potential role for NADA at the CNS highlighting the potential of endocannabinoids and N-acyldopamines as therapeutic agents for the treatment of inflammatory diseases and neuroprotection.

As well as NADA, HIF-1 α involvement in neuroprotection drove us to test the relationship between them. Our results show for the first time the effect of NADA on HIF-1 α levels. Furthermore, since SIAH2 is a protein at the apex of the hypoxia response that rises the transcription factor HIF-1 α we tested the possibility that NADA could modulate HIF-1 α by means of a primarily down-regulation of SIAH2. In short, we found that NADA mediates SIAH2 down-regulation with clear outcomes in HIF-1 α levels.

The relation between SIAH2 and tumourigenesis has been widely described in the literature (House et al, 2009; Telerman & Amson, 2009). The role of this ubiquitin ligase as an expression modulator of the pro-angiogenic transcription factor HIF-1 α , has brought an interest in the development of mechanisms able to regulate its expression (Qi et al, 2010; Qi et al, 2008). Different approaches have shown promising results, underlining the importance that SIAH2 modulation can exert on hypoxia-mediated angiogenesis (Ahmed et al, 2008; Moller et al, 2009; Schmidt et al, 2007). A recent study performed on *Siah2*^{-/-} mice has demonstrated how this protein attenuates HIF1 α -mediated angiogenesis improving responses to chemotherapy, showing once more the importance of this upstream regulator of hypoxia (Wong et al, 2012). Thus SIAH inhibition would decrease the response of different tumourigenic pathways such as DNA damage signalling networks (Calzado et al, 2009; Matsuzawa & Reed, 2001), Ras pathway (Ahmed et al, 2008; Schmidt et al, 2007) and estrogen receptors (Jansen et al, 2009). In this dissertation we have shown a new way whereby the endocannabinoid NADA down-regulates SIAH2 levels.

The regulation of ubiquitin ligases is essential for the control of substrate expression. Although different common regulatory mechanisms for E3 ligases, such as deubiquitinating and sumoylation, have been described, little is known about the role of phosphorylation on ubiquitin ligases (de Bie & Ciechanover, 2011; Lipkowitz & Weissman, 2011). Others and we have shown that SIAH2 can be phosphorylated affecting its activity. To our knowledge, only two kinases have been described: HIPK2 in human SIAH2 and p38 in mice (Calzado et al, 2009; Khurana et al, 2006). In this context, the present study shows for the first time the ability of DYRK2 to interact and phosphorylate human SIAH2 in at least five residues (Ser16, Thr26, Ser28, Ser68 and Thr119), two of which have not been described before. This ability of DYRK2 to interact with an E3 ubiquitin ligase coincides with recent studies that seem to demonstrate a possible role of this kinase in protein proteolysis (Maddika & Chen, 2009; Varjosalo et al, 2008). In this study we also show that SIAH2 phosphorylation state affects its activity, increasing PHD3 degradation and consequently HIF-1 α levels, possibly due to a change in cell localization. These results are consistent with previous reports describing how SIAH1/2 phosphorylation is able to modulate its activity on certain substrates (House et al, 2009; Winter et al, 2008). We have also observed how this control of the hypoxia response pathway has a consequence on angiogenesis development. In this sense, although there are reports showing the relation between SIAH2 expression and tumourigenesis, the role of SIAH2 phosphorylation has not been

investigated previously. It will therefore be relevant to investigate potential changes of SIAH2 phosphorylation and its regulating events in physiological and pathophysiological settings in the future.

On the other hand, our findings also show that SIAH2 is able to regulate DYRK2 expression by an ubiquitination mechanism that is enhanced under hypoxia conditions. Protein kinases are important for all fundamental processes and thus their activities must be tightly controlled, as unrestrained kinase activities as they occur for example in the oncogenic mutant versions of Raf-1 or Src kinases can lead to tumor development (Mansour et al, 1994). Cis-autophosphorylation of DYRK2 results in a constitutively active kinase that needs no additional activation signals from upstream kinases (Lochhead et al, 2005), thus raising the need to control DYRK2 activities by other mechanisms. These include DNA damage-induced nuclear translocation (Taira et al, 2007) and ubiquitin/proteasome-mediated control of its protein stability. Accordingly, DYRK2 levels are kept low by constant ubiquitination that can be mediated by Mdm2 (Taira et al, 2010) and also by SIAH2, as revealed in this study. The relative contribution of both E3 ligases for the steady-state-levels of DYRK2 are currently not known, but the strong upregulation of DYRK2 protein levels in the presence of a SIAH2-specific siRNA point to an important role of SIAH2.

Although DYRK2 functional role is not well known, recent publications by Yoshida K. group have risen the interest on this kinase and its modulation due to its relevant role on tumour progression control. First, DYRK2 exerts an important role on the regulation of the p53 tumour suppressor through its phosphorylation on Ser46, which is necessary for the induction of apoptosis in response to DNA damage (Taira et al, 2007). More recently, they have described the role exerted by DYRK2 on cell cycle progression through c-Jun and c-Myc phosphorylation, and how DYRK2 inactivation has a relevant role on proliferation and tumour progression (Taira et al, 2012). However, DYRK2 expression in human tumours is uncertain, and there is no concluding study about this subject. While mutations of DYRK2 are not often found in cancer cells, a deregulated expression was described by several groups. Overexpression of DYRK2 was reported in esophageal and lung adenocarcinomas (Miller et al, 2003), but on the other hand recent published data point at a reduced or abolished DYRK2 expression in multiple human tumour tissues, which correlates with invasiveness in the case of human breast cancer (Taira et al, 2012). Our data show that DNA damage-induced p53 Ser46 phosphorylation is strongly diminished under

hypoxic conditions, which is due to degradation of DYRK2 and probably also HIPK2, another p53-phosphorylating kinase that is downregulated under hypoxic conditions (Calzado et al, 2009). These mechanisms are of potential clinical relevance in solid tumors, as their central regions are typically hypoxic and thus show diminished p53 phosphorylation and in addition these regions are not easily accessible for chemotherapeutic drugs. SIAH2 inhibition would increase HIPK2 and DYRK2 levels increasing cell sensibility to DNA damage induced apoptosis.

Taken together, our findings support a coordinated regulation model between SIAH2 and DYRK2 (Figure 35). On one hand, DYRK2 is able to phosphorylate SIAH2 modifying its activity on relevant substrates as PHD3, modulating the hypoxia response pathway. On the other hand, SIAH2 is capable of interact and polyubiquitinate DYRK2 promoting its degradation by the proteasome, and altering the p53-dependent apoptosis in response to DNA damage. Further research is needed to explain how this equilibrium is altered and which cell stimuli are necessary to tip the balance in favour of one or the other.

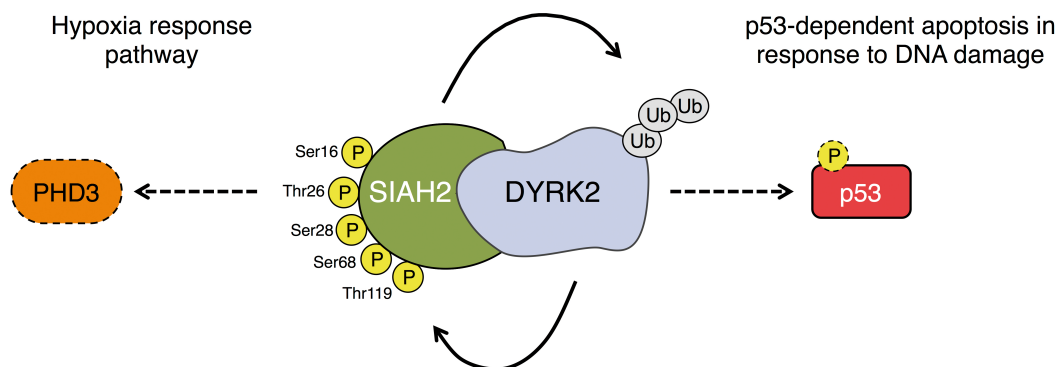


Figure 35. Schematic model summarizing the coordinate regulation between SIAH2 and DYRK2.

In short, we have found that NADA activates a redox-sensitive p38 pathway that stabilizes COX-2 mRNA resulting in the accumulation of the COX-2 protein, which leads to regulation of inflammation, immunomodulation, blood flow, apoptosis and fever. As well as that, we have described a modulatory effect of NADA over SIAH2, which is widely described as a major ubiquitin ligase involved in tumorigenesis and hypoxia. In parallel with the latter effect, we show for the first time the ability of DYRK2 to directly phosphorylate SIAH2 and, conversely, SIAH2-dependent DYRK2 degradation. Finally, we reveal that such dual regulation has clear outcomes in both

PHD3 and p53 responses. These findings suggest new ways to target inflammation, tumorigenesis and apoptosis and urges further research to elucidate which stimuli, and under what circumstances, tip the balance to tumorigenesis or apoptosis.

Conclusions

CONCLUSIONS

A number of conclusions can be drawn from this dissertation:

1. NADA induces p38 MAPK phosphorylation which instigates COX-2 expression in brain endothelial cells.
2. NADA-induced HIF-1 α expression correlates with SIAH2.
3. DYRK2 directly phosphorylates SIAH2 in five residues (S16, T26, S28, S68 and T119).
4. SIAH2 phosphorylation by DYRK2 makes it less stable and more efficient to degrade PHD3.
5. SIAH2 ubiquitinates DYRK2, which is degraded by the proteasome.
6. DYRK2 degradation by SIAH2 in hypoxia have important effects on p53 Ser46 phosphorylation.

References

Achiron A, Miron S, Lavie V, Margalit R, Biegon A (2000) Dexanabinol (HU-211) effect on experimental autoimmune encephalomyelitis: implications for the treatment of acute relapses of multiple sclerosis. *J Neuroimmunol* **102**: 26-31

Ahmed AU, Schmidt RL, Park CH, Reed NR, Hesse SE, Thomas CF, Molina JR, Deschamps C, Yang P, Aubry MC, Tang AH (2008) Effect of disrupting seven-in-absentia homolog 2 function on lung cancer cell growth. *J Natl Cancer Inst* **100**: 1606-1629

Appelhoff RJ, Tian YM, Raval RR, Turley H, Harris AL, Pugh CW, Ratcliffe PJ, Gleadle JM (2004) Differential function of the prolyl hydroxylases PHD1, PHD2, and PHD3 in the regulation of hypoxia-inducible factor. *J Biol Chem* **279**: 38458-38465

Aranda S, Laguna A, de la Luna S (2011) DYRK family of protein kinases: evolutionary relationships, biochemical properties, and functional roles. *FASEB J* **25**: 449-462

Bain J, Plater L, Elliott M, Shpiro N, Hastie CJ, McLauchlan H, Klevernic I, Arthur JS, Alessi DR, Cohen P (2007) The selectivity of protein kinase inhibitors: a further update. *Biochem J* **408**: 297-315

Bartek J, Lukas J (2003) Chk1 and Chk2 kinases in checkpoint control and cancer. *Cancer Cell* **3**: 421-429

Becker W, Joost HG (1999) Structural and functional characteristics of Dyrk, a novel subfamily of protein kinases with dual specificity. *Prog Nucleic Acid Res Mol Biol* **62**: 1-17

Becker W, Weber Y, Wetzels K, Eirimbter K, Tejedor FJ, Joost HG (1998) Sequence characteristics, subcellular localization, and substrate specificity of DYRK-related kinases, a novel family of dual specificity protein kinases. *J Biol Chem* **273**: 25893-25902

Bezuglov VV, Manevich EM, Archakov AV, Bobrov M, Kuklev DV, Petrukhina GN, Makarov VA, Buznikov GA (1997) [Artificially functionalized polyenoic fatty acids--a new lipid bioregulators]. *Bioorg Khim* **23**: 211-220

Bhanot M, Smith S (2012) TIN2 stability is regulated by the E3 ligase Siah2. *Mol Cell Biol* **32**: 376-384

Bobrov MY, Lizhin AA, Andrianova EL, Gretskaya NM, Frumkina LE, Khaspekov LG, Bezuglov VV (2008) Antioxidant and neuroprotective properties of N-arachidonoyldopamine. *Neurosci Lett* **431**: 6-11

Brognard J, Hunter T (2011) Protein kinase signaling networks in cancer. *Curr Opin Genet Dev* **21**: 4-11

Calzado MA, de la Vega L, Moller A, Bowtell DD, Schmitz ML (2009a) An inducible autoregulatory loop between HIPK2 and Siah2 at the apex of the hypoxic response. *Nat Cell Biol* **11**: 85-91

Calzado MA, de la Vega L, Munoz E, Schmitz ML (2009b) Autoregulatory control of the p53 response by Siah-1L-mediated HIPK2 degradation. *Biol Chem* **390**: 1079-1083

Campbell LE, Proud CG (2002) Differing substrate specificities of members of the DYRK family of arginine-directed protein kinases. *FEBS Lett* **510**: 31-36

- Cao C, Matsumura K, Shirakawa N, Maeda M, Jikihara I, Kobayashi S, Watanabe Y (2001) Pyrogenic cytokines injected into the rat cerebral ventricle induce cyclooxygenase-2 in brain endothelial cells and also upregulate their receptors. *Eur J Neurosci* **13**: 1781-1790
- Carlucci A, Adornetto A, Scorziello A, Viggiano D, Foca M, Cuomo O, Annunziato L, Gottesman M, Feliciello A (2008) Proteolysis of AKAP121 regulates mitochondrial activity during cellular hypoxia and brain ischaemia. *EMBO J* **27**: 1073-1084
- Carthew RW, Neufeld TP, Rubin GM (1994) Identification of genes that interact with the *sina* gene in *Drosophila* eye development. *Proc Natl Acad Sci U S A* **91**: 11689-11693
- Caterina MJ, Schumacher MA, Tominaga M, Rosen TA, Levine JD, Julius D (1997) The capsaicin receptor: a heat-activated ion channel in the pain pathway. *Nature* **389**: 816-824
- Caughey GE, Cleland LG, Gamble JR, James MJ (2001) Up-regulation of endothelial cyclooxygenase-2 and prostanoid synthesis by platelets. Role of thromboxane A₂. *J Biol Chem* **276**: 37839-37845
- Charames GS, Bapat B (2003) Genomic instability and cancer. *Curr Mol Med* **3**: 589-596
- Chu CJ, Huang SM, De Petrocellis L, Bisogno T, Ewing SA, Miller JD, Zipkin RE, Daddario N, Appendino G, Di Marzo V, Walker JM (2003) N-oleoyldopamine, a novel endogenous capsaicin-like lipid that produces hyperalgesia. *J Biol Chem* **278**: 13633-13639
- Cok SJ, Morrison AR (2001) The 3'-untranslated region of murine cyclooxygenase-2 contains multiple regulatory elements that alter message stability and translational efficiency. *J Biol Chem* **276**: 23179-23185
- Cortez D, Wang Y, Qin J, Elledge SJ (1999) Requirement of ATM-dependent phosphorylation of *brca1* in the DNA damage response to double-strand breaks. *Science* **286**: 1162-1166
- D'Orazi G, Cecchinelli B, Bruno T, Manni I, Higashimoto Y, Saito S, Gostissa M, Coen S, Marchetti A, Del Sal G, Piaggio G, Fanciulli M, Appella E, Soddu S (2002) Homeodomain-interacting protein kinase-2 phosphorylates p53 at Ser 46 and mediates apoptosis. *Nat Cell Biol* **4**: 11-19
- de Bie P, Ciechanover A (2011) Ubiquitination of E3 ligases: self-regulation of the ubiquitin system via proteolytic and non-proteolytic mechanisms. *Cell Death Differ* **18**: 1393-1402
- De Petrocellis L, Melck D, Bisogno T, Di Marzo V (2000) Endocannabinoids and fatty acid amides in cancer, inflammation and related disorders. *Chem Phys Lipids* **108**: 191-209
- Della NG, Senior PV, Bowtell DD (1993) Isolation and characterisation of murine homologues of the *Drosophila* *seven in absentia* gene (*sina*). *Development* **117**: 1333-1343

- Deng X, Ewton DZ, Mercer SE, Friedman E (2005) Mirk/dyrk1B decreases the nuclear accumulation of class II histone deacetylases during skeletal muscle differentiation. *J Biol Chem* **280**: 4894-4905
- Depaux A, Regnier-Ricard F, Germani A, Varin-Blank N (2006) Dimerization of hSiah proteins regulates their stability. *Biochem Biophys Res Commun* **348**: 857-863
- Di Fiore PP, Polo S, Hofmann K (2003) When ubiquitin meets ubiquitin receptors: a signalling connection. *Nat Rev Mol Cell Biol* **4**: 491-497
- Di M, Bisogno T, De Petrocellis L (2000) Endocannabinoids: new targets for drug development. *Curr Pharm Des* **6**: 1361-1380
- Di Marzo V, De Petrocellis L, Fezza F, Ligresti A, Bisogno T (2002) Anandamide receptors. *Prostaglandins Leukot Essent Fatty Acids* **66**: 377-391
- Dixon DA, Kaplan CD, McIntyre TM, Zimmerman GA, Prescott SM (2000) Post-transcriptional control of cyclooxygenase-2 gene expression. The role of the 3'-untranslated region. *J Biol Chem* **275**: 11750-11757
- Donzelli M, Draetta GF (2003) Regulating mammalian checkpoints through Cdc25 inactivation. *EMBO Rep* **4**: 671-677
- Dubois RN, Abramson SB, Crofford L, Gupta RA, Simon LS, Van De Putte LB, Lipsky PE (1998) Cyclooxygenase in biology and disease. *FASEB J* **12**: 1063-1073
- Falck J, Coates J, Jackson SP (2005) Conserved modes of recruitment of ATM, ATR and DNA-PKcs to sites of DNA damage. *Nature* **434**: 605-611
- Fanelli M, Fantozzi A, De Luca P, Caprodossi S, Matsuzawa S, Lazar MA, Pelicci PG, Minucci S (2004) The coiled-coil domain is the structural determinant for mammalian homologues of Drosophila Sina-mediated degradation of promyelocytic leukemia protein and other tripartite motif proteins by the proteasome. *J Biol Chem* **279**: 5374-5379
- Ferguson JE, 3rd, Wu Y, Smith K, Charles P, Powers K, Wang H, Patterson C (2007) ASB4 is a hydroxylation substrate of FIH and promotes vascular differentiation via an oxygen-dependent mechanism. *Mol Cell Biol* **27**: 6407-6419
- Fernandez-Capetillo O, Lee A, Nussenzweig M, Nussenzweig A (2004) H2AX: the histone guardian of the genome. *DNA Repair (Amst)* **3**: 959-967
- Fogal V, Gostissa M, Sandy P, Zacchi P, Sternsdorf T, Jensen K, Pandolfi PP, Will H, Schneider C, Del Sal G (2000) Regulation of p53 activity in nuclear bodies by a specific PML isoform. *EMBO J* **19**: 6185-6195
- Frew IJ, Hammond VE, Dickins RA, Quinn JM, Walkley CR, Sims NA, Schnall R, Della NG, Holloway AJ, Digby MR, Janes PW, Tarlinton DM, Purton LE, Gillespie MT, Bowtell DD (2003) Generation and analysis of Siah2 mutant mice. *Mol Cell Biol* **23**: 9150-9161
- Fukuba H, Takahashi T, Jin HG, Kohriyama T, Matsumoto M (2008) Abundance of asparaginyl-hydroxylase FIH is regulated by Siah-1 under normoxic conditions. *Neurosci Lett* **433**: 209-214

- Gatei M, Zhou BB, Hobson K, Scott S, Young D, Khanna KK (2001) Ataxia telangiectasia mutated (ATM) kinase and ATM and Rad3 related kinase mediate phosphorylation of Brca1 at distinct and overlapping sites. In vivo assessment using phospho-specific antibodies. *J Biol Chem* **276**: 17276-17280
- Geiger JN, Knudsen GT, Panek L, Pandit AK, Yoder MD, Lord KA, Creasy CL, Burns BM, Gaines P, Dillon SB, Wojchowski DM (2001) mDYRK3 kinase is expressed selectively in late erythroid progenitor cells and attenuates colony-forming unit-erythroid development. *Blood* **97**: 901-910
- Giusti S, Fiszer de Plazas S (2012) Neuroprotection by hypoxic preconditioning involves upregulation of hypoxia-inducible factor-1 in a prenatal model of acute hypoxia. *J Neurosci Res* **90**: 468-478
- Guimera J, Casas C, Pucharcos C, Solans A, Domenech A, Planas AM, Ashley J, Lovett M, Estivill X, Pritchard MA (1996) A human homologue of Drosophila minibrain (MNB) is expressed in the neuronal regions affected in Down syndrome and maps to the critical region. *Hum Mol Genet* **5**: 1305-1310
- Guo X, Williams JG, Schug TT, Li X (2010) DYRK1A and DYRK3 promote cell survival through phosphorylation and activation of SIRT1. *J Biol Chem* **285**: 13223-13232
- Gwack Y, Sharma S, Nardone J, Tanasa B, Iuga A, Srikanth S, Okamura H, Bolton D, Feske S, Hogan PG, Rao A (2006) A genome-wide Drosophila RNAi screen identifies DYRK-family kinases as regulators of NFAT. *Nature* **441**: 646-650
- Habelhah H, Frew IJ, Laine A, Janes PW, Relaix F, Sassoon D, Bowtell DD, Ronai Z (2002) Stress-induced decrease in TRAF2 stability is mediated by Siah2. *EMBO J* **21**: 5756-5765
- Habelhah H, Laine A, Erdjument-Bromage H, Tempst P, Gershwin ME, Bowtell DD, Ronai Z (2004) Regulation of 2-oxoglutarate (alpha-ketoglutarate) dehydrogenase stability by the RING finger ubiquitin ligase Siah. *J Biol Chem* **279**: 53782-53788
- Haglund K, Dikic I (2005) Ubiquitylation and cell signaling. *EMBO J* **24**: 3353-3359
- Harrison S, De Petrocellis L, Trevisani M, Benvenuti F, Bifulco M, Geppetti P, Di Marzo V (2003) Capsaicin-like effects of N-arachidonoyl-dopamine in the isolated guinea pig bronchi and urinary bladder. *Eur J Pharmacol* **475**: 107-114
- Harten SK, Ashcroft M, Maxwell PH (2010) Prolyl hydroxylase domain inhibitors: a route to HIF activation and neuroprotection. *Antioxid Redox Signal* **12**: 459-480
- Hershko A, Ciechanover A (1998) The ubiquitin system. *Annu Rev Biochem* **67**: 425-479
- Hewett SJ, Bell SC, Hewett JA (2006) Contributions of cyclooxygenase-2 to neuroplasticity and neuropathology of the central nervous system. *Pharmacol Ther* **112**: 335-357
- Hicke L, Schubert HL, Hill CP (2005) Ubiquitin-binding domains. *Nat Rev Mol Cell Biol* **6**: 610-621

- Himpel S, Panzer P, Eirnbter K, Czajkowska H, Sayed M, Packman LC, Blundell T, Kentrup H, Grotzinger J, Joost HG, Becker W (2001) Identification of the autophosphorylation sites and characterization of their effects in the protein kinase DYRK1A. *Biochem J* **359**: 497-505
- Hirota K, Semenza GL (2005) Regulation of hypoxia-inducible factor 1 by prolyl and asparaginyl hydroxylases. *Biochem Biophys Res Commun* **338**: 610-616
- Hochstrasser M (2000) Evolution and function of ubiquitin-like protein-conjugation systems. *Nat Cell Biol* **2**: E153-157
- Hoeijmakers JH (2001) Genome maintenance mechanisms for preventing cancer. *Nature* **411**: 366-374
- Hoeller D, Hecker CM, Dikic I (2006) Ubiquitin and ubiquitin-like proteins in cancer pathogenesis. *Nat Rev Cancer* **6**: 776-788
- Hofmann TG, Moller A, Sirma H, Zentgraf H, Taya Y, Droge W, Will H, Schmitz ML (2002) Regulation of p53 activity by its interaction with homeodomain-interacting protein kinase-2. *Nat Cell Biol* **4**: 1-10
- Holloway AJ, Della NG, Fletcher CF, Largespada DA, Copeland NG, Jenkins NA, Bowtell DD (1997) Chromosomal mapping of five highly conserved murine homologues of the Drosophila RING finger gene seven-in-absentia. *Genomics* **41**: 160-168
- Hon WC, Wilson MI, Harlos K, Claridge TD, Schofield CJ, Pugh CW, Maxwell PH, Ratcliffe PJ, Stuart DI, Jones EY (2002) Structural basis for the recognition of hydroxyproline in HIF-1 alpha by pVHL. *Nature* **417**: 975-978
- House CM, Hancock NC, Moller A, Cromer BA, Fedorov V, Bowtell DD, Parker MW, Polekhina G (2006) Elucidation of the substrate binding site of Siah ubiquitin ligase. *Structure* **14**: 695-701
- House CM, Moller A, Bowtell DD (2009) Siah proteins: novel drug targets in the Ras and hypoxia pathways. *Cancer Res* **69**: 8835-8838
- Hu G, Chung YL, Glover T, Valentine V, Look AT, Fearon ER (1997a) Characterization of human homologs of the Drosophila seven in absentia (sina) gene. *Genomics* **46**: 103-111
- Hu G, Zhang S, Vidal M, Baer JL, Xu T, Fearon ER (1997b) Mammalian homologs of seven in absentia regulate DCC via the ubiquitin-proteasome pathway. *Genes Dev* **11**: 2701-2714
- Huang SM, Bisogno T, Trevisani M, Al-Hayani A, De Petrocellis L, Fezza F, Tognetto M, Petros TJ, Krey JF, Chu CJ, Miller JD, Davies SN, Geppetti P, Walker JM, Di Marzo V (2002) An endogenous capsaicin-like substance with high potency at recombinant and native vanilloid VR1 receptors. *Proc Natl Acad Sci U S A* **99**: 8400-8405
- Huang TT, Wuerzberger-Davis SM, Wu ZH, Miyamoto S (2003) Sequential modification of NEMO/IKKgamma by SUMO-1 and ubiquitin mediates NF-kappaB activation by genotoxic stress. *Cell* **115**: 565-576

Ivan M, Kondo K, Yang H, Kim W, Valiando J, Ohh M, Salic A, Asara JM, Lane WS, Kaelin WG, Jr. (2001) HIF α targeted for VHL-mediated destruction by proline hydroxylation: implications for O₂ sensing. *Science* **292**: 464-468

Iwai K, Yamanaka K, Kamura T, Minato N, Conaway RC, Conaway JW, Klausner RD, Pause A (1999) Identification of the von Hippel-Lindau tumor-suppressor protein as part of an active E3 ubiquitin ligase complex. *Proc Natl Acad Sci U S A* **96**: 12436-12441

Jaakkola P, Mole DR, Tian YM, Wilson MI, Gielbert J, Gaskell SJ, Kriegsheim A, Hestrestreit HF, Mukherji M, Schofield CJ, Maxwell PH, Pugh CW, Ratcliffe PJ (2001) Targeting of HIF- α to the von Hippel-Lindau ubiquitylation complex by O₂-regulated prolyl hydroxylation. *Science* **292**: 468-472

Jansen MP, Ruigrok-Ritstier K, Dorssers LC, van Staveren IL, Look MP, Meijer-van Gelder ME, Sieuwerts AM, Helleman J, Sleijfer S, Klijn JG, Foekens JA, Berns EM (2009) Downregulation of SIAH2, an ubiquitin E3 ligase, is associated with resistance to endocrine therapy in breast cancer. *Breast Cancer Res Treat* **116**: 263-271

Jeong JW, Bae MK, Ahn MY, Kim SH, Sohn TK, Bae MH, Yoo MA, Song EJ, Lee KJ, Kim KW (2002) Regulation and destabilization of HIF-1 α by ARD1-mediated acetylation. *Cell* **111**: 709-720

Kaelin WG (2005) Proline hydroxylation and gene expression. *Annu Rev Biochem* **74**: 115-128

Kentrup H, Becker W, Heukelbach J, Wilmes A, Schurmann A, Huppertz C, Kainulainen H, Joost HG (1996) Dyrk, a dual specificity protein kinase with unique structural features whose activity is dependent on tyrosine residues between subdomains VII and VIII. *J Biol Chem* **271**: 3488-3495

Khosravi R, Maya R, Gottlieb T, Oren M, Shiloh Y, Shkedy D (1999) Rapid ATM-dependent phosphorylation of MDM2 precedes p53 accumulation in response to DNA damage. *Proc Natl Acad Sci U S A* **96**: 14973-14977

Khurana A, Nakayama K, Williams S, Davis RJ, Mustelin T, Ronai Z (2006) Regulation of the ring finger E3 ligase Siah2 by p38 MAPK. *J Biol Chem* **281**: 35316-3532

Kibel A, Iliopoulos O, DeCaprio JA, Kaelin WG, Jr. (1995) Binding of the von Hippel-Lindau tumor suppressor protein to Elongin B and C. *Science* **269**: 1444-1446

Kilroy G, Kirk-Ballard H, Carter LE, Floyd ZE (2012) The Ubiquitin Ligase Siah2 Regulates PPAR γ Activity in Adipocytes. *Endocrinology* **153**: 1206-1218

Kim H, Scimia MC, Wilkinson D, Trelles RD, Wood MR, Bowtell D, Dillin A, Mercola M, Ronai ZA (2011) Fine-tuning of Drp1/Fis1 availability by AKAP121/Siah2 regulates mitochondrial adaptation to hypoxia. *Mol Cell* **44**: 532-544

Komiyama S, Taniguchi S, Matsumoto Y, Tsunoda E, Ohto T, Suzuki Y, Yin HL, Tomita M, Enomoto A, Morita A, Suzuki T, Ohtomo K, Hosoi Y, Suzuki N (2004) Potentiality of DNA-dependent protein kinase to phosphorylate Ser46 of human p53. *Biochem Biophys Res Commun* **323**: 816-822

Kumagai A, Kim SM, Dunphy WG (2004) Claspin and the activated form of ATR-ATRIP collaborate in the activation of Chk1. *J Biol Chem* **279**: 49599-49608

- Kyriakis JM, Avruch J (2001) Mammalian mitogen-activated protein kinase signal transduction pathways activated by stress and inflammation. *Physiol Rev* **81**: 807-869
- Lasa M, Mahtani KR, Finch A, Brewer G, Saklatvala J, Clark AR (2000) Regulation of cyclooxygenase 2 mRNA stability by the mitogen-activated protein kinase p38 signaling cascade. *Mol Cell Biol* **20**: 4265-4274
- Le Moan N, Houslay DM, Christian F, Houslay MD, Akassoglou K (2011) Oxygen-dependent cleavage of the p75 neurotrophin receptor triggers stabilization of HIF-1alpha. *Mol Cell* **44**: 476-490
- Leder S, Weber Y, Altafaj X, Estivill X, Joost HG, Becker W (1999) Cloning and characterization of DYRK1B, a novel member of the DYRK family of protein kinases. *Biochem Biophys Res Commun* **254**: 474-479
- Lee K, Deng X, Friedman E (2000) Mirk protein kinase is a mitogen-activated protein kinase substrate that mediates survival of colon cancer cells. *Cancer Res* **60**: 3631-3637
- Li K, Zhao S, Karur V, Wojchowski DM (2002a) DYRK3 activation, engagement of protein kinase A/cAMP response element-binding protein, and modulation of progenitor cell survival. *J Biol Chem* **277**: 47052-47060
- Li S, Li Y, Carthew RW, Lai ZC (1997) Photoreceptor cell differentiation requires regulated proteolysis of the transcriptional repressor Tramtrack. *Cell* **90**: 469-478
- Li S, Xu C, Carthew RW (2002b) Phyllopod acts as an adaptor protein to link the sina ubiquitin ligase to the substrate protein tramtrack. *Mol Cell Biol* **22**: 6854-6865
- Liani E, Eyal A, Avraham E, Shemer R, Szargel R, Berg D, Bornemann A, Riess O, Ross CA, Rott R, Engelender S (2004) Ubiquitylation of synphilin-1 and alpha-synuclein by SIAH and its presence in cellular inclusions and Lewy bodies imply a role in Parkinson's disease. *Proc Natl Acad Sci U S A* **101**: 5500-5505
- Lim DS, Kim ST, Xu B, Maser RS, Lin J, Petrini JH, Kastan MB (2000) ATM phosphorylates p95/nbs1 in an S-phase checkpoint pathway. *Nature* **404**: 613-617
- Lipkowitz S, Weissman AM (2011) RINGs of good and evil: RING finger ubiquitin ligases at the crossroads of tumour suppression and oncogenesis. *Nat Rev Cancer* **11**: 629-643
- Lochhead PA, Sibbet G, Kinstrie R, Cleghon T, Rylatt M, Morrison DK, Cleghon V (2003) dDYRK2: a novel dual-specificity tyrosine-phosphorylation-regulated kinase in Drosophila. *Biochem J* **374**: 381-391
- Lochhead PA, Sibbet G, Morrice N, Cleghon V (2005) Activation-loop autophosphorylation is mediated by a novel transitional intermediate form of DYRKs. *Cell* **121**: 925-936
- Lord KA, Creasy CL, King AG, King C, Burns BM, Lee JC, Dillon SB (2000) REDK, a novel human regulatory erythroid kinase. *Blood* **95**: 2838-2846

Lorick KL, Jensen JP, Fang S, Ong AM, Hatakeyama S, Weissman AM (1999) RING fingers mediate ubiquitin-conjugating enzyme (E2)-dependent ubiquitination. *Proc Natl Acad Sci U S A* **96**: 11364-11369

Maddika S, Chen J (2009) Protein kinase DYRK2 is a scaffold that facilitates assembly of an E3 ligase. *Nat Cell Biol* **11**: 409-419

Mahon PC, Hirota K, Semenza GL (2001) FIH-1: a novel protein that interacts with HIF-1alpha and VHL to mediate repression of HIF-1 transcriptional activity. *Genes Dev* **15**: 2675-2686

Malfitano AM, Matarese G, Pisanti S, Grimaldi C, Laezza C, Bisogno T, Di Marzo V, Lechler RI, Bifulco M (2006) Arvanil inhibits T lymphocyte activation and ameliorates autoimmune encephalomyelitis. *J Neuroimmunol* **171**: 110-119

Mansour SJ, Matten WT, Hermann AS, Candia JM, Rong S, Fukasawa K, Vande Woude GF, Ahn NG (1994) Transformation of mammalian cells by constitutively active MAP kinase kinase. *Science* **265**: 966-970

Mark KS, Trickler WJ, Miller DW (2001) Tumor necrosis factor-alpha induces cyclooxygenase-2 expression and prostaglandin release in brain microvessel endothelial cells. *J Pharmacol Exp Ther* **297**: 1051-1058

Matsuo R, Ochiai W, Nakashima K, Taga T (2001) A new expression cloning strategy for isolation of substrate-specific kinases by using phosphorylation site-specific antibody. *J Immunol Methods* **247**: 141-151

Matsuzawa SI, Reed JC (2001) Siah-1, SIP, and Ebi collaborate in a novel pathway for beta-catenin degradation linked to p53 responses. *Mol Cell* **7**: 915-926

Maya R, Balass M, Kim ST, Shkedy D, Leal JF, Shifman O, Moas M, Buschmann T, Ronai Z, Shiloh Y, Kastan MB, Katzir E, Oren M (2001) ATM-dependent phosphorylation of Mdm2 on serine 395: role in p53 activation by DNA damage. *Genes Dev* **15**: 1067-1077

Mbonye UR, Wada M, Rieke CJ, Tang HY, Dewitt DL, Smith WL (2006) The 19-amino acid cassette of cyclooxygenase-2 mediates entry of the protein into the endoplasmic reticulum-associated degradation system. *J Biol Chem* **281**: 35770-35778

Melnikova I, Golden J (2004) Targeting protein kinases. *Nat Rev Drug Discov* **3**: 993-994

Melvin A, Mudie S, Rocha S (2011) The chromatin remodeler ISWI regulates the cellular response to hypoxia: role of FIH. *Mol Biol Cell* **22**: 4171-4181

Mercer SE, Ewton DZ, Deng X, Lim S, Mazur TR, Friedman E (2005) Mirk/Dyrk1B mediates survival during the differentiation of C2C12 myoblasts. *J Biol Chem* **280**: 25788-25801

Mercer SE, Friedman E (2006) Mirk/Dyrk1B: a multifunctional dual-specificity kinase involved in growth arrest, differentiation, and cell survival. *Cell Biochem Biophys* **45**: 303-315

- Mifflin RC, Saada JI, Di Mari JF, Adegboyega PA, Valentich JD, Powell DW (2002) Regulation of COX-2 expression in human intestinal myofibroblasts: mechanisms of IL-1-mediated induction. *Am J Physiol Cell Physiol* **282**: C824-834
- Miller CT, Aggarwal S, Lin TK, Dagenais SL, Contreras JI, Orringer MB, Glover TW, Beer DG, Lin L (2003) Amplification and overexpression of the dual-specificity tyrosine-(Y)-phosphorylation regulated kinase 2 (DYRK2) gene in esophageal and lung adenocarcinomas. *Cancer Res* **63**: 4136-4143
- Miyata Y, Nishida E (1999) Distantly related cousins of MAP kinase: biochemical properties and possible physiological functions. *Biochem Biophys Res Commun* **266**: 291-295
- Moller A, House CM, Wong CS, Scanlon DB, Liu MC, Ronai Z, Bowtell DD (2009) Inhibition of Siah ubiquitin ligase function. *Oncogene* **28**: 289-296
- Moolwaney AS, Igwe OJ (2005) Regulation of the cyclooxygenase-2 system by interleukin-1beta through mitogen-activated protein kinase signaling pathways: a comparative study of human neuroglioma and neuroblastoma cells. *Brain Res Mol Brain Res* **137**: 202-212
- Nadeau RJ, Toher JL, Yang X, Kovalenko D, Friesel R (2007) Regulation of Sprouty2 stability by mammalian Seven-in-Absentia homolog 2. *J Cell Biochem* **100**: 151-160
- Nakayama K, Frew IJ, Hagensen M, Skals M, Habelhah H, Bhoumik A, Kadoya T, Erdjument-Bromage H, Tempst P, Frappell PB, Bowtell DD, Ronai Z (2004) Siah2 regulates stability of prolyl-hydroxylases, controls HIF1alpha abundance, and modulates physiological responses to hypoxia. *Cell* **117**: 941-952
- Nakayama K, Qi J, Ronai Z (2009) The ubiquitin ligase Siah2 and the hypoxia response. *Mol Cancer Res* **7**: 443-451
- Navarrete CM, Fiebich BL, de Vinuesa AG, Hess S, de Oliveira AC, Candelario-Jalil E, Caballero FJ, Calzado MA, Munoz E (2009) Opposite effects of anandamide and N-arachidonoyl dopamine in the regulation of prostaglandin E and 8-iso-PGF formation in primary glial cells. *J Neurochem* **109**: 452-464
- O'Sullivan SE, Kendall DA, Randall MD (2004) Characterisation of the vasorelaxant properties of the novel endocannabinoid N-arachidonoyl-dopamine (NADA). *Br J Pharmacol* **141**: 803-812
- Oda K, Arakawa H, Tanaka T, Matsuda K, Tanikawa C, Mori T, Nishimori H, Tamai K, Tokino T, Nakamura Y, Taya Y (2000) p53AIP1, a potential mediator of p53-dependent apoptosis, and its regulation by Ser-46-phosphorylated p53. *Cell* **102**: 849-862
- Pause A, Lee S, Worrell RA, Chen DY, Burgess WH, Linehan WM, Klausner RD (1997) The von Hippel-Lindau tumor-suppressor gene product forms a stable complex with human CUL-2, a member of the Cdc53 family of proteins. *Proc Natl Acad Sci U S A* **94**: 2156-2161
- Peers C (1997) Oxygen-sensitive ion channels. *Trends Pharmacol Sci* **18**: 405-408

- Polekhina G, House CM, Traficante N, Mackay JP, Relaix F, Sassoon DA, Parker MW, Bowtell DD (2002) Siah ubiquitin ligase is structurally related to TRAF and modulates TNF-alpha signaling. *Nat Struct Biol* **9**: 68-75
- Pommier Y, Weinstein JN, Aladjem MI, Kohn KW (2006) Chk2 molecular interaction map and rationale for Chk2 inhibitors. *Clin Cancer Res* **12**: 2657-2661
- Pryce G, Ahmed Z, Hankey DJ, Jackson SJ, Croxford JL, Pocock JM, Ledent C, Petzold A, Thompson AJ, Giovannoni G, Cuzner ML, Baker D (2003) Cannabinoids inhibit neurodegeneration in models of multiple sclerosis. *Brain* **126**: 2191-2202
- Puca R, Nardinocchi L, Sacchi A, Rechavi G, Givol D, D'Orazi G (2009) HIPK2 modulates p53 activity towards pro-apoptotic transcription. *Mol Cancer* **8**: 85
- Qi J, Nakayama K, Cardiff RD, Borowsky AD, Kaul K, Williams R, Krajewski S, Mercola D, Carpenter PM, Bowtell D, Ronai ZA (2010) Siah2-dependent concerted activity of HIF and FoxA2 regulates formation of neuroendocrine phenotype and neuroendocrine prostate tumors. *Cancer Cell* **18**: 23-38
- Qi J, Nakayama K, Gaitonde S, Goydos JS, Krajewski S, Eroshkin A, Bar-Sagi D, Bowtell D, Ronai Z (2008) The ubiquitin ligase Siah2 regulates tumorigenesis and metastasis by HIF-dependent and -independent pathways. *Proc Natl Acad Sci U S A* **105**: 16713-16718
- Rennefahrt U, Janakiraman M, Ollinger R, Troppmair J (2005) Stress kinase signaling in cancer: fact or fiction? *Cancer Lett* **217**: 1-9
- Ridley SH, Dean JL, Sarsfield SJ, Brook M, Clark AR, Saklatvala J (1998) A p38 MAP kinase inhibitor regulates stability of interleukin-1-induced cyclooxygenase-2 mRNA. *FEBS Lett* **439**: 75-80
- Ritterhoff S, Farah CM, Grabitzki J, Lochnit G, Skurat AV, Schmitz ML (2010) The WD40-repeat protein Han11 functions as a scaffold protein to control HIPK2 and MEKK1 kinase functions. *EMBO J* **29**: 3750-3761
- Roepstorff P, Fohlman J (1984) Proposal for a common nomenclature for sequence ions in mass spectra of peptides. *Biomed Mass Spectrom* **11**: 601
- Roysarkar T, Sharan S, Wang J, Pawar SA, Cantwell CA, Johnson PF, Morrison DK, Wang JM, Sterneck E (2011) Identification of a Src Tyrosine Kinase/SIAH2 E3 Ubiquitin Ligase Pathway that Regulates C/EBPdelta Expression and Contributes to Transformation of Breast Tumor Cells. *Mol Cell Biol*
- Sacher F, Moller C, Bone W, Gottwald U, Fritsch M (2007) The expression of the testis-specific Dyrk4 kinase is highly restricted to step 8 spermatids but is not required for male fertility in mice. *Mol Cell Endocrinol* **267**: 80-88
- Saito S, Goodarzi AA, Higashimoto Y, Noda Y, Lees-Miller SP, Appella E, Anderson CW (2002) ATM mediates phosphorylation at multiple p53 sites, including Ser(46), in response to ionizing radiation. *J Biol Chem* **277**: 12491-12494
- Saleem A, Datta R, Yuan ZM, Kharbanda S, Kufe D (1995) Involvement of stress-activated protein kinase in the cellular response to 1-beta-D-arabinofuranosylcytosine and other DNA-damaging agents. *Cell Growth Differ* **6**: 1651-1658

- Sancho R, Macho A, de La Vega L, Calzado MA, Fiebich BL, Appendino G, Munoz E (2004) Immunosuppressive activity of endovanilloids: N-arachidonoyl-dopamine inhibits activation of the NF-kappa B, NFAT, and activator protein 1 signaling pathways. *J Immunol* **172**: 2341-251
- Schmidt RL, Park CH, Ahmed AU, Gundelach JH, Reed NR, Cheng S, Knudsen BE, Tang AH (2007) Inhibition of RAS-mediated transformation and tumorigenesis by targeting the downstream E3 ubiquitin ligase seven in absentia homologue. *Cancer Res* **67**: 11798-11810
- Schnell JD, Hicke L (2003) Non-traditional functions of ubiquitin and ubiquitin-binding proteins. *J Biol Chem* **278**: 35857-35860
- Schofield CJ, Ratcliffe PJ (2004) Oxygen sensing by HIF hydroxylases. *Nat Rev Mol Cell Biol* **5**: 343-354
- Semenza GL (2003) Targeting HIF-1 for cancer therapy. *Nat Rev Cancer* **3**: 721-732
- Shevchenko A, Wilm M, Vorm O, Mann M (1996) Mass spectrometric sequencing of proteins silver-stained polyacrylamide gels. *Anal Chem* **68**: 850-858
- Shindoh N, Kudoh J, Maeda H, Yamaki A, Minoshima S, Shimizu Y, Shimizu N (1996) Cloning of a human homolog of the Drosophila minibrain/rat Dyrk gene from "the Down syndrome critical region" of chromosome 21. *Biochem Biophys Res Commun* **225**: 92-99
- Smart D, Gunthorpe MJ, Jerman JC, Nasir S, Gray J, Muir AI, Chambers JK, Randall AD, Davis JB (2000) The endogenous lipid anandamide is a full agonist at the human vanilloid receptor (hVR1). *Br J Pharmacol* **129**: 227-230
- Smeenk L, van Heeringen SJ, Koepffel M, Gilbert B, Janssen-Megens E, Stunnenberg HG, Lohrum M (2011) Role of p53 serine 46 in p53 target gene regulation. *PLoS One* **6**: e17574
- Song WJ, Sternberg LR, Kasten-Sportes C, Keuren ML, Chung SH, Slack AC, Miller DE, Glover TW, Chiang PW, Lou L, Kurnit DM (1996) Isolation of human and murine homologues of the Drosophila minibrain gene: human homologue maps to 21q22.2 in the Down syndrome "critical region". *Genomics* **38**: 331-339
- Stolze IP, Tian YM, Appelhoff RJ, Turley H, Wykoff CC, Gleadle JM, Ratcliffe PJ (2004) Genetic analysis of the role of the asparaginyl hydroxylase factor inhibiting hypoxia-inducible factor (FIH) in regulating hypoxia-inducible factor (HIF) transcriptional target genes [corrected]. *J Biol Chem* **279**: 42719-42725
- Taira N, Mimoto R, Kurata M, Yamaguchi T, Kitagawa M, Miki Y, Yoshida K (2012) DYRK2 priming phosphorylation of c-Jun and c-Myc modulates cell cycle progression in human cancer cells. *J Clin Invest*
- Taira N, Nihira K, Yamaguchi T, Miki Y, Yoshida K (2007) DYRK2 is targeted to the nucleus and controls p53 via Ser46 phosphorylation in the apoptotic response to DNA damage. *Mol Cell* **25**: 725-738
- Taira N, Yamamoto H, Yamaguchi T, Miki Y, Yoshida K (2010) ATM augments nuclear stabilization of DYRK2 by inhibiting MDM2 in the apoptotic response to DNA damage. *J Biol Chem* **285**: 4909-4919

Tang AH, Neufeld TP, Kwan E, Rubin GM (1997) PHYL acts to down-regulate TTK88, a transcriptional repressor of neuronal cell fates, by a SINA-dependent mechanism. *Cell* **90**: 459-467

Tatebe H, Shimada K, Uzawa S, Morigasaki S, Shiozaki K (2005) Wsh3/Tea4 is a novel cell-end factor essential for bipolar distribution of Tea1 and protects cell polarity under environmental stress in *S. pombe*. *Curr Biol* **15**: 1006-1015

Telerman A, Amson R (2009) The molecular programme of tumour reversion: the steps beyond malignant transformation. *Nat Rev Cancer* **9**: 206-216

Topol L, Jiang X, Choi H, Garrett-Beal L, Carolan PJ, Yang Y (2003) Wnt-5a inhibits the canonical Wnt pathway by promoting GSK-3-independent beta-catenin degradation. *J Cell Biol* **162**: 899-908

Toth A, Kedei N, Wang Y, Blumberg PM (2003) Arachidonyl dopamine as a ligand for the vanilloid receptor VR1 of the rat. *Life Sci* **73**: 487-498

Tseng CF, Iwakami S, Mikajiri A, Shibuya M, Hanaoka F, Ebizuka Y, Padmawinata K, Sankawa U (1992) Inhibition of in vitro prostaglandin and leukotriene biosyntheses by cinnamoyl-beta-phenethylamine and N-acyldopamine derivatives. *Chem Pharm Bull (Tokyo)* **40**: 396-400

Varjosalo M, Bjorklund M, Cheng F, Syvanen H, Kivioja T, Kilpinen S, Sun Z, Kallioniemi O, Stunnenberg HG, He WW, Ojala P, Taipale J (2008) Application of active and kinase-deficient kinome collection for identification of kinases regulating hedgehog signaling. *Cell* **133**: 537-548

Winter M, Sombroek D, Dauth I, Moehlenbrink J, Scheuermann K, Crone J, Hofmann TG (2008) Control of HIPK2 stability by ubiquitin ligase Siah-1 and checkpoint kinases ATM and ATR. *Nat Cell Biol* **10**: 812-824

Wong CS, Sceneay JE, House CM, Halse HM, Liu MC, George J, Potdevin Hunnam TC, Parker BS, Haviv I, Ronai ZA, Cullinane C, Bowtell DD, Moeller A (2012) Vascular normalization by loss of Siah2^{-/-} results in increased chemotherapeutic efficacy. *Cancer Res*

Woods YL, Cohen P, Becker W, Jakes R, Goedert M, Wang X, Proud CG (2001) The kinase DYRK phosphorylates protein-synthesis initiation factor eIF2Bepsilon at Ser539 and the microtubule-associated protein tau at Thr212: potential role for DYRK as a glycogen synthase kinase 3-priming kinase. *Biochem J* **355**: 609-615

Yamashita S, Chujo M, Moroga T, Anami K, Tokuishi K, Miyawaki M, Kawano Y, Takeno S, Yamamoto S, Kawahara K (2009) DYRK2 expression may be a predictive marker for chemotherapy in non-small cell lung cancer. *Anticancer Res* **29**: 2753-2757

Yeo SJ, Yoon JG, Yi AK (2003) Myeloid differentiation factor 88-dependent post-transcriptional regulation of cyclooxygenase-2 expression by CpG DNA: tumor necrosis factor-alpha receptor-associated factor 6, a diverging point in the Toll-like receptor 9-signaling. *J Biol Chem* **278**: 40590-40600

Yoshida K, Liu H, Miki Y (2006) Protein kinase C delta regulates Ser46 phosphorylation of p53 tumor suppressor in the apoptotic response to DNA damage. *J Biol Chem* **281**: 5734-5740

Zhang J, Guenther MG, Carthew RW, Lazar MA (1998) Proteasomal regulation of nuclear receptor corepressor-mediated repression. *Genes Dev* **12**: 1775-1780

Zhao H, Piwnica-Worms H (2001) ATR-mediated checkpoint pathways regulate phosphorylation and activation of human Chk1. *Mol Cell Biol* **21**: 4129-4139

Zhao HL, Ueki N, Hayman MJ (2010) The Ski protein negatively regulates Siah2-mediated HDAC3 degradation. *Biochem Biophys Res Commun* **399**: 623-628

Zhou BP, Liao Y, Xia W, Spohn B, Lee MH, Hung MC (2001) Cytoplasmic localization of p21Cip1/WAF1 by Akt-induced phosphorylation in HER-2/neu-overexpressing cells. *Nat Cell Biol* **3**: 245-252

Zygmunt PM, Petersson J, Andersson DA, Chuang H, Sorgard M, Di Marzo V, Julius D, Hogestatt ED (1999) Vanilloid receptors on sensory nerves mediate the vasodilator action of anandamide. *Nature* **400**: 452-457

Oral presentation and Publications

ORAL PRESENTATION

First award to the best oral communication in Cancer Session of the 2nd IMIBIC Young Researchers Conference. Cordoba, Spain, 2011.

Moisés Pérez Aguilera, Carmen García-Limones, Moreno P, Salvatierra A, Eduardo Muñoz and Marco A. Calzado. "Mecanismos de regulación de SIAH2 mediados por quinasas involucradas en la respuesta a estrés oncogénico". II Jornadas de Jóvenes Investigadores en Biomedicina del IMIBIC. Córdoba.

PUBLICATIONS DERIVED FROM PhD THESIS

Authors: **Navarrete CM***, **Perez M***, García de Vinuesa A, Collado JA, Fiebich BL, Calzado MA, Muñoz E.

Title: Endogenous N-acyl-dopamines induce COX-2 expression in brain endothelial cells by stabilizing mRNA through a p38 dependent pathway.

Journal: Biochem Pharmacol. Jun 15;79(12):1805-14.

Date of publication: 2010

Further information: Impact factor (2009): **4,254**. Subject category: Pharmacology & Pharmacy. Number of Journals: 237. Ranking: 43. **(Q1)**. * **Equally contributed to this work.**

Authors: **Moisés Pérez Aguilera**, Carmen García-Limones, Inés Zapico, Anabel Marina, Eduardo Muñoz and Marco A. Calzado.

Title: Mutual regulation between SIAH2 and DYRK2 controls hypoxic and genotoxic signaling pathways.

Journal: Under revision.

PUBLICATIONS IN COLLABORATION DURING THE PhD THESIS

Authors: Márquez N, Calzado MA, Sánchez-Duffhues G, **Pérez M**, Minassi A, Pagani A, Appendino G, Diaz L, Muñoz-Fernández MA, Muñoz E.

Title: Differential effects of Phorbol-13-monoesters on Human Immunodeficiency Virus Reactivation.

Journal: Biochem Pharmacol. 2008 Mar 15;75(6):1370-80

Date of publication: 2008

Further information: Impact factor (2009): **4,254**. Subject category: Pharmacology and Pharmacy. Number of Journals: 237. Ranking: 34. **(Q1)**

Authors: Liliana Avila, **Moises Perez**, Gonzalo Sanchez-Duffhues, Rosario Hernández-Galán, Eduardo Muñoz, Fabio Cabezas, Winston Quiñones, Fernando Torres, Fernando Echeverri.

Title: Effects of diterpenes from latex of Euphorbia lactea and Euphorbia laurifolia on human immunodeficiency virus type 1 reactivation.

Journal: **Phytochemistry**. 2008. Mar 15;75(6):1370-80

Date of publication: 2008

Further information: Impact factor (2009): **2,946**. Subject category: Pharmacology and Pharmacy. Number of Journals: 156. Ranking: 21. **(Q1)**

Authors: **Pérez M**, García de Vinuesa A, Sanchez-Duffhues G, Marquez N, Bellido ML, Muñoz-Fernandez MA, Moreno S, Castor TP, Calzado MA, Muñoz E

Title: Bryostatins synergize with histone deacetylase inhibitors to reactivate HIV-1 from latency.

Journal: **Current HIV Research**. Sep 1;8(6):418-29.

Date of publication: 2010

Further information: Impact factor (2009): **1,978**. Subject category: Virology. Number of Journals: 30. Ranking: 21. **(Q3)**

Authors: Sánchez-Duffhues G, Vo MQ, **Pérez M**, Calzado MA, Appendino G, Muñoz E

Title: Activation of latent HIV-1 expression by protein kinase C agonists. A novel therapeutic approach to eradicate HIV-1 reservoirs.

Journal: Current Drug Targets. 2011 Mar 1;12(3):348-56.

Date of publication: 2010

Further information: Impact factor (2009): **3,932**. Subject category: Pharmacology and Pharmacy. Number of Journals: 237. Ranking: 41. **(Q1)**

Authors: **Moisés Pérez**, Carmen G. Limones, Irene Cantarero, Juan A. Collado, María L. Bellido, Olov Sterner, Marco A. Calzado and Eduardo Muñoz

Title: The fungus metabolite Galiellalactone inhibits HIV-1 replication by interfering with the nuclear import of NF- κ B.

Journal: Under revision



Endogenous *N*-acyl-dopamines induce COX-2 expression in brain endothelial cells by stabilizing mRNA through a p38 dependent pathway

Carmen M. Navarrete^{a,1}, Moisés Pérez^{a,1}, Amaya García de Vinuesa^a, Juan A. Collado^a, Bernd L. Fiebich^c, Marco A. Calzado^{a,b}, Eduardo Muñoz^{a,b,*}

^aDepartamento de Biología Celular, Fisiología e Inmunología, Universidad de Córdoba. Facultad de Medicina. Avda de Menéndez Pidal s/n, 14004 Córdoba, Spain

^bInstituto Maimónides de Investigación Biomédica de Córdoba, Córdoba, Spain

^cNeurochemistry Research Group, Department of Psychiatry, University of Freiburg Medical School. Hauptstrasse 5, D-79104 Freiburg, Germany

ARTICLE INFO

Article history:

Received 4 December 2009

Accepted 24 February 2010

Keywords:

N-Arachidonoyl-dopamine

COX-2

p38 MAPK

mPGES-1

Endothelial cells

ABSTRACT

Cerebral microvascular endothelial cells play an active role in maintaining cerebral blood flow, microvascular tone and blood brain barrier (BBB) functions. Endogenous *N*-acyl-dopamines like *N*-arachidonoyl-dopamine (NADA) and *N*-oleoyl-dopamine (OLDA) have been recently identified as a new class of brain neurotransmitters sharing endocannabinoid and endovanilloid biological activities. Endocannabinoids are released in response to pathogenic insults and may play an important role in neuroprotection. In this study we demonstrate that NADA differentially regulates the release of PGE₂ and PGD₂ in the microvascular brain endothelial cell line, b.end5. We found that NADA activates a redox-sensitive p38 MAPK pathway that stabilizes COX-2 mRNA resulting in the accumulation of the COX-2 protein, which depends on the dopamine moiety of the molecule and that is independent of CB₁ and TRPV1 activation. In addition, NADA inhibits the expression of mPGES-1 and the release of PGE₂ and upregulates the expression of L-PGD synthase enhancing PGD₂ release. Hence, NADA and other molecules of the same family might be included in the group of lipid mediators that could prevent the BBB injury under inflammatory conditions and our findings provide new mechanistic insights into the anti-inflammatory activities of NADA in the central nervous system and its potential to design novel therapeutic strategies to manage neuroinflammatory diseases.

© 2010 Elsevier Inc. All rights reserved.

1. Introduction

The past decade has seen a sudden spurt of interest in the endocannabinoid system (ECs). This system regulates a plethora of biological effects and is composed of cannabinoid and vanilloid receptors, endogenous signaling molecules (called endocannabinoids) and metabolism-related enzymes [1,2]. Endocannabinoids are a class of lipid mediators found in several tissues and based on a polyunsaturated fatty acid amide or ester motifs [3]. Anandamide (AEA) and 2-arachidonoylglycerol (2-AG) are the most characterized endocannabinoids acting in the brain and in peripheral tissues mainly through the activation CB₁ and CB₂ cannabinoid receptors, respectively. AEA can also interact with the vanilloid receptor type

1 TRPV1 [4,5]. This non-selective cation channel is activated by vanilloids, such as capsaicin, and also by endogenous ligands *N*-acyl-dopamines (neurolipins), such as *N*-arachidonoyl-dopamine (NADA) and *N*-oleoyl-dopamine (OLDA) [6–8]. While NADA binds TRPV1 [7,9], and CB₁ receptor [10], OLDA is a capsaicin-like lipid with full TRPV1 agonist activity but devoid of affinity for CB receptors [8]. NADA induces several biological activities such as hyperalgesia [8], smooth muscle contraction in the guinea pig bronchi and bladder [11], vasorelaxation in blood vessels [12], and also has immunomodulatory, neuroprotective and antiinflammatory properties [13–15]. Their saturated analogs *N*-palmitoyl-dopamine (PALDA) and *N*-stearoyl-dopamine (STEARDA) were also identified as endogenous substances not activating TRPV1, although they significantly enhanced the TRPV1-mediated effects of NADA [8].

Endocannabinoids may play a major role in the central nervous system (CNS), immune control and neuroprotection by regulating the cellular network of communication between the nervous and immune system during neuroinflammation and neuronal damage [16–18]. In addition, *N*-acyl-dopamines influence the lipoxygenase pathway of arachidonic acid cascade as substrates or inhibitors and may also be involved in the regulation of inflammation [19,20].

* Corresponding author at: Departamento de Biología Celular, Fisiología e Inmunología. Facultad de Medicina. Avda. de Menéndez Pidal s/n, 14004 Córdoba, Spain. Tel.: +34 957218267; fax: +34 957218229.

E-mail addresses: b72naruc@uco.es (C.M. Navarrete), l02peagm@uco.es (M. Pérez), v52gaana@uco.es (A.G. de Vinuesa), md2coroj@uco.es (J.A. Collado), bernd.fiebich@klinikum.uni-freiburg.de (B.L. Fiebich), bq2cacam@uco.es (M.A. Calzado), fi1muble@uco.es (E. Muñoz).

¹ C.M.N. and M.P. equally contributed to this work.

Title: Mutual regulation between SIAH2 and DYRK2 controls hypoxic and genotoxic signaling pathways.

Authors: Moisés Pérez Aguilera¹, Carmen García-Limones¹, Inés Zapico², Anabel Marina², Eduardo Muñoz¹ and Marco A. Calzado^{1*}.

¹Instituto Maimónides de Investigación Biomédica de Córdoba (IMIBIC), Universidad de Córdoba, 14004 Córdoba, Spain. ²Centro de Biología Molecular Severo Ochoa, CSIC-Universidad Autónoma de Madrid, 28049 Madrid, Spain.

***Corresponding Author:** Marco A. Calzado Ph.D.

Departamento de Biología Celular, Fisiología e Inmunología. Facultad de Medicina, Universidad de Córdoba.

C/ María, Virgen y Madre s/n. 14004, Córdoba, Spain

Phone: + 34 957218267; Fax: + 34 957218266

e-mail: mcalzado@uco.es

Running title: Coordinate regulation between SIAH2 and DYRK2.

Character count: 54.993